The AGE of Biomaterials:

Preserving the myocardium after infarction to promote heart repair and function

Nicholas Blackburn

A Thesis submitted to the

Faculty of Graduate and Postdoctoral Studies

in partial fulfillment of the requirements for the

PhD degree in Cellular and Molecular Medicine

Department of Cellular and Molecular Medicine

Faculty of Medicine

University of Ottawa

Acknowledgements

Not all can be mentioned, but none will be forgotten.

First I would like to thank the current and former members of the Suuronen lab. Principally I would like to thank Drs. Brian McNeill and Branka Vulesevic whom were instrumental to my learning and development as a student and a scientist. I would also like to thank Rick Seymour, Suzanne Crowe, and the animal care team at the University of Ottawa Heart Institute.
I would like to thank Drs. Chao Deng, Zhiyuan Zhong and the members from their labs at Soochow University, People's Republic of China for graciously hosting me in Suzhou. I am forever grateful for this deeply cherished experience.

I would like to thank my thesis committee Dr. Marc Ruel, Dr. Nadine Wiper-Bergeron, and Dr. Katey Rayner. Each member not only was a valuable contribution to the work, but also my own personal and professional development.

I would like to thank my friends and family for their support. I would, especially, like thank my loving partner Gabrielle Cyr for all her help and understanding through what often proved to be a very challenging endeavour.

Finally, I would like to thank my supervisor Dr. Erik Suuronen. I, having had been away from science for a number of years, accepting me into his program was a risk. I thank him for taking that risk, and for his guidance and mentorship all these years. Erik's door is always open, and I could not have asked for a better supervisor.

Abstract

Myocardial infarction (MI) persists as one of the leading causes of death worldwide. Often patients whom survive the initial injury will develop heart failure characterized by a dilated and functionally incompetent heart. Heart failure (HF) carries a worse prognosis than most cancers, and the only curative therapy to date is heart transplantation. A better understanding of the repair and remodeling processes post-MI, and the development of novel therapies are required to combat this burgeoning medical challenge.

This thesis research sought to identify a novel mediator of the impaired cardiac remodeling that often occurs post-MI, and to characterize a biomaterial hydrogel therapy as a novel treatment. We investigated the role of methylglyoxal (MG), an important precursor to advanced glycation end-products (AGE), using a transgenic mouse model to over-express glyoxalase 1 (GLO1). GLO1 is the primary enzyme involved in metabolizing MG and preventing its accumulation. The role for MG and AGEs in MI and HF had been alluded to in the literature, yet no study to date has causally linked them with the loss of function and impaired remodeling of the post-MI heart. We also assessed an injectable hydrogel for the treatment of MI using a mouse model and evaluated the impact of delivery timing on its therapeutic efficacy.

In this thesis, we confirmed that MG derived AGEs accumulate post-MI (Chapter 3.1). We show that preventing their accumulation, through GLO1 over-expression, mitigates the loss of function post-MI and positively influences remodeling through reducing final infarct sizes and end-systolic volumes. We demonstrate that this may possibly occur through improving the bone marrow response post-MI by restoring ECM-cell signaling. In Chapter 3.2, we present results of a study assessing the efficacy of a collagen based injectable hydrogel for the treatment of MI, and

assessing the role that timing plays into the benefits associated with this therapy by studying 3 separate timepoints including 3 hours, 7 days and 14 days post-MI. We found that the injectable hydrogel preserved cardiac function and reduced infarct sizes. It also positively interacted with the host repair response by reducing chronic inflammation and cell death. The benefits of the therapy depended on when the material was delivered, and we found that the earliest timepoint (3 hours post-MI) proved most beneficial. In Chapter 3.3, we combined the knowledge gained from Chapters 3.1 and 3.2 and functionalized our hydrogel with a flavonoid, Fisetin, that has been shown to scavenge MG and increase the activity of GLO1. We show that this novel functionalized material may be able to restore some function in MI, particularly in settings of low baseline cardiac function.

Taken together, the results of this thesis demonstrate that MG accumulates as a result of the ischemia and contributes to the impaired repair resolution and remodeling processes post-MI. This identifies MG as a possible novel target for the treatment of MI. Indeed, we also confirm the role that delivery timing plays into injectable hydrogels post-MI, and present promising results for a functionalized material design to intervene on MG production.

Table of Contents

Abstract iii

List of Figures ix

List of Tables xi

Acronyms and Abbreviations xii

Chapter 1 1

Introduction 1

1.1 Coronary Heart Disease, Myocardial Infarction and Heart Failure 2
1.2 Current Treatments and Possible Opportunities 5
1.3 Cardiac Repair and Remodeling Post-Myocardial Infarction 6
1.3.1 Early Inflammatory Phase 7
1.3.2 The Proliferation/Wound Healing Phase 10
1.3.3 The Maturation Phase 11
1.3.4 The Cardiac Extracellular Matrix and its Evolution throughout the Remodeling Process 12
1.4 Introduction to Glycation and Advanced Glycation End-Products (AGEs) 13
1.4.1 Introduction to Methylglyoxal 16
1.4.2 Methylglyoxal in Physiological Systems 19
1.4.3 The Glyoxalase System 20
1.4.4 Regulation of Glyoxalase 21
1.4.5 Methylglyoxal in Disease 22
1.4.6 Studies of Methylglyoxal and AGEs in Cardiovascular Disease 26
1.4.7 Transgenic hGLO1 Mice 28
1.4.8 Modifications to the Extracellular Matrix 29
1.5 Emerging Therapies for the Treatment of MI – Biomaterials 31
1.5.1 Biomaterials for the Treatment of Myocardial Infarction 31
1.5.2 Acellular, Injectable Hydrogels 32
1.6 Thesis Objectives and Aims 36

1.7 Hypotheses 37

Chapter 2 38

Materials and Methods 38

2.1 Methods – Common 39
2.1.1 Experimental MI Model and Cardiac Echocardiography 39
2.1.2 Animal Studies Randomization & Blinding 40
2.1.3 Histology and Immunohistochemistry 40
2.1.4 Statistical Analysis 41
2.2 Methods – Aim 1 41
2.2.1 Transgenic hGlo1 Mice 41
2.2.2 MG-derived AGE Determination 42
2.2.3 Histology and Immunohistochemistry 43
2.2.4 Collagen Gels and Methylglyoxal Glycation 44
2.2.5 In Vitro MG-Modified Collagen and Peripheral Blood Mononuclear Cells (PBMCs) 44
2.2.6 Flow Cytometry 46
2.2.7 Circulating Angiogenic Cell (CAC) Viability, Chemotaxis and Adhesion 46
2.2.8 In vitro HUVEC ECMatrix™ Angiogenesis Assay 47
2.3 Methods – Aim 2 48
2.3.1 Study Design 48
2.3.2 Matrix Preparation and Injection 48
2.3.3 Cytokine Array 49
2.3.4 Bone Marrow-derived Macrophage Culture 50
2.4 Methods – Aim 3 50
2.4.1 HA-PBLG-LA and PEG-PolyC Polymers 50
2.4.2 Loading Fisetin into HA-PBLG-LA or PEG-PolyC Nanoparticles 51
2.4.3 Fisetin Release Study 51
2.4.4 In vitro Cytotoxicity Assay 52
2.4.5 In vitro HUVEC ECMatrix™ Angiogenesis Assay 52
2.4.6 Fisetin Hydrogel Preparation and Injection 52

Chapter 3 54

Results 54

3.1 Glyoxalase-1 over-expression improves cardiac remodeling and function post-myocardial infarction 55

Brief Introduction to AIM 1 55

3.1.1 MI Stimulates MG-AGE production and GLO1 prevents MG-AGE accumulation 56

3.1.2 GLO1 Over-Expression Preserves Cardiac Function 58

3.1.3 GLO1 Over-Expression Reduces Scar Size and Cell Death 60

3.1.4 Vascular Density and c-kit^{+} Cell Recruitment is Enhanced in GLO1 mice Post-MI 60

3.1.5 MG Modification of ECM Proteins Impairs the Angiogenic Properties of PBMCs 64

3.2 Timing underpins the benefits associated with injectable collagen biomaterial therapy for the treatment of myocardial infarction 68

Brief Introduction to AIM 2 68

3.2.1 Delivery Timing Influences the Efficacy of Collagen-based Hydrogel Therapy for MI 70

3.2.2 Collagen Matrix Treatment Improves Vascular Density and Reduces Ongoing Cell Death in the Post-MI Myocardium 71

3.2.3 Collagen Matrix Therapy Reduces Chronic Inflammation in the MI Heart 75

3.2.4 Early (3 hours) Collagen Matrix Therapy Improves Parameters of Remodeling Post-MI 76

3.2.5 Early Myocardial Neovascularization and Cell Death in Response to 3-hour Collagen Matrix Treatment 79

3.2.6 Inflammatory Response to Early Collagen Matrix Biomaterial Therapy 80

3.2.7 Early Treatment Delivery of Collagen Matrix Biomaterial Preserves Cardiac Function Long-term 83

3.3 A Fisetin-loaded collagen hydrogel improves cardiac function post-MI 85

Brief Introduction to AIM 3 85

3.3.1 Fisetin Prevents MG-mediated Impairment of Angiogenesis and does not Affect Cell Viability 87

3.3.2 Designing a Delivery Platform for in vivo Fisetin Injection 88

3.3.3 Combined Fisetin - Biomaterial Improves Cardiac Function Post-MI 95

3.3.4 Hydrogel Therapies Reduce Final Infarct Sizes Post-MI 97

3.3.5 Hydrogel Therapies Improve Vascular Density and Mitigate Chronic Macrophage Recruitment to the Myocardium 99

Chapter 4 101

Discussion 101

4.1 Summary 102
4.2 The Contribution of MG to Post-MI Cardiac Remodeling 104
4.2.1 Clinical Studies on the Effects of MG and AGEs in CVD 104
4.2.2 In vivo and in vitro Studies of the Effects of MG and AGEs in CVD 106
4.2.3 GLO1 Over-expression Improves Cardiac Remodeling and Function Post-MI 108
4.2.4 Mechanisms of MG Action 109
4.2.4a Cell Death 109
4.2.4b Contributions of the Bone Marrow 111
4.2.4c Modifications to the ECM 112
4.2.4d Additional Mechanisms of MG 115
4.2.5 The PPE-1 hGLO1 Animal Model to Study Effects of MG on Post-MI Cardiac Remodeling 115
4.3 Timing underpins the benefits associated with injectable collagen biomaterial therapy for the treatment of myocardial infarction 118
4.3.1 Timing the Injection of Hydrogels Post-MI 118
4.3.2 Mechanisms of Action 124
4.3.2a Mechanical Reinforcement vs. Bioactivity 124
4.3.2b Inflammation and Cell Death 127
4.3.2c Angiogenesis and Cell-ECM Interactions 129
4.3.3 Limitations – Injection Methods, Animal Models, Additional Mechanisms 130
4.3.3a Injection Methods 130
4.3.3b Disease Models 131
4.3.3c Additional Mechanisms 132
4.4 A Functionalized Hydrogel for Targeting MG Post-MI 133
4.4.1 Targeting MG, and AGEs – a Role for Fisetin 134
4.4.2 Functionalizing Hydrogel Biomaterials for Post-MI Cardiac Therapy with Nanoparticles 136
4.5 General Summary and Conclusions 139
Appendices 141

Appendix A - Supplemental Data 142
Appendix B – Permissions and authorizations 145
References 152

List of Figures

Figure 1.1 Ventricular remodeling after myocardial infarction……..4

Figure 1.2 The phases of repair post-MI……..9

Figure 1.3 (a) AGE cross-linking between matrix proteins surrounding the cardiac muscle fibres
(b) AGE-receptor interaction influencing various pathways……14

Figure 1.4. Methylglyoxal and the Glyoxalase System……18

Figure 1.5. Intra- and extra-cellular targets of MG, AGEs and RAGE……..24

Figure 1.6. Acellular biomaterials for cardiac tissue repair……..34

Figure 2.1 In vitro modification of collagen gels by MG……45

Figure 3.1 MG and AGEs accumulate in the myocardium post-MI……57

Figure 3.2. Preventing MG-AGE accumulation through GLO1 over-expression preserves cardiac geometry and function……59

Figure 3.3. GLO1 over-expression reduces infarct scar size and cell death in mice post-MI……62

Figure. 3.4. GLO1 over-expression increases vascular density, and recruitment and vascular contribution of c-kit+ cells in the MI heart……63

Figure 3.5. MG glycates collagen in vivo and impairs pro-angiogenic properties of cultured human PBMCS in vitro……66

Figure 3.6. MG-modified collagen impairs cell survival and phenotype in vitro……..67

Figure 3.7 Delivering collagen-based biomaterial matrix offers optimal functional benefits……71

Figure 3.8 Collagen hydrogel improves vessel density and mitigates apoptosis……..74

Figure 3.9 Collagen matrix mitigates chronic inflammation in vivo and alters cytokine secretion of macrophages in vitro……77

Figure 3.10 Early collagen matrix delivery improves ventricular remodeling, cardiac performance and reduces final scar size and fibrosis……78
Figure 3.11 3-hour collagen matrix delivery improves neovascularization and reduces cell death 2 days after treatment……80
Figure 3.12 3-hour collagen matrix delivery does not exacerbate the acute inflammatory response early post-MI……82
Figure 3.13 Long-term functional preservation in mice treated with collagen matrix at 3 hours post-MI. ……84
Figure 3.14 Fisetin is not cytotoxic and does not impair angiogenesis in vitro……89
Figure 3.15 Characterizing Fisetin HA NPs……92
Figure 3.16 Fisetin in vitro release from collagen matrix biomaterial……94
Figure 3.17 Combined Fisetin collagen matrix hydrogel improves cardiac function and ventricular volumes post-MI……96
Figure 3.18 Hydrogel therapies reduce final scar sizes at 5 weeks post-treatment……98
Figure 3.19 Hydrogel therapies improve vascular density and reduce macrophage recruitment at 5 weeks post-treatment……100
Figure 4.1 Application of potential therapies to reduce myocardial salvage in relation to ischemic time. ……121
Figure A1 Collagen matrix effects on tissue level cytokine profile……142
Figure A2 Measuring Fisetin using fluorescence spectroscopy at 365nm excitation and 540nm emission……143
Figure A3. Baseline LVEF (pre-injection) of animals treated with fisetin hydrogel, hydrogel, fisetin and PBS 3 hours post-MI……144

List of Tables

Table 1. Size and poly-dispersion indices for various nanoparticle formulations with or without Fisetin……..91

Acronyms and Abbreviations

3-Deoxyglucosone	3DG
Advanced Glycation End-Products	AGEs
Amino Acid	AA
Anti-Oxidant Response Element	ARE
Bone Marrow Derived Macrophages	BMDMs
Cardiac Output	CO
Chemokine (C-C motif) ligand 5	CCL5
Congestive Heart Failure	CHF
Coronary Artery Disease	CAD
Coronary Heart Disease	CHD
Chemokine (C-X-C motif) ligand 5	CXCL5
Danger-Associated Molecular Patterns	DAMPs
Dihydroxyacetone-phosphate	DHAP
Dimethyl Sulfoxide	DMSO
Dynamic Light Scattering	DLS
Early Gene 2 Factor Isoform 4	E2F4

End-diastolic	ED
End-diastolic Area	EDA
End-diastolic Diameter	EDD
End-diastolic Volume	EDV
End-systolic	ES
End-systolic Area	ESA
End-systolic Diameter	ESD
End-systolic Volume	ESV
Extracellular Matrix	ECM
Fractional Area Change	%FAC
Fractional Shortening	%FS
Fibroblast Growth Factor-2	FGF-2
Glyceraldehyde-3-phosphate	GA3P
Glyoxalase 1 / Glyoxalase 2	GLO1/GLO2
Glutathione	GSH
Hyaluronic Acid	HA
Human Umbilical Vein Endothelial Cells	HUVECs

Insulin Response Element	IRE
Interleukin-4	IL-4
Interleukin-10	IL-10
Ischemic Heart Failure	IHF
Ischemia/Reperfusion	I/R
Left Ventricle/Ventricular	LV
Left Ventricular Ejection Fraction	LVEF
Macrophage Inflammatory Protein α	MIP-1α
Macrophage Inflammatory Protein γ	MIP-1γ
Matrix Metalloproteinase	MMP
Methylglyoxal	MG
Methylglyoxal derived AGEs	MG-AGEs
MG Hydroimidazolone	MG-H1
Mitogen-Activated Protein Kinases	MAPK
Myocardial infarction	MI
Nanoparticles	NPs
Nuclear Factor-Erythroid 2 p45 Subunit Related Factor 2	Nrf2

Peripheral Blood Mononuclear Cells	PBMCs
Phosphate Buffered Saline	PBS
Polydispersion Index	PDI
Polyethylene Glycol	PEG
Preproendothelin-1	PPE-1
Reactive Oxygen Species	ROS
Receptor for AGEs	RAGE
ST-Elevated Myocardial Infarction	STEMI
α-smooth muscle actin	α-SMA
Soluble Tumour Necrosis Factor Receptor	sTNFR
Streptozotocin	STZ
Tissue Culture Polystyrene	TCPS
Tissue Inhibitor of Matrix Metalloproteinase 2	TIMP-2
Tissue Inhibitor of MMP	TIMP
Transforming Growth Factor Beta	TGF-β
Tumour Necrosis Factor – α	TNF-α
Type II Diabetes Mellitus	TIIDM

Chapter 1

Introduction

1.1 Coronary Heart Disease, Myocardial Infarction and Heart Failure

Coronary heart disease (CHD) and myocardial infarction (MI) persist as the leading causes of heart failure and death in developed nations (Nabel and Braunwald, 2012). CHD is characterized by fatty build up in the coronary arteries and precedes MI, a condition in which a coronary artery becomes either partially or fully obstructed and prevents blood flow to supplied regions of the heart. In the US, approximately every 42 seconds someone will suffer an MI (Mozaffarian et al., 2016). Approximately 660 000 Americans will suffer a new coronary event and 305 000 will suffer a recurrent one each year (Mozaffarian et al., 2016). CHD was an underlying cause in about 1 in every 7 deaths in the US in 2013, and MI mortality was 116 793 (Mozaffarian et al., 2016). Despite these alarming statistics, between 2003 and 2013, the annual death rate attributable to CHD declined by 38% (Mozaffarian et al., 2016). This trend in improvement may be in large part attributable to changes in risk factors including lower total cholesterol, lower systolic blood pressure, lower smoking prevalence and increased physical activity (Mozaffarian et al., 2016). Although, some of these benefits are offset by increases in other risk factors contributing to CHD and MI including increases in body-mass index (BMI) and diabetes mellitus (DM) (Mozaffarian et al., 2016).

In what seems to be almost paradoxical, these significant advances in care, treatment, lowering of risk factors and improved outcomes over the last several decades precede a growing prevalence of patients with congestive heart failure (CHF) (Nabel and Braunwald, 2012; Neubauer, 2007). CHF is a clinical syndrome characterized by impaired systolic and/or diastolic function and various clinical signs such as fatigue,

dyspnea, fluid retention and cachexia (Hofmann and Frantz, 2013). A recent report released by the American Heart Association (AHA) projects that the prevalence of CHF will increase 46% from 2012 to 2030, resulting in over 8 million people with this clinical syndrome (Mozaffarian et al., 2016). This is particularly alarming given that symptomatic heart failure has about 30 to 40% mortality within the first year of diagnosis, a worse prognosis than most cancers (Jessup and Brozena, 2003; Neubauer, 2007). This reflects both the success in addressing the immediate concerns of MI, i.e. reperfusion of the blocked artery, but also a failure in our understanding of the mechanisms governing the progression of the disease thereafter, i.e. gross cardiac and molecular remodeling (Figure 1.1) (Jessup and Brozena, 2003). To date the most common cause of CHF is ischemic heart disease (Braunwald, 2013); therefore, elucidating the mechanisms that contribute to negative remodeling and the continued loss of viable cardiac tissue following infarction is necessary for the development of successful therapies.

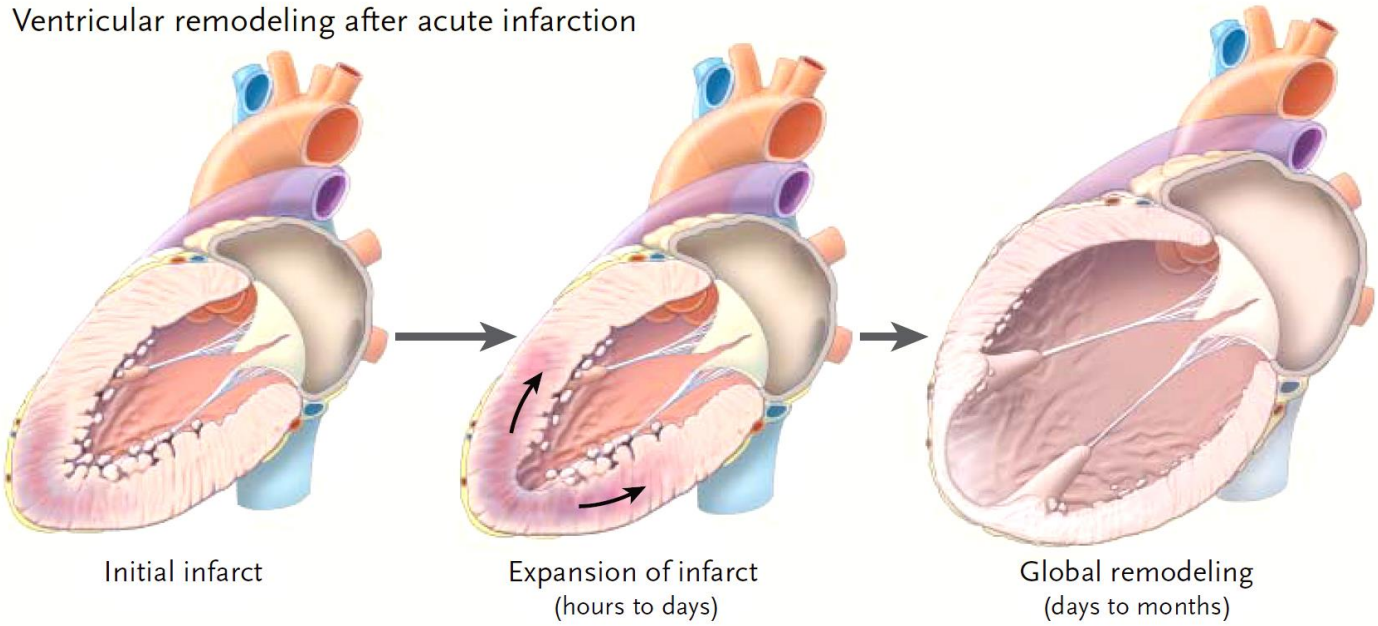

Figure 1.1 Ventricular remodeling after myocardial infarction. At the onset of MI there is no significant change to the ventricular geometry. Within hours to days the infarcted portion of the myocardium begins to expand and thin. Within days to months, global remodeling may occur resulting in overall dilatation of the ventricle decreasing systolic function, and promoting mitral-valve dysfunction and aneurysm formation.

Reproduced with permission from (Jessup, M., and Brozena, S. (2003). Heart failure. N Engl J Med *348*, 2007-2018.

1.2 Current Treatments and Possible Opportunities

Current treatments for MI include timely reperfusion strategies, the process of reopening the blocked artery, and pharmacotherapy including β-blockers, statins, mineralocorticoid receptor blockers, and angiotensin-converting enzyme (ACE) inhibitors (Fraccarollo et al., 2012). These therapies have been shown to improve prognosis by limiting the size of the infarct, preventing arrhythmia, and limiting post-infarction adverse remodeling (Fraccarollo et al., 2012); however, to prevent the development of heart failure following either a large MI or recurrent one, it has been suggested that additional strategies are required.

For one, though reperfusion remains as the best strategy to-date in preventing MI related mortality, it has been accepted that this therapy contributes to collateral damage of the myocardium (Yellon and Hausenloy, 2007). Several mechanisms have been identified as culprits including reactive oxygen species (ROS) formation (Yellon and Hausenloy, 2007). Indeed, animal studies suggest that reperfusion injury may account for up to 50% of the final infarct size (Yellon and Hausenloy, 2007). Therefore, one line of scientific inquiry should involve pharmacological or non-pharmacological means of limiting this type of injury (Yellon and Hausenloy, 2007). Pre-conditioning the myocardium prior to reperfusion, termed ischemic preconditioning, has been investigated and has shown promise in animals, but its translation to the clinic is challenged by the necessity that these therapies are delivered prior to an event, yet the occurrence of MI is not often predictable (Heusch and Rassaf, 2016).

Stem and progenitor cell therapies have also been investigated to enhance the repair of damaged myocardium (van Berlo and Molkentin, 2014). Unfortunately, the results thus far have not met the initial expectations and it seems we are still far from being able to restore damaged myocardium to sufficiently improve mortality or quality of life in patients (Shah and Shalia, 2011).

Finally, another opportunity seems to be to target adverse cardiac remodeling and infarct wound healing during the early phases of the injury. Perhaps successfully intervening during this early period may obviate the need for potentially costly regenerative therapies. In this scenario, cardiac function would be preserved such that patients may lead a fulfilling life, unobstructed by the limitations of their damaged heart. This thesis discusses work that both serves to identify a novel mediator of the early damage that occurs post-MI, and a novel therapy to target this mediator to sustain cardiac function and morphology.

1.3 Cardiac Repair and Remodeling Post-Myocardial Infarction

Adverse cardiac remodeling that occurs following an MI is the structural basis for ischemic heart failure (IHF). What appears to be the fundamental determinant of whether post-MI remodeling resolves into a stable, functioning heart or progresses into failure, at least clinically, is the extent of the initial injury and the efficiency of the repair/resolution mechanisms (Prabhu and Frangogiannis, 2016). The molecular mechanisms that characterize post-infarction repair and remodeling mechanisms are vast and complex, temporally dependent, and thus are outside the scope of the review

in this thesis. Several excellent reviews are available (Dobaczewski et al., 2010; Fraccarollo et al., 2012; Prabhu and Frangogiannis, 2016; Sutton and Sharpe, 2000). The major principles of cardiac repair will be covered.

1.3.1 Early Inflammatory Phase

As mentioned, MI starts when a coronary artery becomes obstructed, because of CHD, and limits or altogether prevents blood flow to an area of the myocardium. The onset of ischemia then precipitates a cascade of cellular and molecular events that subdivide loosely into different phases. In the literature, these overlapping phases are often identified as the inflammatory phase, the reparative and proliferative phase and the maturation phase (Fig 1.2) (Dobaczewski et al., 2010; Fraccarollo et al., 2012; Prabhu and Frangogiannis, 2016). Despite the number of papers that exist investigating the regulation of post-infarct repair and remodeling, our understanding of this highly complex process is still incomplete.

Structurally, this first phase post-MI is characterized by early thinning of the infarcted portion of the left ventricle (Burchfield et al., 2013). The onset of hypoxia during ischemia precipitates the early events of inflammation, which in rodents lasts for about 48 hours (Dobaczewski et al., 2010). However, in the chronic MI rodent model, peak immune cell infiltration appears to occur between 3 and 7 days post-MI (Yan et al., 2013). The exact timeline in larger mammals and humans is longer, but less well understood (Dewald et al., 2004). Hypoxia impairs endothelial cell integrity in the myocardial vasculature increasing its permeability and promoting leukocyte infiltration into the myocardium (Prabhu and Frangogiannis, 2016). Irreversible cell death can occur

in cardiomyocytes and other myocardial cell populations in as early as 20 minutes (Thygesen et al., 2012).

Necrosis appears to characterize the majority of this early cell death, though apoptosis and autophagy also play secondary roles (Eltzschig and Carmeliet, 2011). As mentioned previously, an additional source of cellular injury may derive from reperfusion of the myocardium resulting in ROS production and inflammation (Eltzschig and Carmeliet, 2011; Hori and Nishida, 2009; Yellon and Hausenloy, 2007). These combined sources of cellular necrosis, apoptosis, and damage to the extracellular matrix (ECM) release danger-associated molecular patterns (DAMPs) triggering an acute inflammatory phase (Prabhu and Frangogiannis, 2016). DAMPs lead to pro-inflammatory gene expression and a robust production of pro-inflammatory molecules such as cytokines, chemokines and adhesion molecules. This results in the invasion of activated immune cells, and may serve to further precipitate apoptosis and necrosis in the myocardium (Thygesen et al., 2012; Yan et al., 2013). Neutrophils and monocytes are the principal cell types attracted in the early inflammatory period and once they arrive will begin to respond to inflammatory stimuli further promoting the infiltration of additional immune cells namely neutrophils, macrophages, dendritic cells, and T cells (Lister et al., 2016; Yan et al., 2013). The recruited immune cells further amplify the inflammatory response, clear necrotic tissue and other cellular debris from the myocardium (efferocytosis), and promote tissue digestion by releasing proteases and oxidases into the myocardium (Lister et al., 2016; Prabhu and Frangogiannis, 2016).

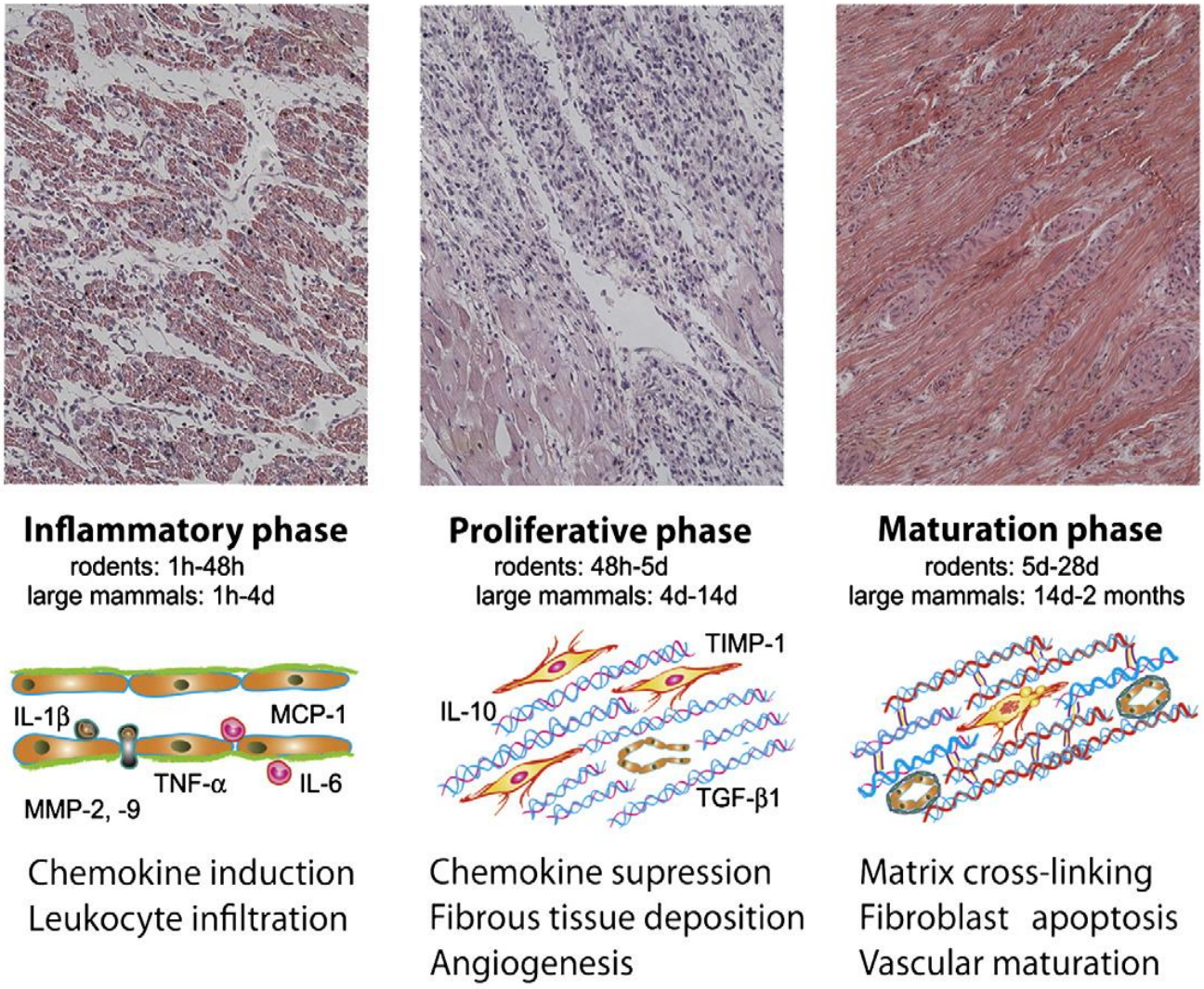

Figure 1.2 The phases of repair post-MI. MI triggers a repair response that falls into three overlapping phases. In the early inflammatory phase, leukocytes are recruited to the infarct due to the upregulation of chemokines, cytokines and other adhesion molecules. Mesenchymal cells will begin to infiltrate the myocardium as the inflammatory phase subsides, marking the transition to the proliferative phase. ECM is deposited by myofibroblasts, while a rich capillary network is formed. During the maturation phase the cellularity of the infarct decreases and the ECM begins to cross-link to form a dense, rigid collagen based scar. The images show hematoxylin/eosin stained sections of reperfused canine infarcts after 1 hour of coronary occlusion.

Modified From (Dobaczewski, M., Gonzalez-Quesada, C., and Frangogiannis, N.G. (2010). The extracellular matrix as a modulator of the inflammatory and reparative response following myocardial infarction. J Mol Cell Cardiol *48*, 504-511) Reprinted with permission from Oxford University Press

Efficient clearance of apoptotic cells is important for inflammation to resolve and the transition from the inflammatory phase into the pro-reparative/wound healing phase of infarction. Defects in the resolution of inflammation have been associated with adverse cardiac remodeling and heart failure in patients surviving MI (Frangogiannis, 2012).

1.3.2 The Proliferation/Wound Healing Phase

Replacement of the necrotic myocardium with granulation tissue marks, approximately, the beginning of the wound healing / proliferation phase post-MI. Principal events in this phase include neovascularization, the infiltration of fibroblasts, and reorganization of the cardiac extracellular matrix (Fraccarollo et al., 2012). Neovascularization relies on the tight coordination of endothelial, perivascular, and vascular smooth muscle cells and the ECM (Fraccarollo et al., 2012). This new vessel formation is required to supply the granulation tissue that is forming. Mobilization of pro-angiogenic bone marrow cells appear to aid in the coordination of the neovascularization response (Fazel et al., 2006). At the same time, migrated fibroblasts begin a phenotypic switch to contractile myofibroblasts (Dobaczewski et al., 2010). Myofibroblasts serve to deposit new collagen-rich ECM, which forms the infarct scar and its primary purpose is to stabilize the infarcted myocardium and prevent rupture (Fraccarollo et al., 2012).

1.3.3 The Maturation Phase

The maturation phase occurs between approximately 5 – 28 days post-MI in mice and 14 days to 2 months in larger mammals, such as canines (Dewald et al., 2004; Dobaczewski et al., 2010). During this period the myocardial scar matures through ECM cross-linking by lysyl oxidases increasing its tensile strength (Li et al., 2014). Additionally, myofibroblasts and vascular cells are cleared via apoptosis (Li et al., 2014). Impaired ECM and scar maturation compromises the integrity of the ventricular wall resulting in the potential for aneurysm formation and, ultimately, cardiac rupture (Li et al., 2014). Even with proper scar formation, cardiac dysfunction can ensue given that the scar is rigid and does not contribute to proper, synchronous pumping of the ventricle. Whether the heart functionally stabilizes following proper scar formation or continues to adversely remodel seems to depend on the initial size of the infarct and how efficiently inflammation is resolved post-MI. Improper resolution can lead to progressive decompensation marked first by hypertrophy of the surviving myocardium and then, as the heart struggles and ultimately fails to compensate for the loss of contractile muscle, it dilates leading to cardiac failure (Burchfield et al., 2013; Fedak et al., 2005). Unfortunately, attempts at targeting inflammation post-MI have yet to yield significant clinical results, likely owing to the complex, over-lapping and often seemingly conflicting roles that many of the effectors play in this process (Hedayat et al., 2010; Prabhu and Frangogiannis, 2016). For example, the cytokine TNF-α is systemically elevated in CHF and is associated with cellular hypertrophy, apoptosis and severity of disease (Fedak et al., 2005; Yokoyama et al., 1997). It is a product of pro-inflammatory macrophages, but

it can also be produced by cardiomyocytes. TNF-α produced from myocytes is important because it may confer key autocrine and paracrine effects on local myocardial cells including endothelial, vascular smooth muscle and cardiac fibroblast cells. In a mouse model of ischemia/reperfusion (I/R), $TNF^{-/-}$ mice exhibit smaller infarcts, attenuated inflammatory cell infiltration, and lower expression of chemokines (Maekawa et al., 2002). However, mice with dual TNF receptor deficiency exhibit worse outcomes post-MI (Kurrelmeyer et al., 2000). These conflicting results highlight the often-pleiotropic roles cytokines play in the post-MI machinery and pose a challenge in developing novel immune modulation therapies for this pathology.

1.3.4 The Cardiac Extracellular Matrix and its Evolution throughout the Remodeling Process

The ECM is intricately involved in the signaling, function and survival of cells (Discher et al., 2009). In particular, the cardiac ECM is important for proper mechanical function of the heart, (Fomovsky et al., 2010) for cell-matrix interactions primarily through the integrins, (Heino, 2000) and it also sequesters important signaling molecules (Schultz and Wysocki, 2009). It also has been identified as a direct modulator of the inflammatory and reparative response (Dobaczewski et al., 2010). It is a complex and dynamic scaffold composed of a broad array of fibrillar collagens, elastins, proteoglycans, and adhesive proteins such as laminin and fibronectin (Fedak et al., 2005; Fomovsky et al., 2010). It is dynamic because it is remodeled by resident cells in response to stimuli including disease and inflammation. For example, during the inflammatory phase of MI, cytokines such as TNF-α and IL-1β enhance matrix

metalloproteinase (MMP) expression and activity on matrix degradation (Dobaczewski et al., 2010). Conversely, pro-healing cytokines such as TGF-β and IL-10 promote Tissue Inhibitor of Metalloproteinase (TIMP) activity, which stimulates matrix deposition and preservation (Dobaczewski et al., 2010). Adverse remodeling that occurs post-MI is thought to be attributed, in part, to an imbalance in the regulation of MMPs and TIMPs (Dobaczewski et al., 2010).

1.4 Introduction to Glycation and Advanced Glycation End-Products (AGEs)

Advanced glycation end-products (AGEs) are a heterogeneous group of post-translational modifications formed by the non-enzymatic binding of free sugars and reactive carbonyls to proteins (Ward et al., 2013). The modifications to proteins may be reversible or irreversible and serve to alter their structure and function (Jahan and Choudhary, 2015). A causative role for AGEs has been shown in many pathologies owing to the disruption of the physiological folding of proteins, cross-linking and degradation, and through ligand interactions with their receptor, RAGE (receptor for AGEs) (Jahan and Choudhary, 2015; Ramasamy et al., 2012). Indeed, ECM cross-linking and AGE – receptor interactions have been identified as possibly culpable in heart failure (Figure 1.3) (Hartog et al., 2007b). Given that AGEs are the product of reducing sugars or dicarbonyls and proteins, they have received much attention in hyperglycemic disorders such as Diabetes Mellitus (Koenig et al., 1976; Maessen et al., 2015; Rabbani and Thornalley, 2012).

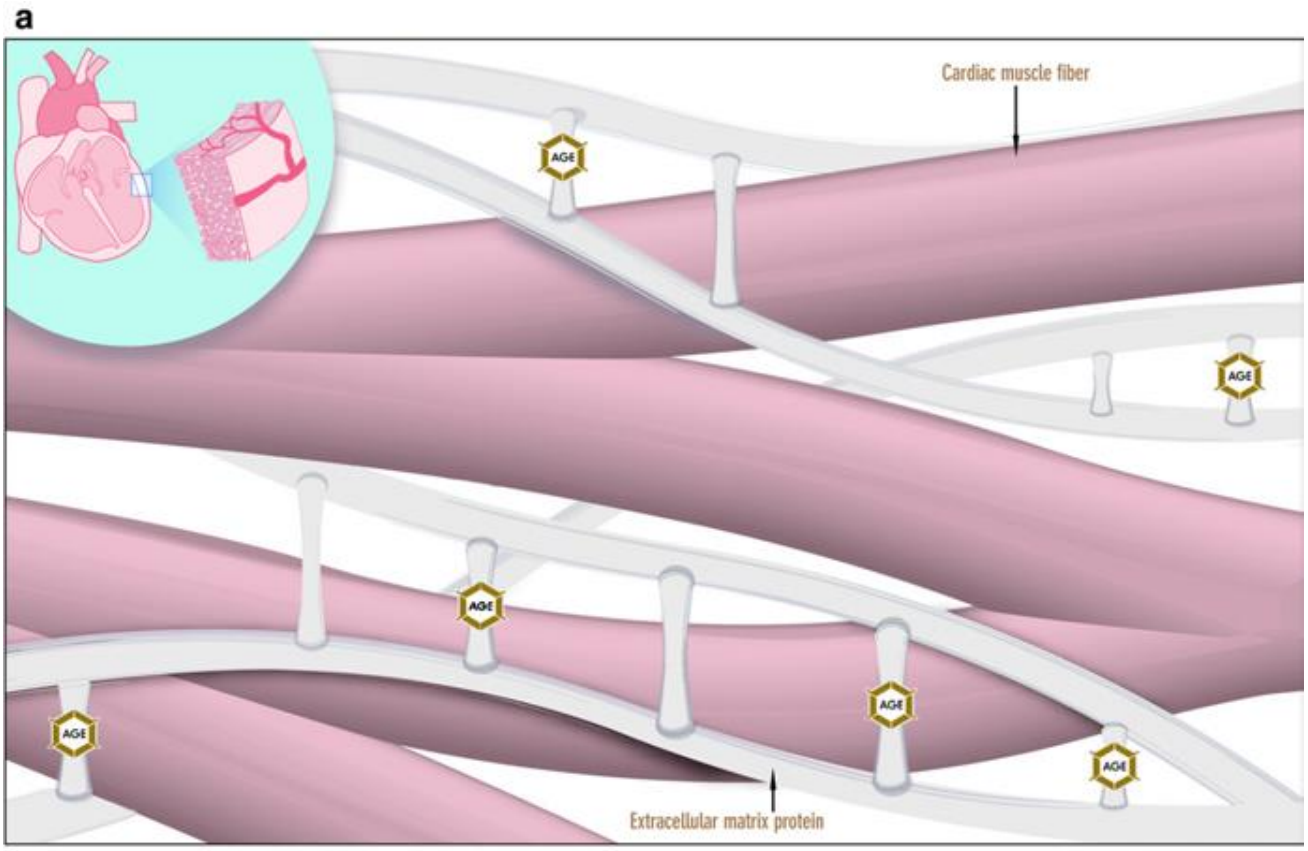
a
Cardiac muscle fiber
AGE
Extracellular matrix protein
b
CORONARY ARTERY DISEASE / ENDOTHELIAL DYSFUNCTION
Atherosclerosis
Vasoconstriction
Thrombosis
VASCULAR/ MYOCARDIAL STIFFNESS
Fibrosis / ECM accumulation
Increased production of collagen
IMPAIRED CONTRACTION/RELAXATION
Impaired calcium metabolism
Delayed calcium re-uptake
Decreased levels of intracellular calcium
Foam cell production
Macrophage
Pro-inflammatory cytokines
Oxidized-LDL
Monocyte
Monocyte / Macrophage adhesion
Decreased NO levels
increased endothelin-1 synthesis
PAI-1, Tissue factor
TGF-ß
Fibroblast
Myocyte
Enhanced expression of TGF-ß
AGEs
AGE receptor
Upregulation AGE receptor
Upregulation VCAM-1, ICAM-1,
Decreased eNOS activity
Increased NO inactivation
Nuclear Transcription Factors
Second Messenger
DNA
Endothelial cell

Figure 1.3 (a) AGE cross-linking between matrix proteins surrounding the cardiac muscle fibres. (b) AGE-receptor interaction influencing various pathways. AGE receptors have been demonstrated in a number of cell types including endothelial cells, monocytes, macrophages and myocytes. The most important receptor identified in the context of MI and heart failure is the receptor for AGEs (RAGE) (Aleshin et al., 2008; Basta, 2002; Bucciarelli et al., 2006; Tsoporis et al., 2010). RAGE is a multiligand receptor of the immunoglobulin superfamily. Distinct families of ligands, among which are S100/calgranulins, amphoterin, and amyloid-β-peptide, have been shown to interact with RAGE. This figure focuses on the effects of AGE-ligands. Activation of RAGE stimulates second messenger pathways, and the production of ROS via the NADPH oxidase pathway (Goldin et al., 2006; Hartog et al., 2004). In turn, second messengers activate or prolong activation of nuclear transcription factors (e.g. nuclear factor-κB), that subsequently upregulate the production of endothelin-1, vascular cell adhesion molecule-1 (VCAM-1), intercellular adhesion molecule-1 (ICAM-1), E-selectin, plasminogen activator inhibitor-1 (PAI-1), tissue factor, and transforming growth factor-β (TGF-β). Activation of RAGE upregulates RAGE expression itself as well (Bento et al., 2010c; Dobler et al., 2006; Pedchenko et al., 2005; Queisser et al., 2010; Tanaka et al., 2000). In turn, activation of these signaling pathways could perpetuate inflammation, such as the culpable mechanism in atherosclerosis, force vasoconstriction, contribute to pathogenic thrombosis, and perpetuate fibrogenesis.

Modified from Hartog, J.W., Voors, A.A., Bakker, S.J., Smit, A.J., and van Veldhuisen, D.J. (2007a). Advanced glycation end-products (AGEs) and heart failure: pathophysiology and clinical implications. European journal of heart failure 9, 1146-1155. Reprinted with permission from John Wiley and Sons.

Glucose-derived AGEs are some of the most commonly researched in the literature. They are formed via a Schiff-base intermediate when the glucose molecule reacts with the protein N-terminal and lysyl side chain amino groups (Hartog et al., 2007a; Rabbani and Thornalley, 2012). The production of a Schiff-base intermediate is reversible, but the process can continue with the conversion to another intermediate, an Amadori product, and finally the re-arrangement to a more stable AGE end-product such as *Nε*-fructosyl-lysine (FL) (Hartog et al., 2007a; Rabbani and Thornalley, 2012).

Other AGE precursors have been also characterized such as reactive dicarbonyl metabolites – methylglyoxal (MG), glyoxal and 3-deoxyglucosone (3DG) (Rabbani and Thornalley, 2012). Pathologic accumulation of these reactive dicarbonyls is often referred to as "dicarbonyl stress", akin to oxidative stress, and implies a physiological system that is over-producing dicarbonyls, failing to eliminate them sufficiently or both. Methylglyoxal appears to be the most important of these precursors in the development of disease (Rabbani and Thornalley, 2012).

1.4.1 Introduction to Methylglyoxal

Methylglyoxal, a potent α-oxoaldehyde, was first identified to modify proteins *in vivo* over a decade ago and is potentially the most important AGE precursor (Rabbani and Thornalley, 2012; Shamsi et al., 1998). MG is produced through a number of mechanisms, but the majority is generated through the spontaneous degradation of the triose phosphate intermediates of glycolysis: dihydroxyacetone-phosphate (DHAP) and glyceraldehyde-3-phosphate (GA3P) (Phillips and Thornalley, 1993; Rabbani and

Thornalley, 2012) (Rabbani et al., 2016b). MG can also be produced from the catabolism of threonine, degradation of proteins glycated by glucose, the diet, and ketone body metabolism (Cai et al., 2012; Rabbani et al., 2016b). MG-derived AGE (MG-AGE) adducts can form and accumulate both intra- and extra-cellularly. Though AGEs are not membrane permeable, most of their precursors, including MG, are. The majority of MG basally produced is metabolized and rendered inert by the glyoxalase system through a 2-step process (Figure 1.4)(Rabbani and Thornalley, 2012; Xue et al., 2012). In the first step, GLO1 facilitates the formation of an S-D-Lactoylglutathione intermediate from the hemithioacetal that is formed by the non-enzymatic reaction between MG and glutathione (GSH). During the second step GLO2 hydrolyzes the S-D-lactoylglutathione to D-lactate and thus recycles the GSH that was used to create the hemithioacetal intermediate (Rabbani and Thornalley, 2012; Thornalley, 2003b). GLO1 is the rate limiting enzyme, and its activity is proportional to the cellular concentration of GSH (Figure 1.4) (Thornalley, 2003b).

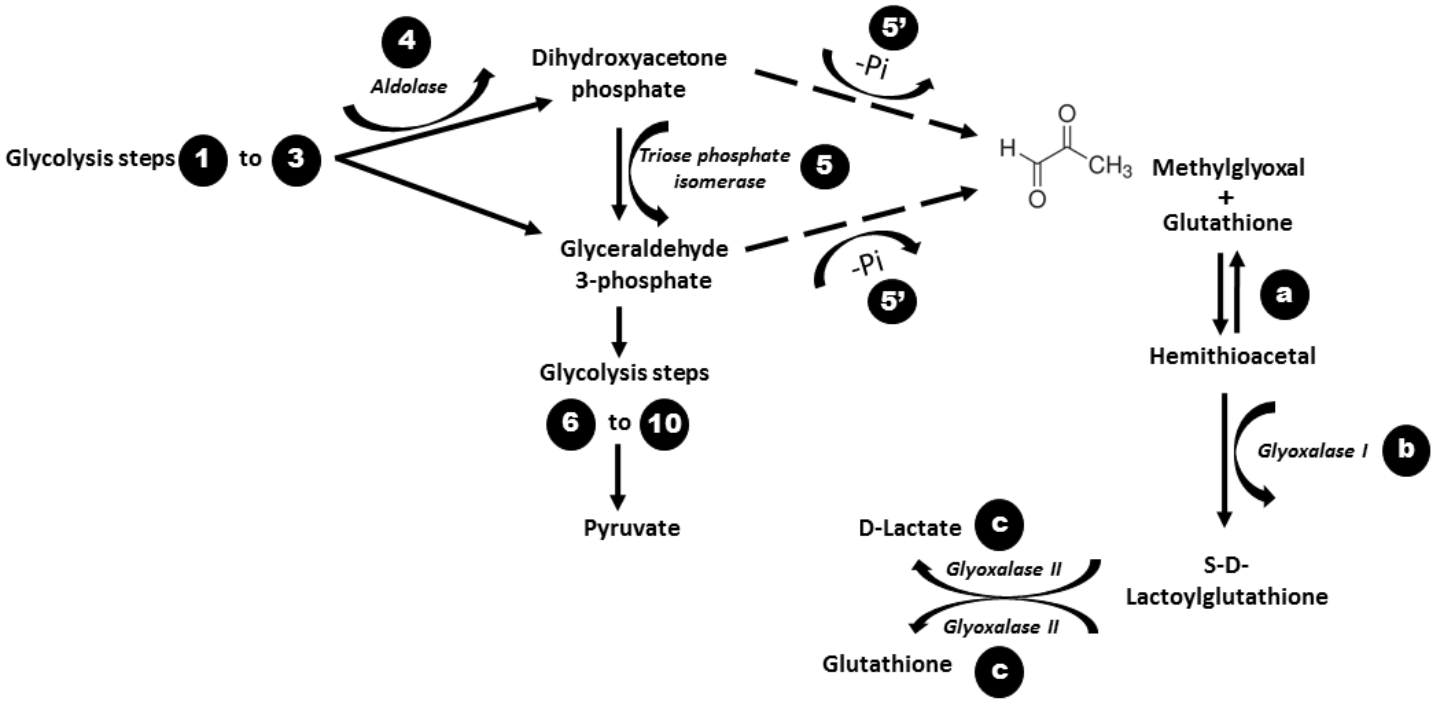

Figure 1.4. Methylglyoxal and the Glyoxalase System. MG is produced via the spontaneous degradation of the triose phosphate intermediates dihydroxyacetone phosphate and glyceraldehyde 3-phosphate. In physiological systems, methylglyoxal is eliminated via the glyoxalase system. The first step involves the production of a hemithioacetal intermediate from the reaction between MG and GSH, which is converted to S-D-lactoylglutathione. The second step involves the production of D-lactate and recycles GSH.

MG-specific glycation occurs primarily on arginine residues as the major product hydroimidazolone (MG-H1; N_{δ}-(5-hydro-5-methyl-4-imidazolon-2-yl)-ornithine), but MG glycation of lysine and cysteine residues are also main targets (Rabbani and Thornalley, 2012). Other minor adducts include *Nε*-carboxyethyl-lysine, argpyrimidine, lysine-derived 4-methylimidazolium crosslink (MOLD), as well as several others (Rabbani and Thornalley, 2012). The MG-H1 adduct accounts for approximately 90% of all adducts (Lo et al., 1994; Rabbani and Thornalley, 2012). The importance of MG derives from its specific glycation behavior, being that it is often directed to functionally important arginine residues such as those found in the integrin recognition sequences of collagen (Dobler et al., 2006; Pedchenko et al., 2005). MG glycation of proteins is particularly damaging because of the preferential modification of arginine residues that have the highest probability of all amino acids (AAs) to localize to functional sites in proteins (~20%) (Gallet et al., 2000). Likewise, functionally relevant arginine residues seem to be important targets for glycation (Ahmed et al., 2005; Blom et al., 2004; Dobler et al., 2006; Rabbani and Thornalley, 2012; Venkatraman et al., 2001; Yao et al., 2007). Given the reactivity of MG and the prevalence of its adducts in the body, it was a candidate choice dicarbonyl to study.

1.4.2 Methylglyoxal in Physiological Systems

Though it's concentration in the plasma is 50,000-fold less than glucose, MG has received much attention in the literature because it is 10,000 - 50,000 times more

reactive (Rabbani and Thornalley, 2012). The majority (~95%) of free MG in cells is reversibly bound to proteins. Additionally, mechanisms to de-glycate proteins modified by MG are yet to be identified (Rabbani and Thornalley, 2012). Although, a slow reversibility of MG-H1 adducts has been described with a half-life of approximately 12 days (Ahmed et al., 2002). MG concentrations are found to be in the 50 – 150nM in human plasma and 1-4µM in human cells; however, this has been shown to increase by 1.5-3-fold in different diseases resulting in dicarbonyl stress (Rabbani and Thornalley, 2014). Altogether, total formation for MG is estimated to be 125 µmol/kg cell mass per day, to a predicted whole body formation of 3mmol per day in a 70kg individual (Rabbani et al., 2016b). Despite this seemingly high flux of MG produced per day in an individual it is estimated that > 99% is metabolized by the glyoxalase 1 and aldoketo reductase (AKR) isozymes representing the enzymatic defense against glycation (Rabbani et al., 2016b). Overall, less than 1% of MG produced modifies proteins.

1.4.3 The Glyoxalase System

Glyoxalase 1 was first discovered in 1913 and it was initially believed to be the enzymatic unit facilitating a glycolytic bypass through MG to pyruvate (Sousa Silva et al., 2013). Indeed, later research began to provide compelling evidence that MG and GLO1, in fact, did not participate in glycolysis, particularly the discovery that the process required glutathione (GSH) as a co-factor, GSH having no effect on glycolysis, and that the end-product was D-lactate (Sousa Silva et al., 2013). Later, a second enzyme was found to be required in the catalysis from MG to D-lactate and was named GLO2. Since a

role for MG and the GLO pathway in glycolysis was ruled out, other theories were proposed. In the late sixties it was thought to be involved in cell proliferation, but again was later refuted (Sousa Silva et al., 2013). Today, other than providing enzymatic defense against reactive dicarbonyls, the role for the GLO1 and MG in physiology is still not entirely clear. GLO1 appears to be important as it is in the top 15% of proteins in terms of abundance in human cells (Rabbani et al., 2016a; Schwanhausser et al., 2011). The GLO system is often erroneously referred to as *the* enzymatic defense system against MG toxicity; however, others have been identified, including the aldoketo reductases (AKR)(Rabbani et al., 2016a). Other than in the renal medulla, it appears that the *in situ* activity of GLO1 exceeds AKR by approximately 30-fold, thus it is thought to be the *primary* defense against MG formation (Rabbani et al., 2016a).

The GLO system detoxifies MG through a 2-step process. In the first step, GLO1 facilitates the formation of an S-D-Lactoylglutathione intermediate from the hemithioacetal that is formed by the non-ezymatic reaction between MG and GSH. During the second step, GLO2 hydrolyzes the S-D-lactoylgutathione to D-lactate and thus recycles the GSH that was used to create the hemithioacetal intermediate (Rabbani and Thornalley, 2012; Thornalley, 2003a).

1.4.4 Regulation of Glyoxalase

GLO1 is present in the cytosol of all cells in the human body, and nearly all organisms. Human GLO1 exists as a dimer and is expressed at the genetic locus *GLO1* 6p21.2 (Rabbani et al., 2014). GLO1 appears to experience frequent copy number

variation in human and mouse genomes, resulting in approximately 2-4-fold increase in its expression (Rabbani et al., 2014). Human GLO1 contains several regulatory elements including: metal response element (MRE), insulin response element (IRE), early gene 2 factor isoform 4 (E2F4), and activating enhancer-binding protein 2α (AP-2α) (Rabbani et al., 2014). Recently, an anti-oxidant response element (ARE) was identified in the 5'-untranslated region of exon 1, which appears to suggest some level of stress response control via nuclear factor-erythroid 2 p45 subunit related factor 2 (Nrf2) (Xue et al., 2012). Nrf2 activators increased GLO1 mRNA, protein and activity, while decreasing intra- and extracellular concentrations of MG (Xue et al., 2012). $Nrf2^{-/-}$ mice showed decreased GLO1 mRNA and protein in most tissues, as well as increased urinary excretion of MG. GLO1 activity expression seems to be impaired by RAGE activation, though the mechanism is still unknown (Rabbani et al., 2014).

1.4.5 Methylglyoxal in Disease

A role for MG specific glycation in several diseases has gained considerable attention. Indeed, the damage that may accumulate from MG-specific toxicity was highlighted in an article published in 2009 by Schlotterer et al. In this study, the authors demonstrated that MG production was responsible for lifespan reduction in *C. Elegans* kept in hyperglycemia (Schlotterer et al., 2009). The over-expression of GLO1 rescued this loss of lifespan, partially through reducing intracellular ROS accumulation, whereas silencing GLO1 had the opposite effect (Morcos et al., 2008; Schlotterer et al., 2009). Furthermore, promoting MG accumulation, through GLO1 silencing, reduced mean and

maximum lifespan in *C.Elegans* despite normoglycemic conditions. Though specific mechanistic details were not elucidated, this study provided strong evidence for the potential devastating impact that MG-specific glycation could have in disease (Schlotterer et al., 2009).

As mentioned, the primary mechanism through which MG is thought to participate in disease is via arginine directed glycation (Pedchenko et al., 2005; Rabbani and Thornalley, 2012). Between 3-13% of the proteins in the human body may contain an MG-H residue (Wang et al., 2012). MG-H1 becomes causative in disease where either production is increased, metabolism decreases, or both (Rabbani and Thornalley, 2012). MG is accumulated during periods of oxidative stress (Abordo et al., 1999; Sena et al., 2012) and glycolytic metabolism and may contribute to oxidant-induced cytotoxicity (Abordo et al., 1999). Chronic hyperglycemia or acute ischemic insult stimulate the production of MG (Aleshin et al., 2008; Bucciarelli et al., 2006) , and the depletion of glutathione (Abordo et al., 1999), while also down-regulating the expression of GLO1 (Kumagai et al., 2009). The consequence being the GLO system is no longer capable of meeting metabolic demands (Ramasamy et al., 2006). In turn, the supra-production of MG triggers ROS, and the sequence continues as one perpetuates the production of the other. An overview of some of the intra- and extracellular targets of MG, AGEs and RAGE is provided in Figure 1.5.

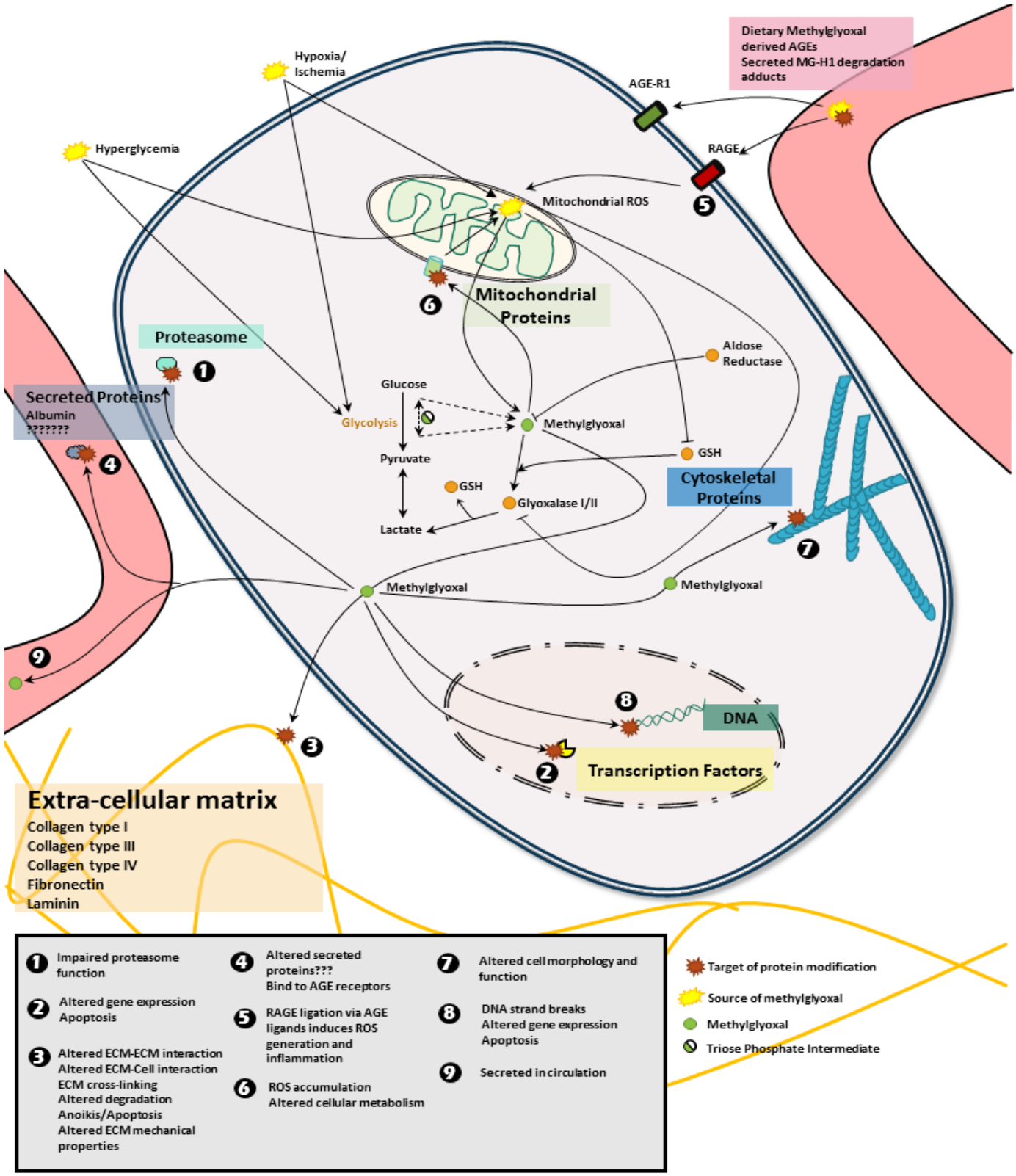
Dietary Methylglyoxal derived AGEs
Secreted MG-H1 degradation adducts
Hypoxia/ Ischemia
AGE-R1
Hyperglycemia
RAGE
Mitochondrial ROS
Mitochondrial Proteins
Proteasome
Aldose Reductase
Secreted Proteins
Albumin
???????
Glucose
Glycolysis
Methylglyoxal
GSH
Pyruvate
Cytoskeletal Proteins
GSH
Glyoxalase I/II
Lactate
Methylglyoxal
Methylglyoxal
DNA
Transcription Factors
Extra-cellular matrix
Collagen type I
Collagen type III
Collagen type IV
Fibronectin
Laminin
1 Impaired proteasome function
2 Altered gene expression
Apoptosis
3 Altered ECM-ECM interaction
Altered ECM-Cell interaction
ECM cross-linking
Altered degradation
Anoikis/Apoptosis
Altered ECM mechanical properties
4 Altered secreted proteins???
Bind to AGE receptors
5 RAGE ligation via AGE ligands induces ROS generation and inflammation
6 ROS accumulation
Altered cellular metabolism
7 Altered cell morphology and function
8 DNA strand breaks
Altered gene expression
Apoptosis
9 Secreted in circulation
Target of protein modification
Source of methylglyoxal
Methylglyoxal
Triose Phosphate Intermediate

Figure 1.5. Intra- and extra-cellular targets of MG, AGEs and RAGE. MG directed glycation involves principally arginine, lysine and cysteine residues. MG can be produced as a result of hyperglycemia, hypoxia, inflammation, reduced GLO1 activity and ROS generation. MG glycation has been shown to impair (**1**) proteasome function (Bento et al., 2010b). It has also been shown to induce (**2**) cell death (Chan and Wu, 2008; Li et al., 2007; Nam et al., 2015) and modify transcription factors and result in altered gene expression (Yao et al., 2007). (**3**) MG modifications of the ECM have been shown to be causative in disease resulting in altered mechanical properties and cell anoikis (Talior-Volodarsky et al., 2012). (**4**) MG has been shown to either directly modify or alter the release of secreted proteins (Bento et al., 2010a) and MG-derived AGEs have been shown to interact with AGE receptors such as RAGE (Xue et al., 2014). (**5-6**) RAGE activation has been shown to induce ROS formation, generate inflammation and influence GLO1 activity (Aleshin et al., 2008; Basta, 2002; Ma et al., 2009; Ramasamy et al., 2008, 2009, 2012; Shang et al., 2010; Tsoporis et al., 2010). MG has been shown to (**7**) modify or alter cytoskeleton protein formation (Fesus et al., 1981; Tatone et al., 2011). (**8**) MG modification of DNA has also been reported (Murata-Kamiya et al., 1999; Murata-Kamiya and Kamiya, 2001; Thornalley et al., 2010). Increased serum levels of MG have been associated with a number of pathologies (Rabbani et al., 2016a, b).

1.4.6 Studies of Methylglyoxal and AGEs in Cardiovascular Disease

The roles for AGEs and MG-AGEs in diabetes and other disorders have been well described (Goh and Cooper, 2008); however, how they participate in the pathogenesis of CVD is less well understood. A brief, non-exhaustive, review of our understanding of the role of MG and AGEs in CVD is discussed.

To date, studies suggesting possible AGE/MG-AGE involvement have been correlative as opposed to causative. For example, in one clinical study, skin autofluorescence – a metric of glycation – was elevated post-STEMI (ST-elevated myocardial infarction) and associated with inflammation, glycemic stress, and predictive of future major adverse cardiac events (Mulder et al., 2009). In another, Serum MG-H1 AGE levels were associated with CVD mortality in non-diabetic women (Kilhovd et al., 2009). Plasma AGEs, particularly levels of CML, have been associated with the prognosis and severity of CHF (Hartog et al., 2007b). However, after correcting for renal function, the association was lost, thus making it difficult to determine if CML was simply a biomarker (Hartog et al., 2007a; Hartog et al., 2007b). More recently, using an integrative genomics framework approach combining 16 separate genome wide association studies (GWAS), *GLO1* was identified as one of several genes that were key drivers in CAD (coronary artery disease)-associated gene networks (Makinen et al., 2014). Coinciding with these results, in a separate study, MG-H1 and CML levels were associated with rupture-prone atherosclerotic plaques from human carotid endarterectomy specimens (Hanssen et al., 2014). This rupture prone phenotype was also characterized by increased levels of pro-inflammatory mediators IL-8, MCP-1 and

decreased GLO1 mRNA versus stable plaque segments (Hanssen et al., 2014). Together, these clinical studies seem to indicate some role for MG and its AGEs in the development of CAD, MI and CHF, but have not determined what that role may be.

To date, no animal study has specifically investigated MG in MI, though several do provide some insight. Of the few animal studies reported, several using an I/R mouse model showed that ischemia was associated with an increase in MG and AGE production in the myocardium, but it did not establish whether MG or its AGEs contributed to the cardiac remodeling (Aleshin et al., 2008; Bucciarelli et al., 2006). *In vitro* research has suggested that MG exacerbates ischemia-reperfusion injury to cultured cardiomyocytes (Wang et al., 2010), but this has not been examined *in vivo*. Chronic administration of MG to rats creates diabetes-like ischemic disease (Crisostomo et al., 2013), but this does not represent the physiological phenomena of MG accumulation. Over-expressing GLO1 in STZ-induced diabetic mice resulted in reduced inflammation, improved capillary density and prevented ventricular dysfunction (Vulesevic et al., 2016), but whether MG contributes to cardiac dysfunction independent of hyperglycemia is still largely unknown. Collectively, the evidence thus far provides a strong foundation to suggest that MG and MG-AGEs may participate in the pathogenesis of cardiac remodeling following MI, though whether they constitute a novel biomarker or play a causative role is still unclear. One objective of this thesis was to answer this question.

1.4.7 Transgenic hGLO1 Mice

In this thesis we employed the use of a transgenic mouse model designed to over-express GLO1 to test the hypothesis that MG contributes to the loss of cardiac function and impaired remodeling post-MI (Geoffrion et al., 2014; Vulesevic et al., 2014; Vulesevic et al., 2016). This mouse was kindly provided by our collaborator Dr. Ross Milne. The transgenic mouse was created by cloning cDNA encoding the *hGLO1* gene with an amino terminal c-myc epitope tag into a Not1-digested PEP8 plasmid. Therefore, in this mouse, the *hGLO1* insert would be under the control of the murine pre-proendothelin promoter. PEP8hGLO1 was micro-injected into pronuclei of fertilized C57BL/6 mouse eggs which were then transferred into the oviducts of pseudo-pregnant foster mothers (Vulesevic et al., 2014).

Immunoreactivity of the c-myc-hGLO1 was detected in all tissues assessed in the *hGLO1*$^{+/-}$ mouse as reported in an earlier publication from our group (Vulesevic et al., 2014). Use of the preproendothelin promoter was reported to limit the expression of the target gene to the vascular compartment of mice (Harats et al., 1995)(Vulesevic et al., 2014). However, characterization of the hGLO1 mouse revealed that extracts of smooth muscle cells, bone marrow derived macrophages and isolated endothelial cells all demonstrated 5 fold greater activity of GLO1 than those from non-transgenic littermates (Vulesevic et al., 2014). In a separate report from our group, we additionally showed that whole-heart activity of GLO1 was increased by 1.8 fold, though immune-

reactivity of the c-myc tag was not detected in isolated cardiomyocytes (Vulesevic et al., 2016).

1.4.8 Modifications to the Extracellular Matrix

The ECM contributes considerably in governing wound repair (Schultz and Wysocki, 2009), through processes including inflammation, the reparatory response (Dobaczewski et al., 2010), and stem cell fate (Watt and Huck, 2013). At the same time, it also appears to be a primary target for modification in post-MI cardiac remodeling (Dobaczewski et al., 2010; Fedak et al., 2005). The composition of the ECM varies between tissues and is dynamic, constantly being remodeled by the cells it supports. Collagen I constitutes approximately 80% of the heart's ECM and the cardiac ECM is significantly altered in the pathogenesis of MI remodeling (Fedak et al., 2005).

Collagens constitute a major target for the accumulation of glycation adducts because they tend to be directly accessible to MG and other AGE precursors and because they exhibit extremely slow turnover (Monnier et al., 2005; Verzijl et al., 2000). Given that the cardiac ECM has an >10-fold longer turn-over than other cardiac proteins, carbonyl modifications may prove to be a central pathogenic mechanism in cardiovascular diseases (Hartog et al., 2007b; Talior-Volodarsky et al., 2012; Yuen et al., 2010). There are several studies pointing to the relevance of MG modifications to the ECM in CVD. For example, disruption of β1 integrin binding to collagen results in

apoptosis of cardiomyocytes, (Amin et al., 2011) and the domain on collagen required for β1 signaling is a primary target for MG-AGE modification (Dobler et al., 2006).

MG modification of the ECM may also affect the adhesion of endothelial cells, resulting in cell death and impaired microvasculature (Dobler et al., 2006). However, anoikis is not the only consequence of collagen glycation. The differentiation of fibroblast to myofibroblasts has been demonstrated to be influenced by glycated collagen *in vitro* (Yuen et al., 2010) and *in vivo* (Talior-Volodarsky et al., 2012). In diabetic cardiomyopathy, collagen glycation weakens integrin-collagen interactions promoting a compensatory expression of integrin alpha11 expression on fibroblasts through TGF-β2. This stimulates collagen synthesis and myofibroblast differentiation contributing to fibrosis and myocardial stiffening (Talior-Volodarsky et al., 2012; Wang et al., 2010). Therefore, it is conceivable that MG-AGEs may surface as key mediators of the pathogenesis of MI and intervening in their production may limit the extent of remodeling and abrogate some of the risk of CHF. It is likely then that this process is exacerbated in diabetic patients presenting with acute or chronic MI. Taken together, these findings indicate that loss of matrix interactions through AGE accumulation on key protein recognition sequences may be an important influence on the survival and function of cardiomyocytes and other cardiac cells post-MI.

1.5 Emerging Therapies for the Treatment of MI – Biomaterials

As indicated earlier, we are witnessing an increase in the prevalence of CHF despite significant improvements in early mortality post-MI. Therefore, there is an urgent need for therapies that can successfully stabilize the heart both functionally and biochemically to prevent the adverse remodeling that results in a dilated and functionally incapable heart. Given the complexity of the cellular and molecular events that characterize post-MI remodeling it is not difficult to imagine that this would challenge the translation of novel therapies required to treat this disease. This part of the thesis will discuss our attempt at designing a strategy to intervene in post-MI remodeling using an acellular injectable hydrogel biomaterial.

1.5.1 Biomaterials for the Treatment of Myocardial Infarction

Burdick et al. have pondered that "the therapeutic merit of regenerating myocardium as a treatment for MI seems obvious; but is it really?" (Burdick et al., 2013). Indeed, the majority of patients who experience MI have adequate cardiac function, and it is only with time that they experience the progressive loss of function and symptoms of CHF (Burdick et al., 2013). It is plausible that intervening early in the process of cardiac repair and remodeling could functionally stabilize the heart. This would serve to maintain the heart at a capacity that is compatible with a relatively healthy and fulfilling life and, thus potentially obviate the need for a regenerative therapy. Biomaterial therapies have emerged as such therapies and have shown promise in pre-clinical animal models. Clinical trials have begun with several alginate-based materials for MI

and HF and are showing promising early results (Anker et al., 2015; Frey et al., 2014; Mann et al., 2016; Ruvinov and Cohen, 2016).

Biomaterials may be composed of synthetic or natural components, may be delivered as acellular therapies or designed to deliver cells, and may be used as left ventricular (LV) restraints, cardiac patches or injectable hydrogels. Many excellent reviews exist on the use of biomaterials post-MI (Burdick et al., 2013; Johnson and Christman, 2013; Lister et al., 2016; Radhakrishnan et al., 2014; Tous et al., 2011) . This section will briefly review the use of injectable, acellular hydrogels.

1.5.2 Acellular, Injectable Hydrogels

Acellular, injectable hydrogels, many based on natural ECM components, are an emerging treatment modality for MI. Whereas many biomaterials were initially designed to act as fillers for tissue defects, they have evolved rapidly into increasingly complex therapies capable of interacting with local cells and tissues and altering the healing process after disease or injury (Figure 1.6) (Burdick et al., 2013). Many have been tested in clinically relevant models of MI and heart failure (Johnson and Christman, 2013; Radhakrishnan et al., 2014).

Several materials have been shown to improve or preserve cardiac function in rodent and swine MI models, as assessed by left ventricular ejection fraction (LVEF), and improved ventricular geometry such as end-diastolic (ED) or end-systolic (ES) diameters (Johnson and Christman, 2013; Radhakrishnan et al., 2014). Injectable hydrogels are

particularly attractive for cardiac applications owing to their ease of use and the possibility of minimally-invasive delivery to the infarcted myocardium. Additionally, naturally derived materials may prove beneficial over synthetic ones given their potential to interact with the host tissue and direct the repair response. Of course, one drawback may be that naturally derived materials often lack the mechanical properties to physically stabilize the wound (Huyer et al., 2015). Regardless, a number of injectable hydrogels have been shown to preserve cardiac function and dimensions potentially through modulating the host repair response, inflammation, mechanical properties or a combination thereof (Huyer et al., 2015; Rane and Christman, 2011). Given that post-MI cardiac remodeling is characterized by temporally sensitive events, the timing of material delivery post-injury would appear to be an important consideration, yet is often overlooked in study design (Huyer et al., 2015). Improperly timed delivery could result in an ineffective therapy or worse, it could exacerbate the pre-existing injury (Huyer et al., 2015). As MI involves distinct necrotic, inflammatory, proliferative and maturation phases, delineation of the ideal time of delivery is important to ensure optimal efficacy of the biomaterial therapy (Radhakrishnan et al., 2014). One aim of the work comprised in this thesis was to assess how the timing of delivery would affect the therapeutic benefit of a collagen-based injectable hydrogel post-MI (Blackburn et al., 2015).

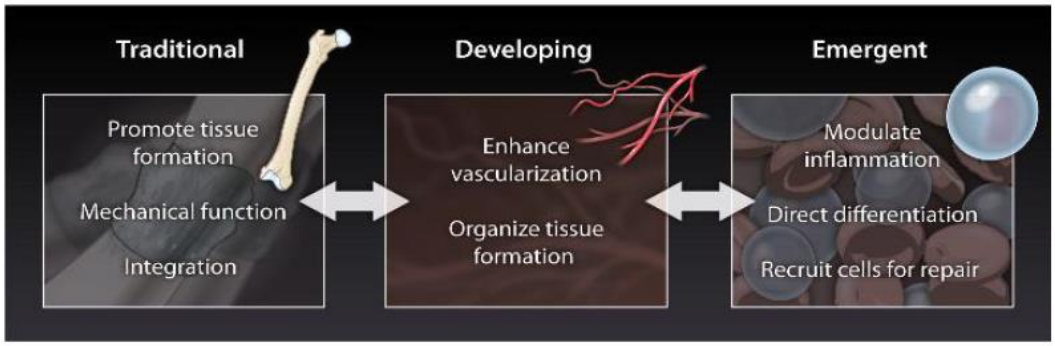
Traditional
Developing
Emergent
Promote tissue formation
Mechanical function
Integration
Enhance vascularization
Organize tissue formation
Modulate inflammation
Direct differentiation
Recruit cells for repair

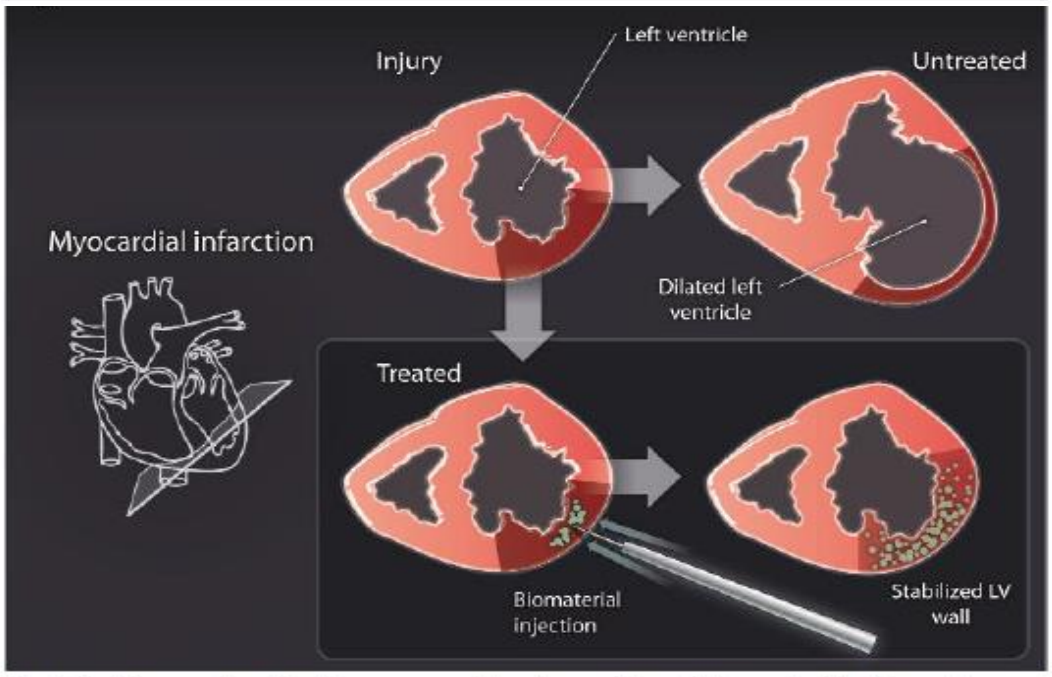
Left ventricle
Injury
Untreated
Myocardial infarction
Dilated left ventricle
Treated
Biomaterial injection
Stabilized LV wall

Figure 1.6. Acellular biomaterials for cardiac tissue repair. (Top) The evolution of acellular materials from traditional approaches of promoting tissue formation, improving mechanical function and host integration, to developing and emergent approaches of interacting with the host tissue repair response. Emerging methods may one day direct the differentiation of cells, recruit specific cells for repair and modulate inflammation. (Bottom) Injectable hydrogels delivered to the myocardium post-MI can functionally stabilize the infarcted LV wall preventing possible future LV dilatation and failure.

From Burdick, J.A., Mauck, R.L., Gorman, J.H., 3rd, and Gorman, R.C. (2013). Acellular biomaterials: an evolving alternative to cell-based therapies. Science translational medicine *5*, 176ps174. Reprinted with permission from AAAS

1.6 Thesis Objectives and Aims

The overall goal of this research was to clarify the role of MG and MG-AGEs in post-MI cardiac remodeling and to test biomaterial therapies that could functionally stabilize the heart through the promotion of wound healing responses and/or intervention on MG-mediated cardiac damage.

AIM 1 - Specifically, our first objective was to investigate MG effects post-MI. A transgenic mouse designed to over-express GLO1 was used to investigate a causative role for MG in the remodeling of the myocardium post-MI.

AIM 2 - Given the contribution of ECM disruption to adverse remodeling post-MI, the next objective was to assess whether an acellular collagen biomaterial, acting as an ECM replacement therapy, could preserve cardiac function and modulate the host response post-MI. Specifically, we sought: 1) to determine whether timing of administration affects the ability of a collagen matrix to improve cardiac function post-MI; and 2) to examine the mechanisms by which the matrix treatment mediates cardiac repair.

AIM 3 – The final objective of this thesis was to combine the injectable hydrogel therapy with a MG-reducing drug (Fisetin) to evaluate if a combined ECM replacement and dicarbonyl scavenger therapy would further serve to preserve cardiac function and geometry post-MI over either strategy alone.

1.7 Hypotheses

It was hypothesized that:

AIM 1 – MI stimulates the acute production of MG and that MG serves to impair post-MI cardiac repair. Intervening on MG production, through GLO1 over-expression, would preserve cardiac function and limit remodeling through improved post-MI cardiac repair.

AIM 2 – An acellular, injectable hydrogel biomaterial would preserve cardiac function and remodeling post-MI, and that delivering the material early post-MI would offer the most benefits.

AIM 3 – Combining the injectable hydrogel with an MG scavenger, Fisetin, would synergize to better preserve cardiac function post-MI vs. either therapy alone.

Chapter 2

Materials and Methods

2.1 Methods – Common

The following materials and methods are common to all the studies conducted in Chapter 3.

2.1.1 Experimental MI Model and Cardiac Echocardiography

All procedures were performed with the approval of the University of Ottawa Animal Care Committee and in accordance with the National Institutes of Health Guide for the Care and Use of Laboratory Animals. Experimental MI was induced in 7-8- weeks old female C57BL/J6 mice (Charles River Laboratories) as previously described (Ahmadi et al., 2014). Briefly, mice were anaesthetized using 2.5% isoflurane, intubated and kept under mechanical ventilation. A left-sided open thoracotomy was performed and the left anterior descending coronary artery was permanently ligated with a 7-0 silk suture 2mm below the tip of the left atrium. MI was confirmed by myocardial blanching in the region supplied by the artery. Short acting buprenorphine was administered at least an hour prior to surgery, and long-acting buprenorphine was administered subcutaneously immediately before surgery for peri-operative analgesia. Cardiac function was assessed by echocardiography on long-axis views with a Vevo770 system (VisualSonics) in B mode with the use of a 707B series real-time microvisualization (RMV) scanhead probe. Echocardiography tracings were performed using the manufacturer's supplied software.

2.1.2 Animal Studies Randomization & Blinding

All surgeries were performed by the same animal technician blinded to treatment allocation. Mice were assigned a code number associated with the study protocol but not treatment. The treatment delivered to each mouse was recorded and only revealed once the final functional and/or histological analyses were completed. Echocardiography tracings and histological assessments were all performed by members of the research team blinded to the treatment assignment.

2.1.3 Histology and Immunohistochemistry

For all histology and immunohistochemistry, hearts were collected, perfused with 2-3ml of saline, snap frozen in OCT and stored at -80°C. Slides were prepared with 8µm sections at different levels. Masson's trichrome or hematoxylin-phloxine saffron (HPS) staining was performed to measure relative final scar size by the midline-arc method, as previously described (Takagawa et al., 2007). Unless otherwise specified, all primary antibodies for immunohistochemistry were purchased from Abcam and all alexa fluor (488, 546) secondary antibodies from Invitrogen. To assess vascularization, tissue sections were stained with antibodies against CD31 (for endothelial cells; Santa Cruz Biotechnology) and α-SMA (for vascular smooth muscle cells). Cell death and apoptosis was identified using a TUNEL kit (Roche) and anti-active caspase 3 antibody, respectively, while cell proliferation was assessed with an anti-Ki67 antibody.

Additionally, Ly6G was used to stain for neutrophils, CD68 or F4/80 for macrophages, and F4/80+CD206 or F4/80+CD86 for M2 and M1 macrophages, respectively. Cell nuclei were stained with 4',6-diamidino-2-phenylindole (DAPI). Imaging was performed with a Zeiss Z1 fluorescence microscope and ZenBlue (2011-12) digital image software. For quantification, 6 random microscopic FOV of the infarct area (except where otherwise indicated) were counted per sample in a blinded fashion.

2.1.4 Statistical Analysis

Statistical analyses were performed using GraphPad Prism 7 software. Data is presented as mean ± standard error (SE). Unless otherwise specified, comparisons of data between multiple groups were performed by a one-way analysis of variance with a post-hoc Tukey test to establish differences between individual groups, while comparisons between two groups were analyzed using a two-tailed student's t-test. Statistical significance was given for $p<0.05$.

2.2 Methods – Aim 1

2.2.1 Transgenic hGlo1 Mice

Human GLO1 over-expressing mice (GLO1 mice) were bred on a C57/BLJ6 background, and carry a transgene encoding *hGlo1* with a cMyc epitope tag under the control of the preproendothelin-1 promoter, as previously reported (Vulesevic et al., 2014). This promoter is appropriate because it is highly expressed in cardiac vasculature and it is up-regulated in the infarcted heart (Harats et al., 1995; Tonnessen et al., 1998). All

experiments used mice hemizygous for the *hGlo1* transgene or their non-transgenic littermates. In whole heart, GLO1 mice showed a 1.8-fold increase in GLO1 activity (p=0.002; as measured by the rate of formation of S-D-lactoylglutathione from hemi-thioacetal), and no difference in the level of the GLO1 co-factor reduced glutathione (p=0.7), compared to non-transgenic littermates.

2.2.2 MG-derived AGE Determination

GLO1 and WT mice underwent surgical MI and tissue was harvested 6 hours later from the infarcted zone of the myocardium. Tissue from age-matched non-infarcted controls was also procured. Tissue was surgically micro-dissected and immediately snap frozen in liquid nitrogen and kept at -80^{o}C until required. Samples were prepared for analysis by LC/MS by sequential proteolytic digestion as previously described (Ahmed et al., 2002). Briefly, tissue was first mechanically homogenized using liquid nitrogen and/or other common methods. Once crushed, an approximately equal volume of QQ water was added to samples and samples were freeze (-80^{o}C) -thawed (thawed on ice) three times and then sonicated. Samples were kept at -80^{o}C until further processing. Prior to proteolytic digestion, sample protein concentrations were first assayed using the BCA method. For sample proteolytic digestion, samples were digested according to the following protocol:

- Day 1: 500ug of protein in 25uL, 10uL of internal standard (provided by PreventAGE Health Care, LLC), 5uL 2mg/ml pepsin (Sigma), and 25uL of 20mM HCl were added to

a 1mL digestion vial then mixed. Samples were purged with N_2, vortexed and incubated at 37°C for 24 hours.

- Day 2: 8uL of 65mM KOH, 25uL of 50mM KPO_4 with gentamicin, and 5uL of 2mg/mL Pronase (Sigma) were added to the vials and mixed. Samples were purged with N_2 and incubated for 24 hours at 37°C.
- Day 3-5: 5uL of 2mg/mL Aminopeptidase (Sigma), 5uL of 2mg/ml Prolidase (Sigma) were added to the vials and mixed. Samples were purged with N_2 and incubated at 37°C for 48 hours. Following the incubation period samples were transferred to cryo-vials for LC/MS.

LC/MS on the proteolytically digested samples was carried out at PreventAGE Health Care, LLC (Dartmouth Regional Technology Center, Lebanon, NH 03766 USA) as described (Beisswenger et al., 2014).

2.2.3 Histology and Immunohistochemistry

An anti-methylglyoxal-derived AGE antibody (MG-AGE 3D11; Cellbiolabs STA-011) and an anti-type I collagen antibody were used to identify MG-AGE modified collagen *in vivo,* as described (Talior-Volodarsky et al., 2012). Briefly, frozen tissue sections were fixed in acetone and washed with TBS-T. To reduce background, goat anti-mouse IgG (1:25 dilution) in 10% fetal bovine serum in PBS was used to block sections for 3h prior to incubating with the primary antibody overnight at 4°C.

2.2.4 Collagen Gels and Methylglyoxal Glycation

Collagen type I (1%; Nippon Ham) gels were prepared as previously described (Artym and Matsumoto, 2010). Gels were incubated overnight at 37°C with PBS or with 1mM MG (Sigma) (Figure 2.1). This concentration is effective at generating glycated collagen *in vitro* to an extent that is comparable to *in vivo* levels of glycated collagen in the ventricles of rats with diabetic cardiomyopathy (Talior-Volodarsky et al., 2012), thus demonstrating that 1mM MG is physiologically relevant. Glycation of the gel was confirmed by Western blot using a monoclonal antibody (1H7C6) against MG-H1 adducts (the major MG adducts), kindly provided by Drs. Xueliang Du and Michael Brownlee.

2.2.5 In Vitro MG-Modified Collagen and Peripheral Blood Mononuclear Cells (PBMCs)

Procedures for the isolation of human peripheral blood mononuclear cells (PBMCs) were approved by the Human Research Ethics Board of the University of Ottawa Heart Institute. With informed consent, total PBMCs were isolated from the blood of healthy volunteers, and cultured for 4 days on fibronectin, as previously described (Kuraitis et al., 2011). PBMCs were cultured on MG-modified or non-modified collagen gels in Endothelial Growth Medium-2 (EGM-2) with FBS, VEGF, R^3-IGF-1 and hEGF supplements (Lonza) at 37°C for 4 days, after which cells and/or conditioned media were collected. PBMCs were evaluated for viability and phenotype (by flow cytometry), adhesion, and angiogenesis.

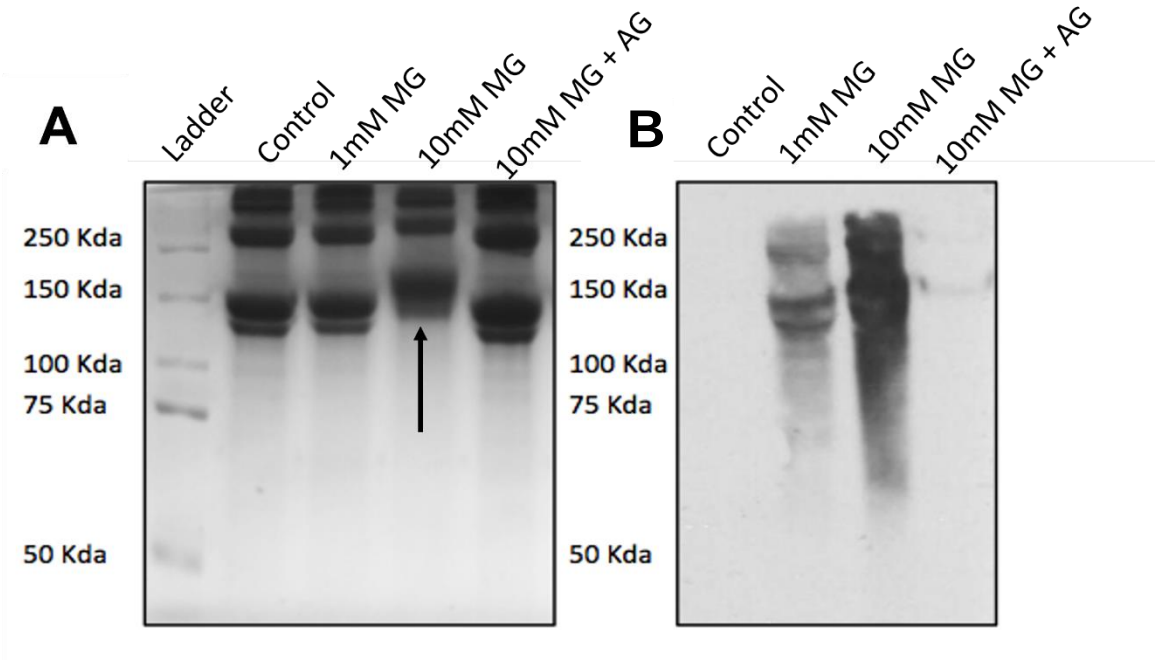

Figure 2.1 *In vitro* modification of collagen gels by MG. (Left) SDS-PAGE gels stained using Coomassie blue showing the shift in migration of collagen modified by methylglyoxal (MG) *in vitro*. Aminoguanidine (AG) is an MG scavenger and served as a control. (B) Western blot of collagen modified by MG.

2.2.6 Flow Cytometry

For the in vivo work, flow cytometry was performed on circulating peripheral blood mononuclear cells collected by saphenous vein bleeds pre-operatively and at Days 2, 7, and 28 post-surgery, as described previously (Vulesevic et al., 2014). Briefly, the mononuclear cell fraction was labelled with antibodies against the following antigens: c-kit (Southern Biotech, Birmingham, USA), CD45 (BD Biosciences, Mississauga, Canada), and flk-1 (mouse vascular endothelial growth factor receptor-2; eBioscience, San Diego, USA), and analysed with a FACSAria flow cytometer (BD Biosciences).

For in vitro studies, flow cytometry was performed as described previously (Kuraitis et al., 2011). Briefly, PBMC phenotype was assessed at baseline and after 4 days culture on collagen gel (± MG modification). Cells were lifted and stained for CD31, CD34, CD133 and CD144 for 30 min at 4^{o}C in HBSS, then washed and re-suspended in 0.5% bovine serum albumin in PBS for immediate analysis by flow cytometry with a FACSAria™ (BD Biosciences). Antibodies used were: CD31-FITC (Beckman Coulter), CD34-PE-Cy7 (eBioscience), CD133-APC (Miltenyi Biotec), CD144-PE (Beckman Coulter) with matched Isotype controls. All data was analyzed using FACSDiva software.

2.2.7 Circulating Angiogenic Cell (CAC) Viability, Chemotaxis and Adhesion

For viability, PBMCs were cultured on collagen gels (± MG modification) for 2 days under serum deprivation and hypoxic conditions as described (Kuraitis et al., 2011). Cells were then stained for CD133, CD34, CD31, CD144 and 7-aminoactonomycin (7-AAD) and

analyzed by flow cytometry. For adhesion, 5×10^5 DAPI-stained PBMCs were seeded on MG-modified or non-modified collagen gels for 60 min, fixed with 4% paraformaldehyde (PFA) and counted per FOV in a blinded fashion (20× magnification). For chemotaxis, PBMCs on the 2 collagen gel substrates were serum starved overnight and placed in Transwell® Permeable Supports (Corning), with 0.05µg/ml of VEGF (Cedarlane) in endothelial basal media (EBM) as the migratory stimulus, as previously described (Kuraitis et al., 2011). After overnight culture, PBMCs were fixed with PFA and the number of migrating PBMCs was quantified.

2.2.8 In vitro HUVEC ECMatrix™ Angiogenesis Assay

PBMCs were stained with DAPI and human umbilical vein endothelial cells (HUVECs; Invitrogen) were labeled with CellTracker Orange™ (Invitrogen) prior to the *in vitro* ECMatrix™ assay (Millipore). HUVECs (5×10^3 cells) were seeded with PBMCs (5×10^3 cells; from collagen gel ±MG modification) in µ-slide angiogenesis slides (Ibidi) coated with 10µl of ECMatrix™. The number of $DAPI^+$ PBMCs contributing to structure formation (co-localization of DAPI and CellTracker™ Orange) and total tubule length were quantified per FOV (10× magnification). Each condition was assayed in triplicate, with a minimum of n=4 per condition.

2.3 Methods – Aim 2

2.3.1 Study Design

A chronic LAD permanent occlusion MI model was used. Three different delivery time-points were tested: 3h, 7d and 14d post-MI (Fig. 3.7A). The primary end-point was the effect of treatment on cardiac function (%LVEF) at 4 weeks post-treatment. Following this determination, mechanisms underlying the observed therapeutic benefits were investigated through histology, immunohistochemistry and molecular analyses. Further follow-up analysis of the 14d treatment cohort was not pursued due to lack of efficacy.

2.3.2 Matrix Preparation and Injection

Preparation of the matrix has been described previously (Kuraitis et al., 2013). Briefly, 1M 2-(N-morpholino) ethanesulfonic acid (MES) buffer (pH 6.0) containing 1:1 (molar equivalent) cross-linking mixture of N-ethyl-N-(3-dimethylaminopropyl) carbodiimide and N-hydroxysuccinimide (EDC/NHS; 13mM) was added to 0.375% rat tail collagen type I (w/v, BD Biosciences) with 100 µL of 40% chondroitin sulfate-C (CS-C; w/v) (Wako Chemicals) and kept on ice. The final pH was adjusted to 7.2–7.4 using NaOH. The collagen-based matrices are liquid at the time of injection but upon exposure to physiological temperatures (~37°C), they solidify into a gel. Using an ultra-sound guided (long axis view) closed-chest procedure, mice were assigned to randomly receive one of the following treatments (3-4 injections; 50 µL total) into the infarct / border

zone: 1) phosphate buffered saline (PBS) or 2) injectable matrix, delivered at 3h, 7d or 14d post-MI (Fig. 3.7 A). The syringe was secured in a micromanipulator (VisualSonics), and both the needle and RMV scanhead probe were aligned along the heart long axis before the injection procedure. The needle was retracted from the ultrasound field-of-view (FOV) with the use of the micromanipulator until the needle tip was in the desired location within the myocardium. The treatment mixture was then injected into the border and infarct zones of the anterior wall. Mice were observed for 4 weeks post-treatment, after which they were sacrificed for histological assessment. Subsets of mice in the 3h cohort were sacrificed at 2d or 3 months post-treatment to assess the short-term effect of the treatment on neovascularization, inflammation and cell death, and the effect of treatment on long-term functional preservation, respectively.

2.3.3 Cytokine Array

At 4 weeks post-treatment, infarct tissue from a subset of mice in the 3h and 7d treatment groups (PBS and matrix) was isolated for cytokine array (Raybiotech). The tissue was micro-dissected from freshly harvested hearts and frozen with liquid nitrogen until use. Protein was extracted using the lysis buffer provided with the cytokine array kit. The concentration of the protein in each sample was quantified using a BCA Kit (Thermo scientific) and appropriately normalized. Fluorescence intensity was assessed and cytokine expression was quantified and normalized using the manufacturer's supplied software.

2.3.4 Bone Marrow-derived Macrophage Culture

Bone marrow-derived macrophages (BMDMs) were generated from the bone marrow of 7-9 week old female mice tibia, as previously described (Cecchini et al., 1987). Matrix-coated 6-well plates were prepared and cells were maintained in DMEM with 10% FBS, 15% L929 media containing M-CSF on standard tissue culture polystyrene (TCPS) or collagen matrices for one week. To assess the effect of matrix interaction on the secretory profile of BMDMs, supernatants were collected after one week. Produced cytokines were quantified in culture supernatants using the Mouse Inflammation Array (Raybiotech), following procedures as described above.

2.4 Methods – Aim 3

2.4.1 HA-PBLG-LA and PEG-PolyC Polymers

The hyaluronic acid-g-poly(c-benzyl-L-glutamate)-lipoic acid (HA-PBLG-LA) graft copolymer was kindly provided by Dr. Deng and Dr. Zhong (Biomedical Polymer Laboratory, Soochow University, Suzhou, People's Republic of China). A description of the synthesis of the polymer has been previously reported (Sun et al., 2016). The polyethylene glycol polycarbonate (PEG-polyC) polymer was also kindly provided by Drs. Deng and Zhong.

2.4.2 Loading Fisetin into HA-PBLG-LA or PEG-PolyC Nanoparticles

Fisetin loading into HA-PBLG-LA or PEG-PolyC nanoparticles was accomplished by dropwise addition of a DMSO solution of HA-PBLG-LA (100µL, 5mg/mL) or PEG-PolyC (100µL, 5mg/mL) and Fisetin (10µL, 10mg/mL) to phosphate buffer (PB) (900µL, 10mM, pH7.4) under constant stirring and room temperature, as described (Sun et al., 2016). The size and poly-dispersion index (PDI) of NPs was evaluated using dynamic light scattering (DLS) following large volume dilution using a Zetasizer (Malvern Instruments).

2.4.3 Fisetin Release Study

Fisetin at a low (40µM) or high (80µM) concentration was added to the collagen hydrogel, prepared as described in section 2.3.2. 200µL of hydrogel was plated in 12 well dishes and 1 mL release media was added to each well. At pre-defined intervals (0, 30, 120, 240, 360 and 1440 minutes), 1 mL solutions containing Fisetin were extracted. Then equal volumes of the extracted solution were mixed in a 1 cm path length cuvette with Triton X-100 (0.52 mM; Sigma) in a 1:1 ratio to maximize the emission intensity fluorescence of Fisetin, which has been proven to be dependent on the polarity of the solution showing maximum intensities under hydrophobic conditions (Guharay et al., 1999). The fluorescence of the resultant solution was measured by a spectrofluorometer. Briefly, the excitation was performed with a 365 nm LED light source and the emission was collected at an angle of 90° making use of an optic fiber (Ocean Optics) and a Flame Miniature Spectrometer (Ocean Optics) as detector. The

emission wavelength was followed at 540 nm. Final concentrations were determined using a calibration curve of Fisetin prepared under the same experimental conditions. All measurements were performed at 25°C.

2.4.4 In vitro Cytotoxicity Assay

The cytotoxicity of Fisetin was assessed using human umbilical vein endothelial cells (HUVECs). Cells were maintained in M200 media supplemented with LS-GS (Gibco) until 80% confluency and then $1x10^5$ cells were plated in wells of a 6 well plate for 24 hours. Cells were then incubated in 0.1% DSMO (control), 10µM, 50µM, 100µM, or 500µM Fisetin for 48 hours at 37°C. Cells were subsequently lifted and stained for 7-AAD to assess viability using flow cytometry as described in 2.2.6.

2.4.5 In vitro HUVEC ECMatrix™ Angiogenesis Assay

Similar to the cytotoxicity assay, HUVECs were pre-treated with 0.1% DSMO (control), 10µM, 50µM, 100µM, or 500µM Fisetin for 48 hours at 37°C. Cells were lifted and $5x10^3$ cells/ well were plated in *in vitro* angiogenesis µ-slides (IBIDI) coated with ECMatrix™ (Millipore). As described previously, total network length was measured using ImageJ software.

2.4.6 Fisetin Hydrogel Preparation and Injection

Preparation of the matrix was performed as described in section 2.3.2 (Kuraitis et al., 2013). In addition, for the combined Fisetin-hydrogel therapy, Fisetin was added during

hydrogel preparation to a final concentration of 80µM in the hydrogel. Mice receiving the Fisetin hydrogel or Fisetin alone therapies received a total of approximately 1.14ug of Fisetin. At 3 hours post-MI, mice were assigned to randomly receive one of the following treatments (3-4 injections; 50 µL total) into the infarct / border zone: 1) phosphate buffered saline (PBS); 2) injectable matrix; 3) Fisetin alone; or 4) the combined Fisetin-hydrogel. Injections were performed using an ultrasound-guided procedure as described in 2.3.2. Mice were observed for 5 weeks post-treatment, after which they were sacrificed for histological assessment. Infarct size, vessel density and macrophage infiltration were all assessed using histological methods as described in

Chapter 3

Results

3.1 Glyoxalase-1 over-expression improves cardiac remodeling and function post-myocardial infarction

Brief Introduction to AIM 1

In the first aim of this thesis, we endeavored to determine the role of MG and MG-AGEs in the development of cardiac remodeling post-MI. To this end, we employed a transgenic mouse that over-expresses GLO1 to determine if reducing MG and MG-AGEs would positively impact cardiac remodeling and preserve cardiac function post-infarction.

Contributions of Authors

Most of the Immunohistochemistry, flow cytometry, mass spectrometry sample preparation, *in vitro* assays and echocardiography were conducted by me. A small number of the initial surgeries and echocardiography was conducted by Ali Ahmadi. The MI surgeries and other relevant animal-related procedures were performed by Rick Seymour. Aleksandra Ostojic assisted with some immohistochemistry. Branka Vulesevic assisted with sample preparation and digestion for mass spectrometry, which was sent to PREVENTAGE Healthcare for measurement. Brian McNeill assisted with flow cytometry and animal echocardiography. Data analysis and writing of the manuscript were conducted by me and assisted by Branka Vulesevic and Brian McNeill, and under the supervision of Dr. Erik Suuronen.

3.1.1 MI Stimulates MG-AGE production and GLO1 prevents MG-AGE accumulation

To assess whether MI stimulates the production of MG-AGEs, we harvested myocardial tissue from GLO1 over-expressing mice and their WT littermates at baseline (no MI) and 6h post-MI (infarct and peri-infarct) and used mass spectrometry to measure AGE content: 1) MG-H1, 2) the MG-derived carboxyethyl-lysine (CEL) and 3) the glyoxal-derived carboxymethyl-lysine (CML)). At 6h post-MI, there was a 52% increase in myocardial MG-H1 content in WT mice compared to non-infarct controls, whereas MG-H1 levels were unchanged in GLO1 mice post-MI compared to GLO1 and WT mice at baseline (baseline = healthy animals/no MI) (Fig. 3.1*A*). In other words, MI stimulated the production and/or accumulation of MG derived glycation adducts. For CML and CEL, myocardial levels did not change in WT mice after MI; but in post-MI GLO1 mice their abundance was reduced compared to non-infarcted hearts (Fig. 3.1 *B* and *C*). To visualize MG-H1 accumulation, immunohistochemistry was performed on myocardial tissue sections of GLO1 and WT mice at 4 weeks post-MI. Diffuse MG-H1 staining was observed within the granulation tissue and in arterioles and cardiomyocytes of the infarct scar; however, less MG-H1 staining intensity was observed in GLO1 compared to WT mice (Fig. 3.1*D*). Therefore, it appears that MI acutely stimulates the production of MG-AGEs and their presence persists in the myocardium for up to 4 weeks.

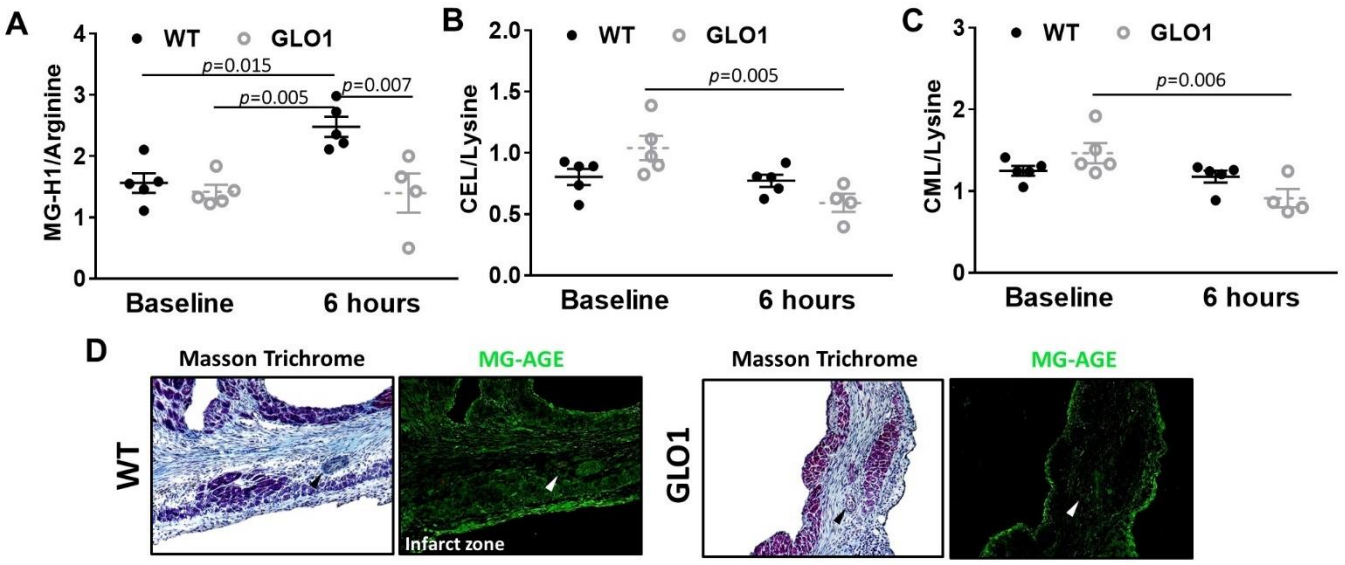

Figure 3.1 MG and AGEs accumulate in the myocardium post-MI. (A-C) Levels of the AGEs (A) MG-H1, (B) CEL and (C) CML in the infarct tissue of mice at 6h post-MI measured by LC/MS (n=4-5). (D) Masson-Trichrome and MG-AGE stained serial tissue sections at 28d post-MI. Arrowheads indicate arterioles. Data are presented as mean ± SEM. (A-C) Analyzed using 2-way ANOVA with Tukey post-hoc test.

3.1.2 GLO1 Over-Expression Preserves Cardiac Function

Since we established that MI stimulates the production of MG and MG-AGEs, our next goal was to determine if preventing AGE accumulation would be beneficial to cardiac function post-MI. We found that reducing MG-AGE levels in the myocardium post-MI (via GLO1 over-expression) significantly limited loss of cardiac function. Notably, echocardiography revealed greater left ventricular ejection fraction (LVEF) in GLO1 mice compared to WT mice at both 1 weeks and 4 weeks post-MI (Fig. 3.2*A*). A higher % fractional area change (%FAC), a reduction in end-systolic volumes (ESV), and a trend towards lower end-diastolic volumes (EDV) were also observed in GLO1 mice at 4 weeks post-MI (Fig. 3.2 *B-D*). There were no differences in cardiac output (CO), LV mass and heart rate between GLO1 and WT mice at 4 weeks post-MI (Fig. 3.2 *E-G*). Together, these results demonstrate that MG-AGEs are produced and accumulate in the post-MI myocardium, and that GLO1 over-expression can prevent their accumulation and limit the loss of cardiac function.

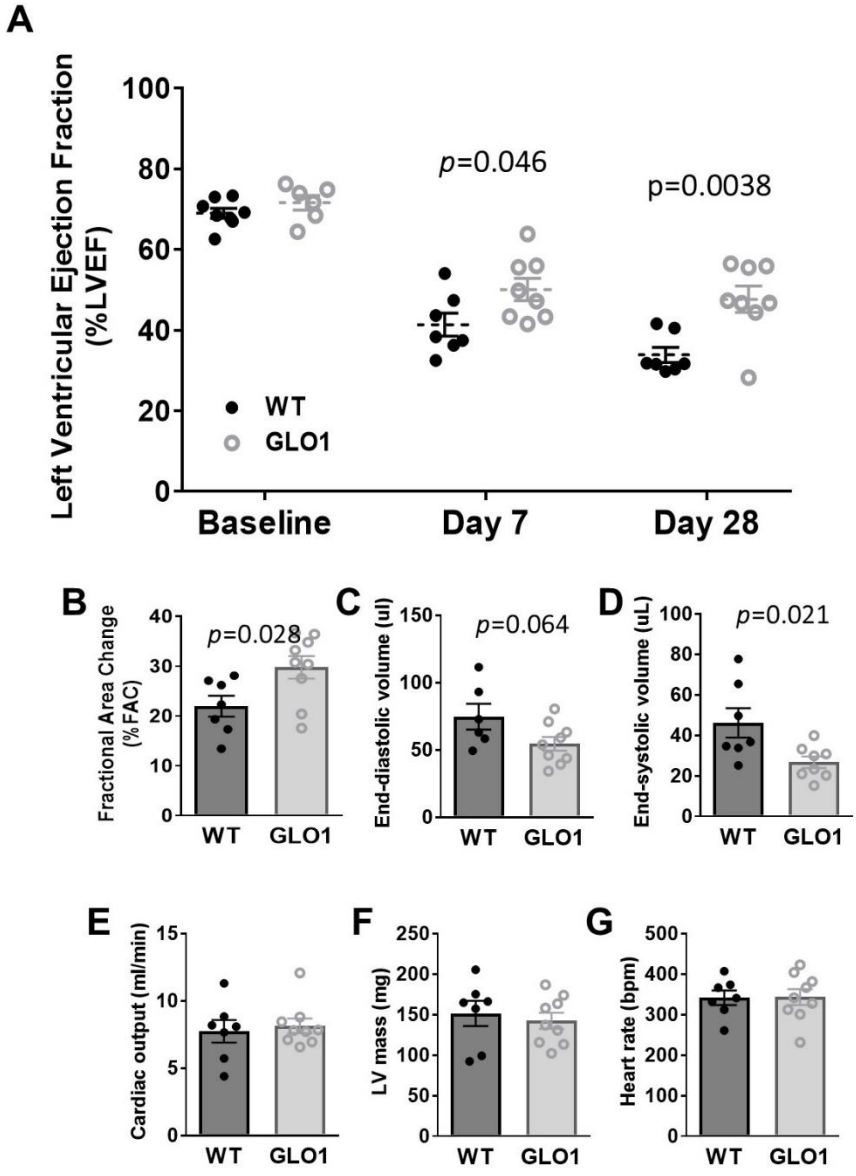

Figure 3.2. Preventing MG-AGE accumulation through GLO1 over-expression preserves cardiac geometry and function. Serial echocardiography assessment of (A) LVEF at baseline (no MI), 7 and 28 days post-MI; and 28 day post-MI assessment of (B) fractional area change, (C) end-diastolic volume, (D) end-systolic volume, (E) cardiac output, (F) LV mass, and (G) heart rate in WT and GLO1 mice at 28d post-MI (GLO1 n=8, WT n=7). Data are presented as mean ± SEM. (A) Analyzed using 2-way ANOVA with Bonferroni correction; (B-G) Analyzed using student's two-tailed t-test.

3.1.3 GLO1 Over-Expression Reduces Scar Size and Cell Death

We next focused on the effects of MG-AGEs on cardiac remodeling and cell death. By Masson Trichrome staining, which can be used to visualize collagen, we found that GLO1 mice had a reduced final scar size compared to WT mice at 4 weeks post-MI (Fig. 3.3 *A* and *B*). GLO1 over-expression also reduced on-going cell death within the myocardium (Fig. 3.3 *C*-*G*). At 4 weeks post-MI, less apoptotic active caspase-3$^+$ cardiomyocytes were present in the infarct and border-zones of GLO1 mice compared to WT littermates (Fig. 3.3*C*), and TUNEL staining confirmed the reduced cardiomyocyte cell death in GLO1 mice (Fig. 3.3*D*). The number of TUNEL$^+$ non-cardiomyocytes was also reduced in GLO1 vs. WT mice (Fig. 3.3*E*). Overall, GLO1 over-expression reduced final scar size at 4 weeks post-MI and reduced on-going cell death in the myocardium.

3.1.4 Vascular Density and c-kit$^+$ Cell Recruitment is Enhanced in GLO1 mice Post-MI

In diabetes, MG has been shown to impair angiogenesis (Dobler et al., 2006); therefore, we assessed vascular density in the hearts of GLO1 and WT mice to determine if MG played a similar role post-MI. In non-infarcted hearts, no difference was observed in vascular density between GLO1 and WT mice (data not shown). However, at 4 weeks post-MI, GLO1 mice had a greater number of CD31$^+$ capillaries and α-SMA$^+$ arterioles compared to WT (Fig. 3.4 *A*-*C*). To understand the mechanism, we focused our attention on the bone marrow (BM) repair response. Others have shown that c-kit$^+$ cells recruited from the BM play a major role in vascular repair post-MI (Fadini et al., 2012; Fazel et al.,

2006). Moreover, we have previously reported that GLO1 overexpression in the BM can reverse defective neovascularization in diabetic mice (Vulesevic et al., 2014). To determine the effect of GLO1 on the BM response post-MI, we evaluated the presence of c-kit$^+$ cells in the myocardium using immunohistochemistry (Fig. 3.4 *D-H*). We found that GLO1 mice had more arterioles with c-kit$^+$ cells incorporated around the vessel vs. WT mice (Fig. 3.4*D*), and the number of c-kit$^+$ cells that were localized within these arterioles was increased in GLO1 mice (Fig. 3.4*E*). The number of c-kit$^+$ cells that co-stained with endothelial marker CD31$^+$ was greater for GLO1 mice vs. WT (Fig. 3.4*F*), as was the overall number of c-kit$^+$ cells recruited to the myocardium (Fig. 3.4*G*). Additionally, we collected peripheral blood mononuclear cells (PBMCs) from mice over time (at 0d, 2d, 7d and 28d post-MI) and assessed the mobilization of c-kit$^+$, c-kit$^+$VEGFR2$^+$CD45$^-$ and c-kit$^+$VEGFR2$^+$CD45$^+$ cells. There was a trend for more c-kit$^+$ and c-kit$^+$VEGFR2$^+$CD45$^-$ cells at 2d and 7d post-MI in GLO1 mice compared to WT (Fig. 3.4 *D* and *E*), while the number of circulating c-kit$^+$VEGFR2$^+$CD45$^+$ cells at 7d was significantly greater in GLO1 mice compared to WT (Fig. 3.4*F*). Together, these results suggest that GLO1 over-expression promotes post-MI neovascularization possibly through superior mobilization, homing and/or survival of c-kit$^+$ cells.

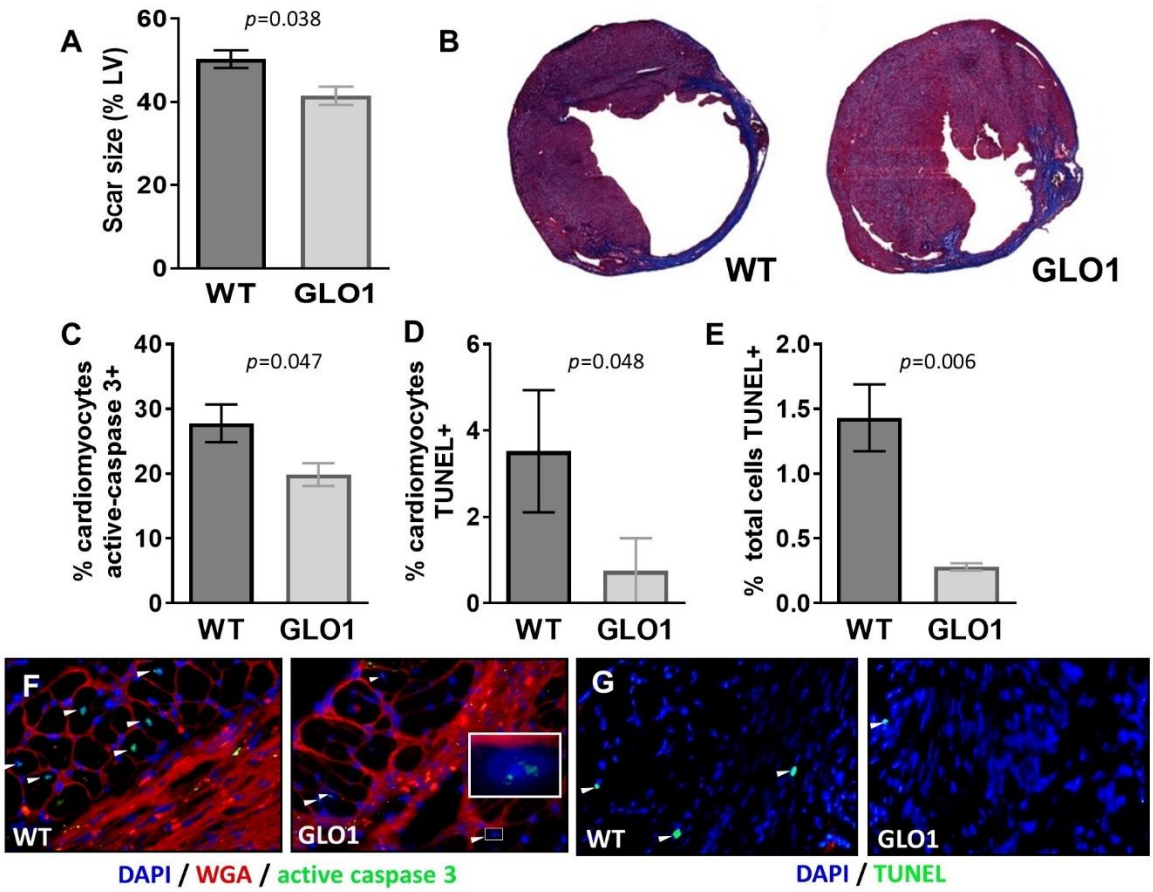

Figure 3.3. GLO1 over-expression reduces infarct scar size and cell death in mice post-MI. (A) Scar size in GLO1 and WT mice at 28d post-MI (n=5). (B) Masson-trichrome stained tissue sections at 28d post-MI. Proportion of (C) apoptotic active caspase 3+ cardiomyocytes, (D) TUNEL+ cardiomyocytes, and (E) TUNEL+ non-cardiomyocyte cells in tissue sections at 28d post-MI, determined by immunohistochemistry (n=5). (F) Representative images of apoptotic cardiomyocytes (active caspase 3+, green, arrowheads) in WT and GLO1 mice (WGA, wheat-germ agglutinin). (G) TUNEL staining (green, arrowheads) of non-cardiomyocyte cells. Data are presented as mean ± SEM. Analyzed using student's two-tailed t-test.

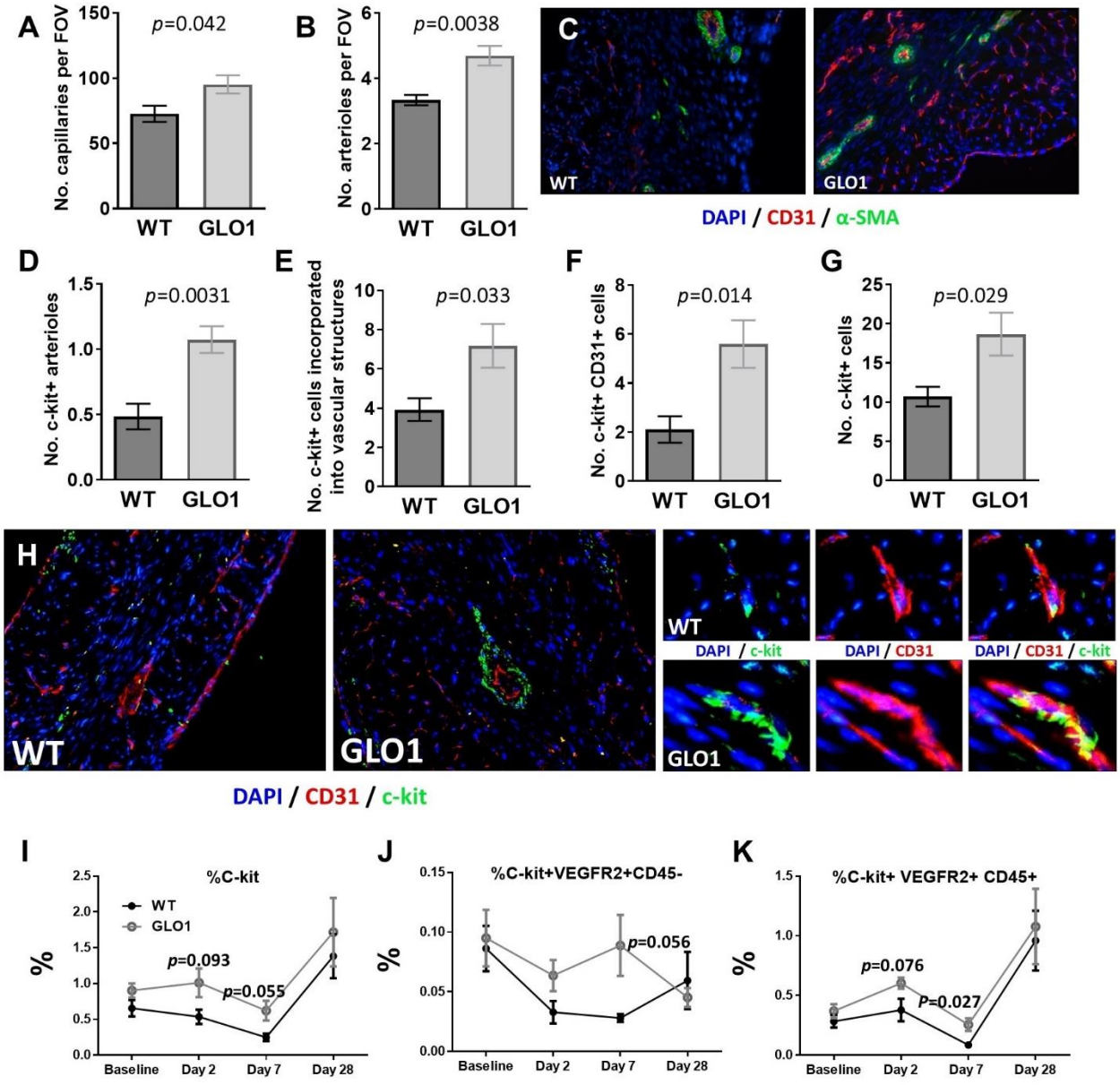

Figure. 3.4. GLO1 over-expression increases vascular density, and recruitment and vascular contribution of c-kit+ cells in the MI heart. (A and B) Number of capillaries (CD31+) and arterioles (α-SMA+CD31+) by immunohistochemistry (n=5). (C) Fluorescence microscopy images of α-SMA+ arterioles (green) and CD31+ capillaries (red). The number of (D) arterioles containing c-kit+ cells, (E) c-kit+ cells incorporated into arterioles, (F) c-kit+CD31+ cells, and (G) total number of c-kit+ in the myocardium at 28d post-MI (n=5). (H) Left panels: Images of recruited c-kit+ cells (green) co-stained with CD31 (red). Right panels: Higher magnification images. (I-K) Percentage of PBMCs in the peripheral circulation that are c-kit+, c-kit+VEGFR2+CD45- and c-kit+VEGFR2+CD45+ over a period of 28d post-MI assessed by flow cytometry (n=3-5). Data are presented as mean ± SEM. (A-G) Analyzed using student's two-tailed t-test. (I-K) Analyzed using 2-way ANOVA with Bonferroni correction.

3.1.5 MG Modification of ECM Proteins Impairs the Angiogenic Properties of PBMCs

The ECM undergoes extensive remodeling post-MI and the deposited scar consists mainly of type I collagen, which is a major target for MG-mediated glycation (Francis-Sedlak et al., 2010; Talior-Volodarsky et al., 2012). Thus, we sought to assess MG modification of type I collagen in the infarcted myocardium and to explore how MG-modified collagen affects angiogenic BM cell function. By fluorescence immunohistochemistry, tissue sections from 28d post-MI were co-stained for MG-H1 and type I collagen. Prominent MG-H1 accumulation was observed surrounding arterioles in the border-zone of the infarcted myocardium (Fig. 3.5*A*). Notably, greater co-localization of MG-H1 and collagen I staining, particularly surrounding the arterioles, was qualitatively observed in WT compared to GLO1 mice (Fig. 3.5*A*).

Collagen glycation has been shown to impair neovascularization in collagen gels *in vitro* and *in vivo* (Francis-Sedlak et al., 2010). Based on this literature and our *in vivo* observations of GLO1 over-expression effects on MG-AGEs, collagen and PBMCs, we performed some *in vitro* experiments to investigate how MG-modified collagen may affect the phenotype and function of PBMCs recruited to the heart post-MI. For clinical relevance, human PBMCs were cultured on MG-modified or non-modified type I collagen. Exposure to MG-modified collagen had no effect on their chemotactic response towards a gradient of vascular endothelial growth factor (VEGF; data not shown); however, fewer PBMCs were capable of adhering to MG-modified collagen vs. non-modified collagen (Fig. 3.5*B*). To evaluate if the interaction between MG-modified collagen and cells would impair angiogenic potential, PBMCs from either substrate (MG-

modified or non-modified collagen) were added together with human umbilical vein endothelial cells (HUVECs) in an angiogenesis assay. With PBMCs from the MG-modified collagen there was reduced total capillary-like network length and less of these PBMCs incorporated into capillary-like structures compared to PBMCs from non-modified collagen (Fig. 3.5 *C-E*). Therefore, the interaction of angiogenic BM cells with MG-modified collagen reduces their angiogenic potential, which appears consistent with our *in vivo* observations.

We next subjected cells to apoptosis-inducing conditions similar to myocardial ischemia (serum/growth factor deprivation and hypoxia). Subjecting cells to apoptotic conditions for 2d did not affect the overall viability of PBMCs, although the endothelial cell fraction ($CD31^+$, $CD144^+$ and $CD31^+CD144^+$ cells) from MG-modified collagen exhibited reduced survival compared to non-modified collagen culture (Fig. 3.6 *A-C*).

We also investigated if MG-modified collagen affected the putative $CD133^+$ and $CD34^+$ progenitor cell subpopulations that participate in post-natal vasculogenesis (Fadini et al., 2012). There was reduced viability of $CD34^+$ cells and $CD133^+$ cells in PBMCs cultured on MG-modified collagen under apoptotic conditions (Fig. 3.6 *D* and *E*). When cultured for 4d under normal conditions, PBMCs on MG-modified collagen had a reduced proportion of $CD34^+$ and $CD133^+$ cells compared to non-modified collagen culture suggesting loss of this phenotype (Fig. 3.6 *F* and *G*). Together these experiments highlight potential negative effects that glycated collagen may have on the angiogenic potency of PBMCs.

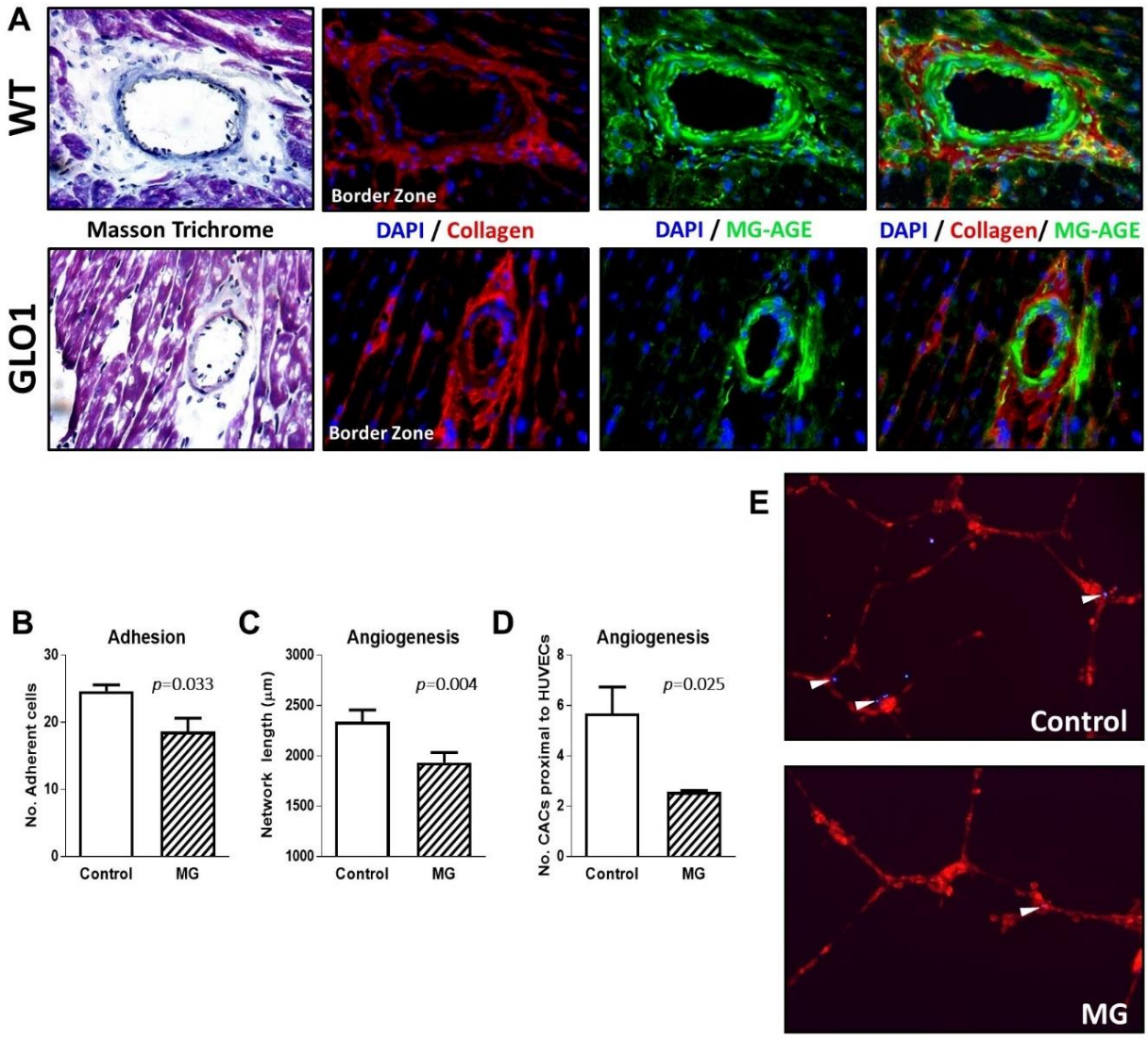

Figure 3.5. MG glycates collagen in vivo and impairs pro-angiogenic properties of cultured human PBMCS in vitro. (A) Masson-Trichrome and immunofluorescence images (MG-AGE and collagen type I) of the MI border zone. (B) Number of human PBMCs adhered to control (non-modified collagen) and MG-modified collagen after 60min in vitro (n=4). (C) Total network length, (D) number of PBMCs proximal to HUVEC structures, and (E) representative images of an angiogenesis assay using HUVECs co-cultured with PBMCs from control or MG-modified collagen culture (PBMCs stained blue and HUVECs orange; n=5). Data are presented as mean ± SEM. Analyzed using student's two-tailed t-test.

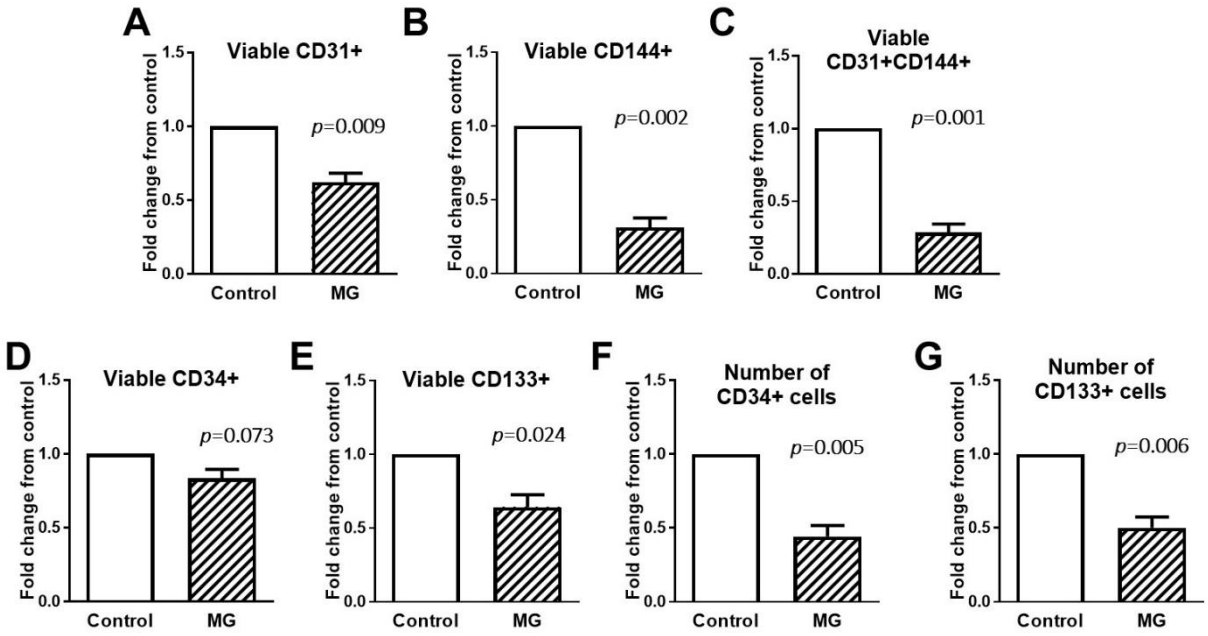

Figure 3.6. MG-modified collagen impairs cell survival and phenotype in vitro. (A-E) Viability of the CD31+, CD144+, CD31+CD144+, CD34+ and CD133+ fractions of PBMCs cultured on control or MG-modified collagen and subjected to apoptotic conditions (n=5). (F and G) Number of CD34+ and CD133+ cells after PBMCs were cultured on control or MG-modified collagen for 4d (n=5). Data are presented as mean ± SEM. Analyzed using ratio-paired two-tailed t-test.

3.2 Timing underpins the benefits associated with injectable collagen biomaterial therapy for the treatment of myocardial infarction

Published work. Reference: *N.J.R Blackburn et al. Biomaterials 39 (2015) 182-192*

Brief Introduction to AIM 2

In the first aim of this thesis we confirmed that MI stimulates the production of MG-AGEs and that limiting their accumulation mitigates functional loss and cardiac remodeling post-MI. This is likely due to several mechanisms, though ECM modification and disruption (for which collagen is a main target) may be a significant contributor. Therefore, the next goal of our work was to determine if a collagen-based biomaterial could serve as a replacement and/or protective therapy to limit post-MI remodeling and loss of cardiac function. In addition, given that the post-MI heart undergoes complex and dynamic changes that are time-dependent, we sought to determine *when* the optimal time to deliver the biomaterial therapy is. Specifically, our goal was to: 1) assess the potential for our collagen biomaterial to preserve cardiac function and anatomy post-MI; 2) determine when post-MI is the optimal time to deliver the therapy and achieve the best results; and 3) understand how the therapy confers its beneficial effects.

Contributions of Authors

Animal work was performed by me and Tanja Sofrenovic. I performed all experiments related the day 0 treated animals and some follow up day 7 animals. Day 7 and 14 time-points were performed by Tanja Sofrenovic. Cardiac echocardiography, immunohistochemistry and cytokine arrays were similarly divided between Tanja Sofrenovic and me for the initial 3 time-point comparison. MI surgeries were performed by Rick Seymour and Ali Ahmadi and echo-guided cardiac injections were performed by Rick Seymour and Brian McNeill. *In vitro* bone marrow derived macrophage culture and cytokine secretion assessment by cytokine array was performed by Drew Kuraitis. All 2-day end-point and 12-week end-point experiments were performed by me. Study design, data analysis and manuscript preparation was conducted by Dr. Erik Suuronen and myself.

3.2.1 Delivery Timing Influences the Efficacy of Collagen-based Hydrogel Therapy for MI

Our first objective for this study was to determine the impact of delivery timing on the preservation of cardiac function post-MI. Therefore, we surgically induced MI by ligating the left anterior descending coronary artery in mice and then randomly assigned the animals for 1) treatment type (collagen matrix or PBS control) and 2) treatment timing (3 hours, 7 days or 14 days post-MI) (Fig. 3.7 A). We did not observe differences in mortality between PBS and Matrix treated animals at any of the delivery time-points assessed. Indeed, 100% of the animals survived the initial MI surgery and 91%, 86% and 83% of the animals survived the 3 hour, 7-day and 14-day treatment time-points. Cardiac function (%LVEF) was assessed using echocardiography at baseline (post-MI / pre-treatment) and at 4 weeks post-treatment (Fig. 3.7 A).

We found that efficacy of the material in preserving cardiac function post-MI was dependent on when the material was delivered post-MI. Figure 3.7 B shows cardiac function (%LVEF) assessed at 28 days post-treatment for each animal cohort (animals treated at 3 hours, 7 or 14 days post-MI) along with their respective PBS treated controls. Mice receiving the material at 14 days post-MI showed no preservation or improvement in cardiac function compared to PBS treated mice (Fig. 3.7 B). Mice having received the material at 7 days post-MI showed a preservation in their function (%LVEF) compared to those treated with PBS (Fig. 3.7 B). An improvement in function occurred in mice that received the material shortly after induction of MI (3 hours) compared to all other treatment groups (Fig. 3.7 B). PBS treated animals from all time-points demonstrated the same level of deterioration in function as no statistically significant

differences in their function (%LVEF) was found at 4 weeks post-treatment. Together, these results highlighted the impact of delivery timing on the efficacy of collagen matrix therapy for MI and demonstrated that the earlier the material is delivered post-MI the greatest extent of functional preservation may be achieved. Given that we did not observe any functional benefits for the 14-day treatment, this delivery time-point was abandoned in favour of focusing on the mechanisms of action for the 3 hour and 7 day treatment time-points.

3.2.2 Collagen Matrix Treatment Improves Vascular Density and Reduces Ongoing Cell Death in the Post-MI Myocardium

To begin to understand the mechanisms through which collagen matrix therapy may preserve cardiac function post-MI and how delivery timing influences this efficacy, we performed a histological comparison of the two treatment time-points that demonstrated functional benefit post-MI (3 hours and 7 days). We first assessed the materials' influence on vascular density and on-going apoptosis in fresh frozen tissue sections of the infarcted myocardium at 4 weeks post-treatment (Fig 3.8).

Both time-points appeared equally effective at improving large vessel density compared to PBS treatment as shown by the superior number of arterioles (α-SMA+ structures with a CD31+ lined lumen) (Fig 3.8 B). However, the 3-hour collagen matrix delivery was superior than PBS and the 7 day time-point at promoting a higher density of capillaries (CD31+ cells) in the infarcted myocardium.

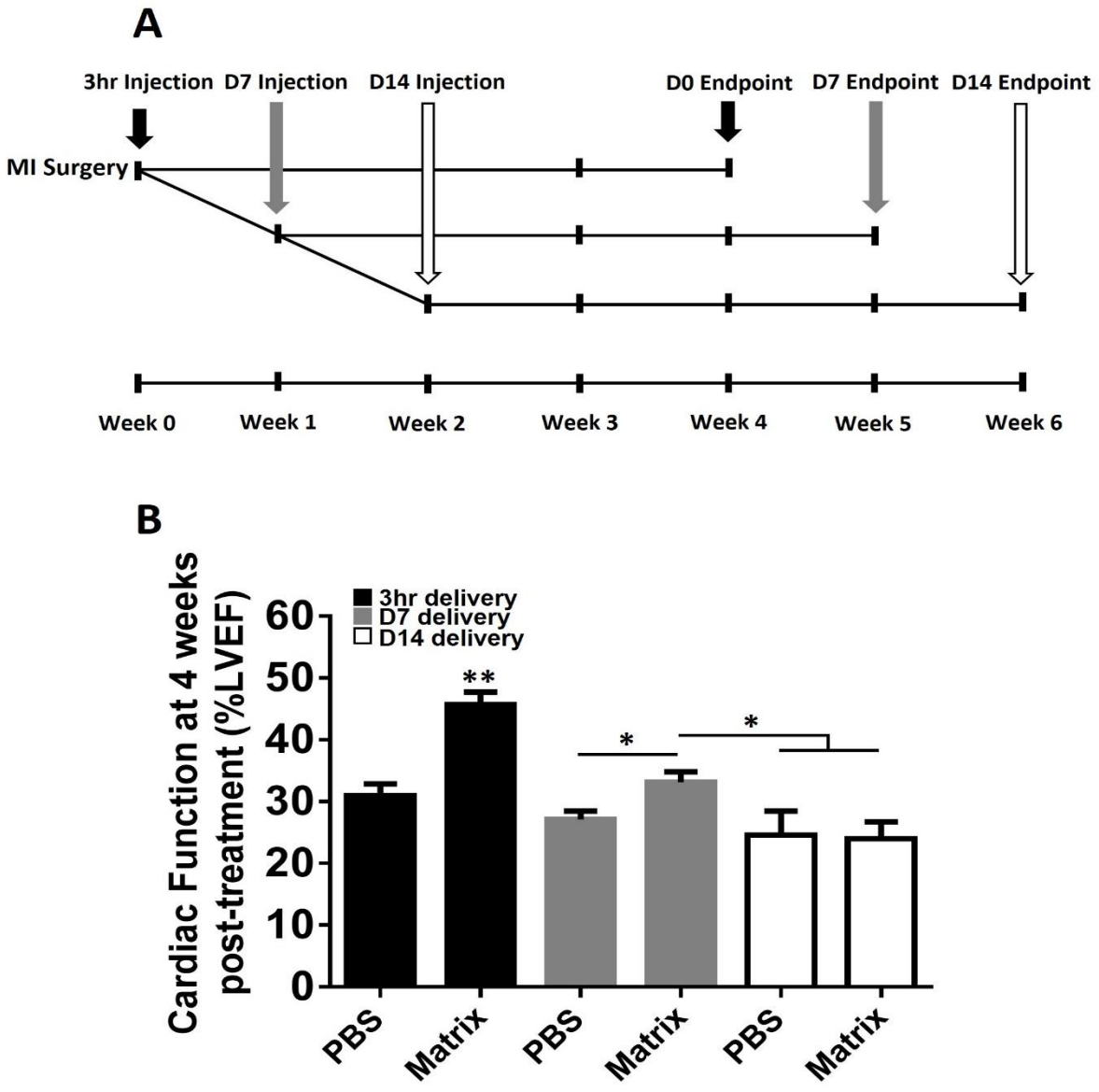

Figure 3.7 Delivering collagen-based biomaterial matrix offers optimal functional benefits. (A) Experimental design. Surgical MI was induced in mice and then animals were randomly assigned to both treatment delivery (PBS or Matrix) and time (3 hours, 7 days or 14 days post-MI) and followed for 4 weeks' post-treatment. (B) %LVEF, cardiac function, assessed using echocardiography at 4 weeks' post-treatment. $^{**}p<0.0001$ vs. all (one-way ANOVA); $^{*}p<0.05$ (Fisher's least significant differences test); n = 15: PBS D0, n=16: Matrix D0, n=14: PBS D7, n=20: Matrix D7, n = 8: PBS D14, n = 5: Matrix D14.

On-going apoptosis in the myocardium may be one of the defining factors of ventricular remodeling and heart failure (Baldi et al., 2002; van Empel et al., 2005; Wencker et al., 2003); therefore, we examined the extent of on-going apoptosis in the heart at 4 weeks post-treatment. Although we did not resolve the exact identity of the cells, we identified apoptotic cells in the myocardium by quantifying those staining positive for active caspase 3. At 4 weeks post-treatment, we found that only the 3 hour delivery of the collagen matrix had the long-term effect of reducing the level of apoptosis in the myocardium compared to control treatment (Fig. 3.8 E). Delivering the material at 7 days post-MI demonstrated a modest reduction that did not reach statistical significance. Altered cytokine expression and regulation has been implicated in ventricular remodeling post-MI (Hedayat et al., 2010; Shah and Mann, 2011); therefore, we next assessed whether our collagen matrix hydrogel therapy altered the cytokine milieu in the myocardium. We harvested peri-infarct/infarct tissue at 4 weeks post-treatment for both the 3 hour and 7 day delivery time-points and assessed cytokine expression using a commercially available array (Appendix A - Figure A1 A,B). While the expression of the majority of the cytokines assessed in the 3 hour time-point were unaffected (Appendix A - Figure A1 A,B), we did detect an increase in FGF-2 compared to all other groups (Fig 3.2 F). Interestingly, several modest differences were observed in the 7 day time-point including a reduction in ALK-1, FGF-2, IFN-gamma, IGFBP-5, MCP-1, SCF, and VEGFR1 (Fig 3.S1 B).

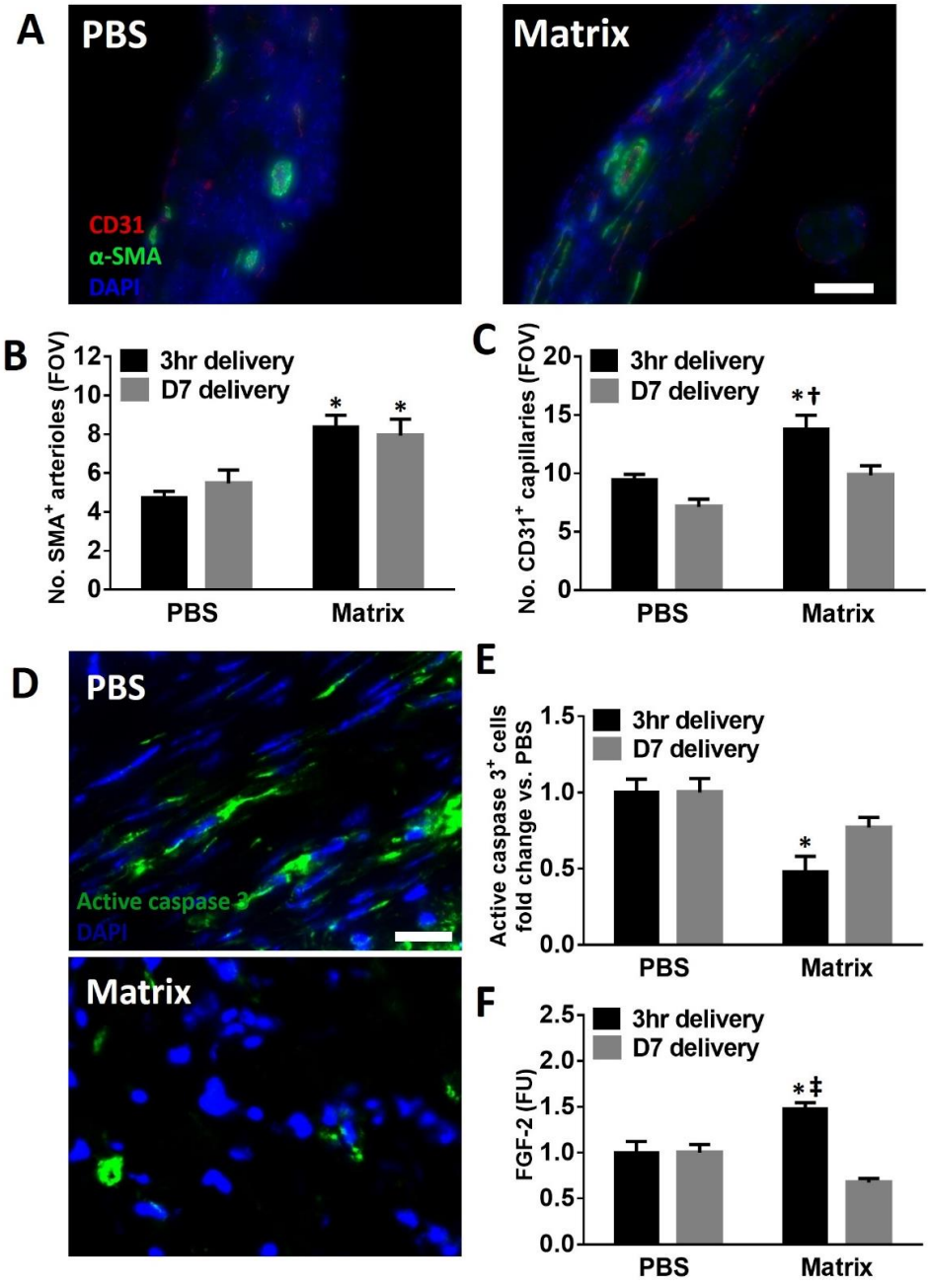

Figure 3.8 Collagen hydrogel improves vessel density and mitigates apoptosis. (A) Representative images of fluorescence immunohistochemical stains of CD31 to identify capillaries and α-SMA to identify arterioles (scale bare = 100µm). (B & C) Quantification of arterioles (B) and capillaries (C) in the infarcted myocardium of 3h and 7-day treatment groups. *p<0.05 vs. PBS, † p<0.05 vs. Matrix D7; n= 5-6. (D) Representative images of active caspase 3 fluorescence immunohistochemical staining (scale bar = 20um). (E) Active caspase 3+ cells (fold change relative to PBS) in infarcted myocardium. *p<0.05 vs. PBS; n= 5-6. (F) FGF-2 levels assessed via cytokine array from infarcted tissue for 3 hour and 7-day treatment groups. *p<0.05 vs. PBS; ‡ p<0.0001 vs. Matrix D7; n=5-6.

3.2.3 Collagen Matrix Therapy Reduces Chronic Inflammation in the MI Heart

One of the determinants of adverse ventricular remodeling and failure is whether inflammation efficiently resolves or persists chronically in the myocardium (Hedayat et al., 2010). Thus, we assessed inflammation in the myocardium post-MI at 4 weeks post-treatment in 3 hour and 7 day treated animals by staining for macrophages (CD68+ cells). We found that the biomaterial therapy delivered at both time-points reduced the quantity of macrophages persisting in the infarcted myocardium (Fig 3.9 B). Similarly, using a cytokine array we found that the 3-hour delivery of the collagen matrix produced a modest, yet significant, reduction in the TNF-α inflammatory cytokine in the myocardium (Fig 3.9 C).

Since we observed that the biomaterial therapy could reduce chronic inflammation in the infarcted myocardium *in vivo*, we further explored this mechanism *in vitro*. To this end, we assessed the cytokine secretion profile of macrophages derived from collagen matrix culture *in vitro*. Bone marrow derived macrophages harvested from mice were cultured on the collagen matrix material or tissue-culture polystyrene (TCPS). After 1 week of culture on either substrate, conditioned media was collected from the cultures to assess secreted cytokines. As shown in Figure 3.9 D, macrophages cultured on the collagen matrix demonstrated a reduction in the release of pro-inflammatory cytokines such as MIP-1α (Ramos et al., 2005), MIP-1γ and CCL5 (Haberstroh et al., 2002; Kraaijeveld et al., 2007); an increase in the anti-inflammatory IL-4 (Van Dyken and Locksley, 2013) and angiogenic CXCL5 (Eyman et al., 2009)

cytokines; a reduction in the soluble TNF receptors sTNFR1 and sTNFR2; and an increase in the matrix remodeling protein TIMP-2.

3.2.4 Early (3 hours) Collagen Matrix Therapy Improves Parameters of Remodeling Post-MI

Having observed that the 3-hour delivery time point of the collagen matrix hydrogel offered superior functional benefits versus the other delivery time points (7 and 14 day), we sought to further explore the benefits of this treatment by assessing final scar size and other metrics of cardiac function and remodeling. As shown in Figure 3.10 B, we found that early delivery of the collagen matrix results in an approximately 40% reduction of final scar size at 4 weeks post-treatment compared to PBS treated animals. Moreover, we found that the early treatment delivery also improved additional metrics of cardiac performance including %fractional area change (FAC) (Fig 3.10 C), cardiac output (CO) (Fig 3.10 D), and stroke volume (SV) (Fig 3.10 E). We also found that mice treated with the collagen matrix hydrogel had reduced end-systolic volumes (ESV) (Fig 3.10 F), a metric for global cardiac remodeling, compared to those treated with PBS. Fibrogenesis is important for scar formation and structural reinforcement of the infarcted myocardium, though penetrating fibrosis into the bordering and remote regions of the myocardium can lead to diastolic stiffness, dyskinetic ventricular contractions and perpetuate negative remodeling (Li et al., 2014). Therefore, we assessed the level of fibrosis in the bordering regions of the infarct. We found that matrix treatment delivered at 3 hours post-MI was associated with reduced penetrating fibrosis compared to PBS treated animals at 4 weeks post-treatment (Fig 3.10 H).

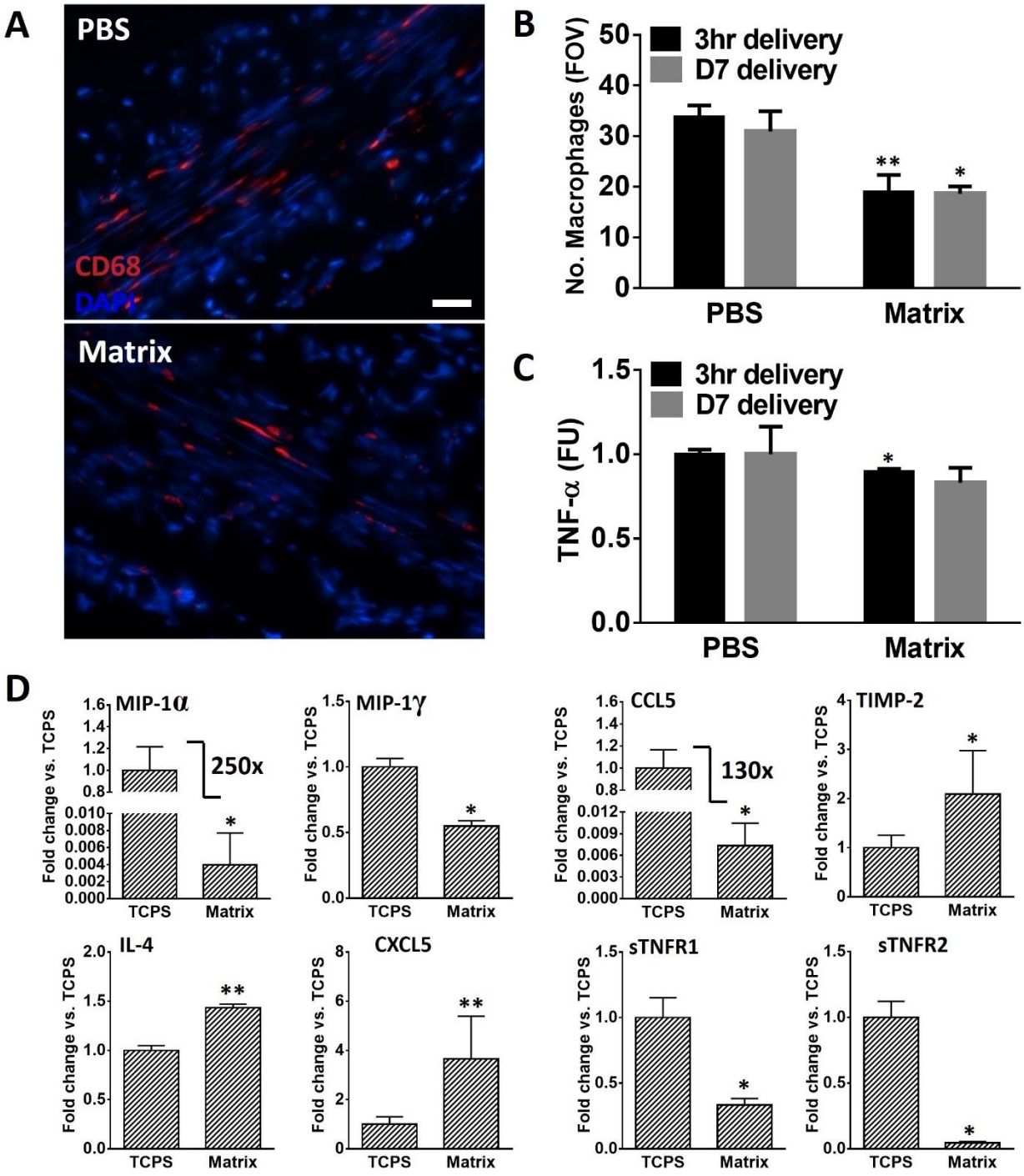

Figure 3.9 Collagen matrix mitigates chronic inflammation *in vivo* and alters cytokine secretion of macrophages *in vitro*. (A) Representative imagine of fluorescent immunohistochemical stains of CD68+ macrophages in myocardial tissue section (scale bar = 20μm). (B) CD68+ macrophage density in the infarcted myocardium of 3 hour and 7-day treatment groups. *$p < 0.05$ vs. PBS, **$p < 0.01$ vs. PBS; n=3-6. (C) TNF-α levels assessed by cytokine array from infarcted tissue. *$p < 0.05$ vs. PBS; n=5-6. (D) Fold-change in cytokine secretion profile for cultured BMDMs on collagen matrix biomaterial or TCPS *in vitro*. *$p < 0.05$ and **$p<0.01$; n=3-4.

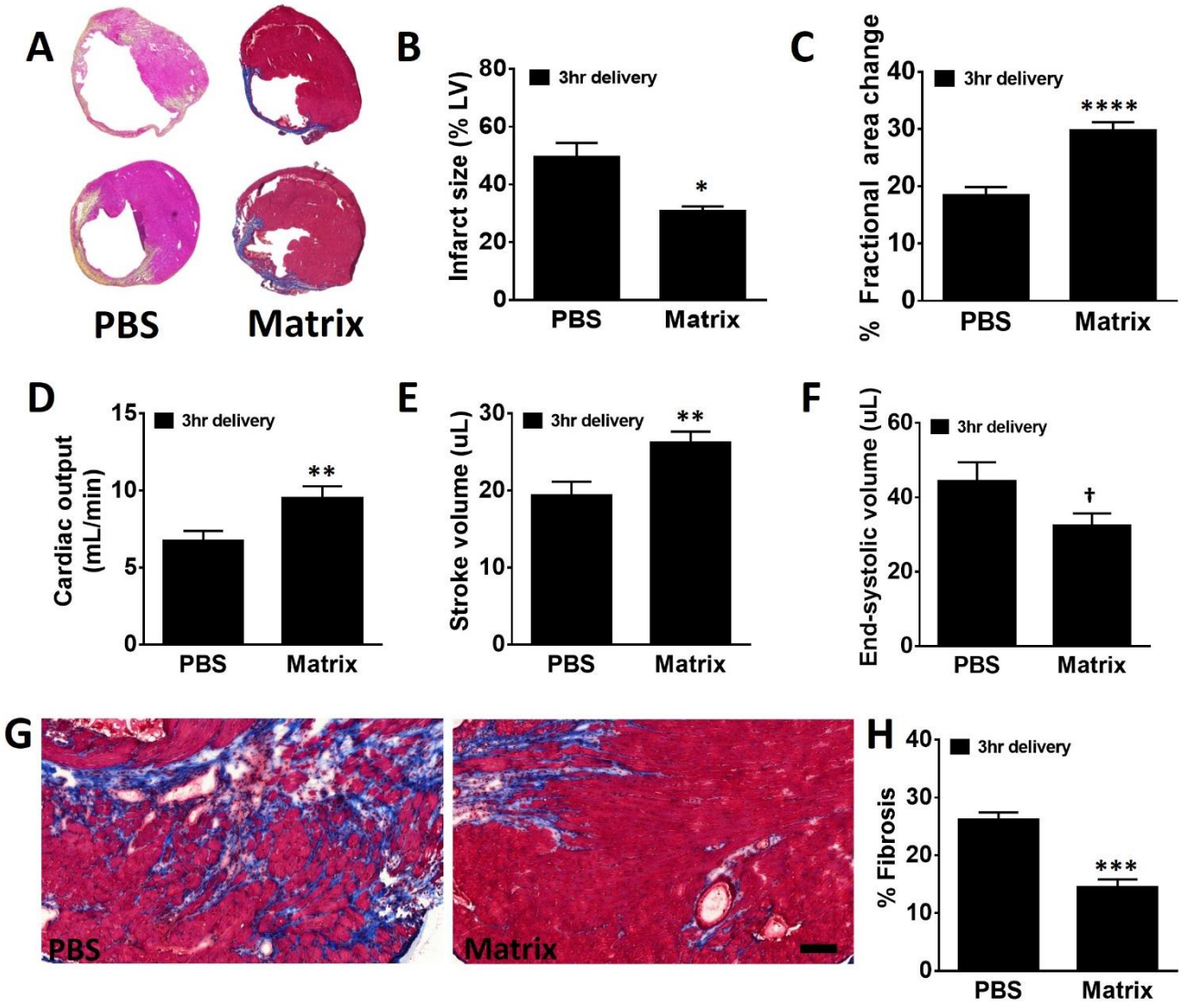

Figure 3.10 Early collagen matrix delivery improves ventricular remodeling, cardiac performance and reduces final scar size and fibrosis. (A) Masson trichrome stained tissue sections of hearts at 4 weeks post-MI from 3 hour treated hearts. (B) Final scar size in 3 hour treated mice (collagen matrix or PBS) at 4 weeks' post-treatment. *$p < 0.05$; n=3-5. (C-F) % Fractional area change, cardiac output (ml/min) and stroke volume (µl) and LV-volume at end-systole (µl) for the 3 h treatment groups assessed at 4 wk post-treatment. **$p < 0.01$, ****$p < 0.0001$, †$p = 0.0545$; n=15-16. (G) Representative images of Masson-trichrome stained tissue demonstrating penetrating fibrosis into the bordering areas of the infarct at 4 weeks post-MI (scale bar=100um). (H) Percentage of fibrosis in the bordering region of the infarcted myocardium at 4 weeks post-MI. ***p<0.001; n=5-6.

Collectively, these results indicate that delivering the collagen matrix therapy early post-MI can protect and support the myocardium by limiting functional decomposition and partially preventing adverse cardiac remodeling.

3.2.5 Early Myocardial Neovascularization and Cell Death in Response to 3-hour Collagen Matrix Treatment

Our next goal was to further interrogate the mechanisms underlying the effects of the 3-hour delivery time-point. We wanted to understand what changes were occurring in the myocardium shortly after the therapy was delivered, but before the 7-day treatment cohort would have received the biomaterial therapy, to possibly explain the benefits of the earlier delivery time-point. We proceeded to assess the host tissue response, specifically looking at vascular density, angiogenesis and cell death at 2 days post-therapy. This would provide insight into the bioactive benefits of delivering the biomaterial 3 hours post-MI that would not be present in mice treated at 7 days (Fig 3.11 A). We first assessed vascular densities in the infarcted myocardium. We did not find any difference in the number of arterioles (α-SMA+ structures) between collagen matrix treated animals and PBS controls at 2 days post-treatment (Fig 3.11 B). However, we did observe a higher density of CD31+ capillaries in mice treated with the matrix vs. PBS controls (Fig 3.11 C). This increase in the number of capillaries is likely due to increased angiogenesis in the infarcted myocardium of collagen matrix treated mice, since a higher number of proliferating CD31+ capillaries were also observed (CD31+ cells co-staining with Ki67) (Fig. 3.11 D). Additionally, proliferating capillaries in collagen matrix treated animals represented a higher proportion of the total number of

proliferating cells in the infarcted myocardium compared to PBS treated animals (Fig. 3.11 E). Our next investigations focused on cell death, a hallmark of myocardial infarction. Indeed, the collagen matrix was able to limit cell death early post-MI as shown by the reduced number of TUNEL+ cells in the infarcted myocardium at 2 days post-treatment compared to PBS treated mice (Fig 3.11 H).

3.2.6 Inflammatory Response to Early Collagen Matrix Biomaterial Therapy

An important consideration for naturally derived hydrogels for the treatment of myocardial infarction is biocompatibility. Therefore, we assessed the acute inflammatory response to the hydrogel at 2 days post-treatment in myocardial tissue sections. We examined two major cell types that are recruited to the myocardium during the initial inflammatory phase shortly after infarction: neutrophils (Ly6G+ cells) and macrophages (F4/80+ cells). Given that we observed differences in cytokine secretion of bone marrow derived macrophages cultured on the material *in vitro*, we also stained for two important subsets of macrophages: the pro-inflammatory M1 macrophage (CD86+ cells) and the pro-wound healing / anti-inflammatory M2 macrophage (CD206+ cells). Collagen matrix therapy did not alter neutrophil recruitment to either the infarcted myocardium or the bordering areas (Fig. 3.12 A). The collagen matrix did not impact the total number of recruited macrophages to the myocardium (Fig 3.12 B). Furthermore, collagen matrix therapy did not affect the number of recruited M2 macrophages (Fig 3.12 C); however, we did see a decrease in the number of M1 macrophages recruited to both the infarcted area and the border zone in collagen matrix treated versus PBS treated animals (Fig 3.12 D).

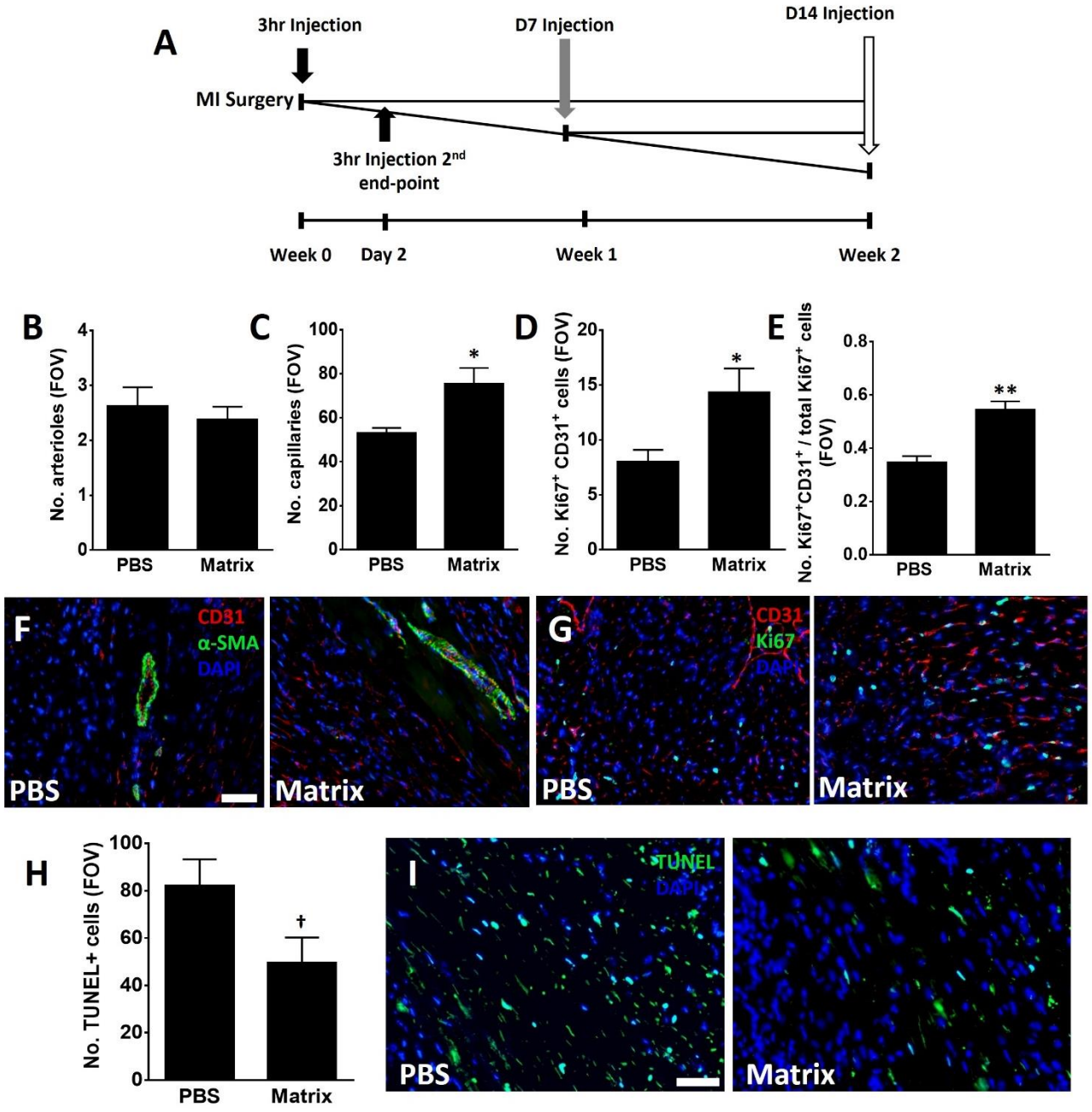

Figure 3.11 3-hour collagen matrix delivery improves neovascularization and reduces cell death 2 days after treatment. (A) Schematic representation of study design. (B & C) Arteriole and capillary densities assessed at 2 days post-treatment in 3 hour treated mice in the infarcted myocardium. *p<0.05; n=4. (D & E) Assessment of the number of Ki67+CD31+ cells, proliferating endothelial cells, and proportion of proliferating endothelial cells (relative to the total number of Ki67+ cells) in the infarcted myocardium. *p<0.05, **p<0.005; n=5. (F & G) Representative images of arterioles (α-SMA+) and capillaries (CD31= cells) and proliferating cells (Ki67+ cells) (Scale bar = 100um). (H) TUNEL stain quantifying the extent of cell death in the myocardium in tissue sections. †p=0.08; n=4. (I) Representative TUNEL stained images of MI heart tissue sections (Scale bar = 100 um).

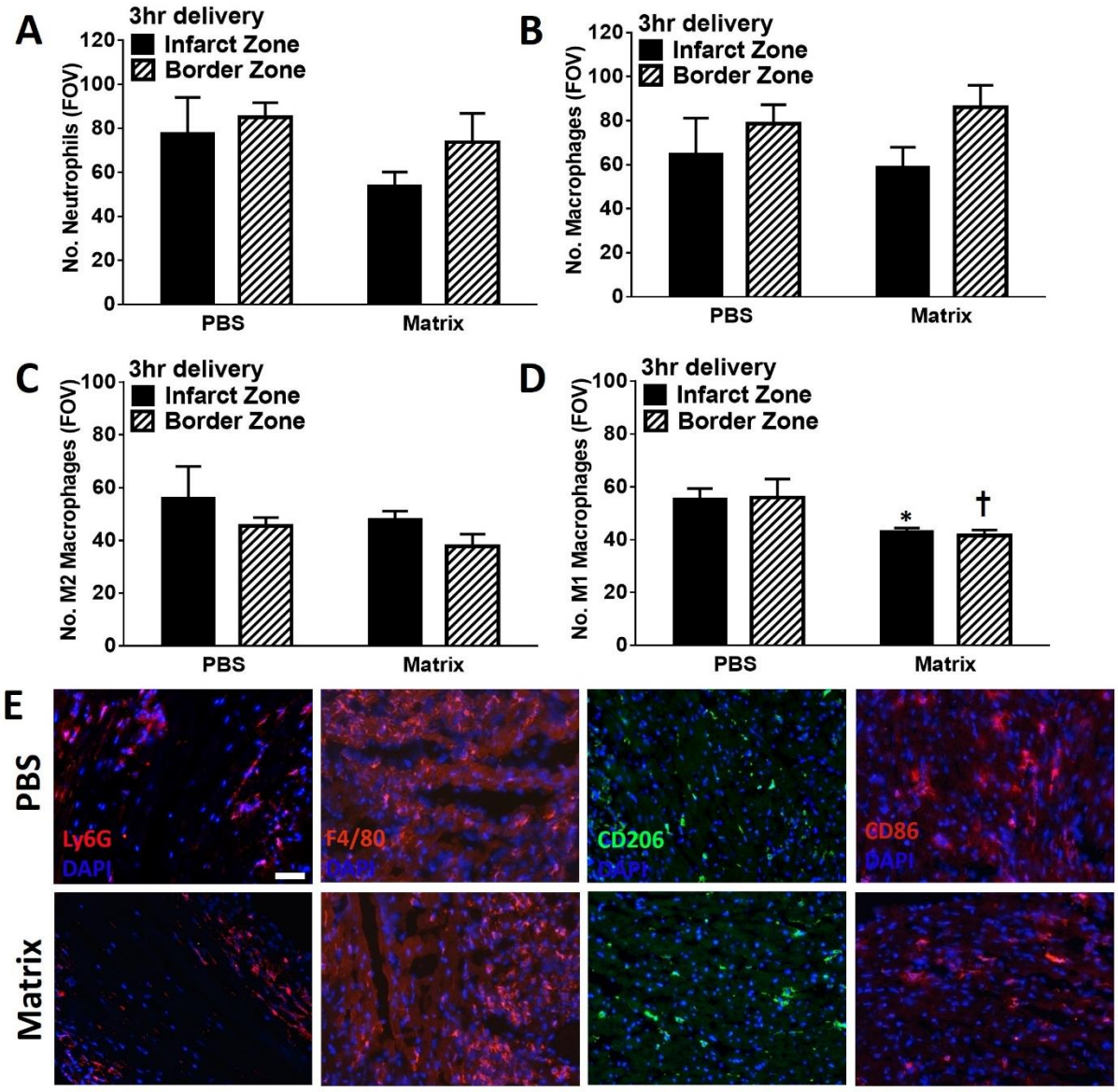

Figure 3.12 3-hour collagen matrix delivery does not exacerbate the acute inflammatory response early post-MI. (A-D) Quantification of inflammatory cells recruited to the infarcted myocardium early post-MI including: (A) neutrophils (Ly6G+ cells), (B) macrophages (F4/80+ cells), (C) M2 macrophages (CD206+ cells) and (D) M1 macrophages (CD86+ cells) in the infarct and bordering areas at 2 days post-treatment. *$p < 0.05$ and †$p = 0.07$ vs. PBS; n = 4. (E) Representative images of fluorescent immunohistochemistry of infiltrating neutrophils, macrophages, M2 macrophages and M1 macrophages in the infarcted myocardium. (Scale bar = 100um).

These results indicate that our collagen biomaterial does not exacerbate the acute inflammatory phase post-MI, thus supporting its biocompatibility.

3.2.7 Early Treatment Delivery of Collagen Matrix Biomaterial Preserves Cardiac Function Long-term

To rule out the possibility of the benefits being transient, the next approach of this study was to ascertain whether the collagen matrix hydrogel therapy, when delivered at 3 hours post-MI, would provide lasting functional benefits. Therefore, experimental MI was induced in a subset of mice and animals were treated at 3 hours post-MI (collagen matrix or PBS), and followed for 3 months post-treatment (Fig 3.13 A). Left ventricular ejection fraction (%LVEF) was assessed in matrix and PBS treated animals at baseline (3 hours post-MI / pre-treatment), and 1, 4, 8 and 12 weeks post-treatment. At baseline (3 hours post-MI / pre-treatment) there were no significant differences in cardiac function (%LVEF) between PBS and matrix treated animals. Prior to the 12-week endpoint for the study, 2 mice from the PBS cohort died, while all collagen matrix treated animals survived. As shown in Figure 3.13 B, mice treated with the collagen matrix at 3 hours post-MI demonstrated a stabilization in cardiac function, whereas animals given PBS experienced progressive functional deterioration. Additionally, matrix treated animals showed superior cardiac output (Fig 3.13 C), and stroke volumes (Fig 3.13 D). Matrix treated animals also had improvements in end-systolic and diastolic volumes (Fig 3.13 E, F) that did not reach statistical significance, possibly owing to the small sample size. Therefore, delivering the collagen matrix hydrogel at 3 hours post-MI offers long-term stability to cardiac function and anatomy.

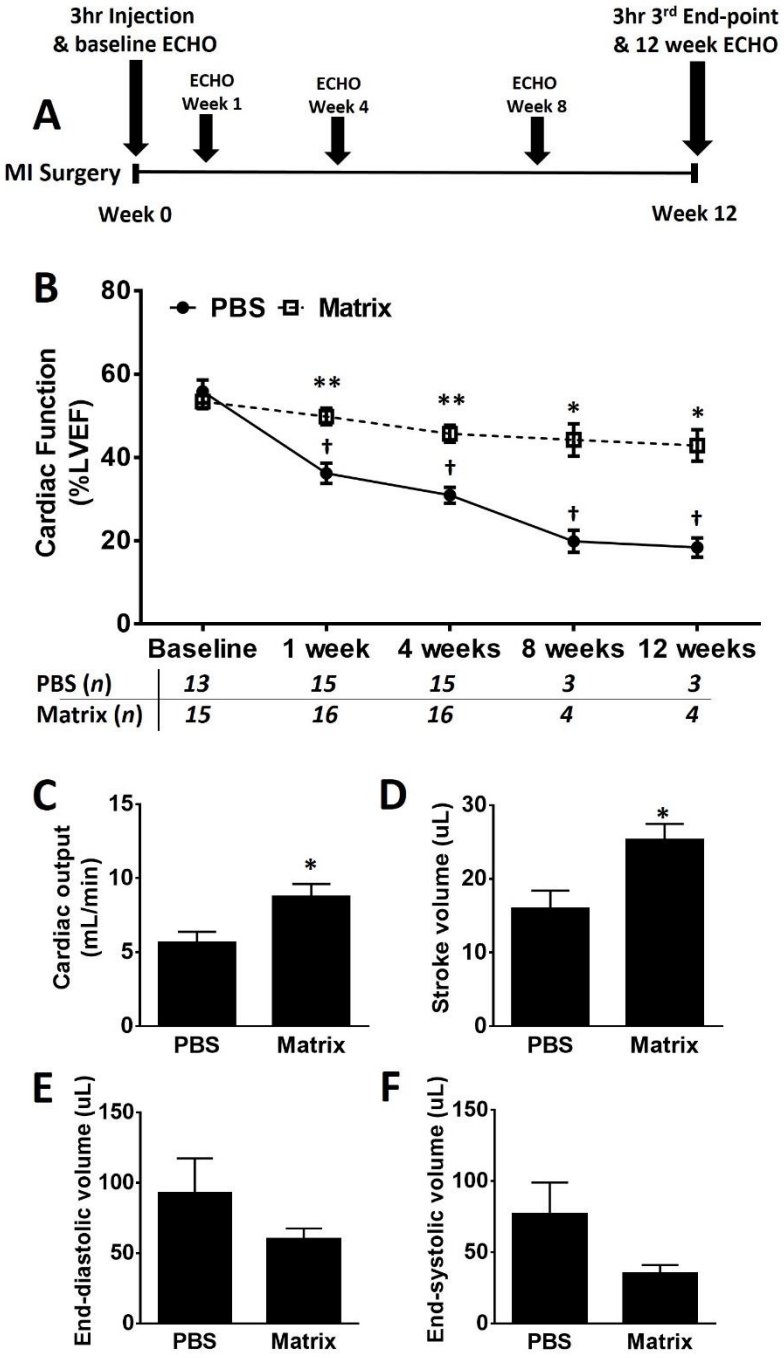

Figure 3.13 Long-term functional preservation in mice treated with collagen matrix at 3 hours post-MI. (A) Schematic of experimental design. (B) Cardiac function, %LVEF, followed for 12 weeks in a subset of mice treated with collagen matrix or PBS at 3 hours post-MI. *$p < 0.001$ vs. PBS, **$p < 0.0001$ vs. PBS, †$p < 0.0001$ vs. baseline PBS. (C-F) Additional functional assessments at 12 weeks post-treatment including (C) cardiac output (ml/min), (D) stroke volume (µl), and left ventricular volumes at (E) end-diastole (µl) and (F) end-systole (µl). *$p < 0.05$; n = 3-4.

3.3 A Fisetin-loaded collagen hydrogel improves cardiac function post-MI

Brief Introduction to AIM 3

The next approach in the thesis research was to combine the knowledge we gained from AIM 1 and AIM 2 to produce a biomaterial therapy strategy to target MG for the treatment of MI. Thus far, we have demonstrated: 1) that MG is produced post-MI and contributes to cardiac dysfunction and adverse remodeling; and 2) that delivering a collagen matrix biomaterial 3 hours post-MI can mitigate cardiac dysfunction and remodeling post-MI. Our ultimate goal was to combine these two findings into a novel therapy for post-MI remodeling. To this end, we combined our biomaterial therapy with the flavonoid Fisetin, an MG scavenger / GLO1 activator, which is an antioxidant shown to increase GSH levels, stimulate the expression of GLO1 and directly scavenge MG (Maher et al., 2011). Methods to release Fisetin from our biomaterial were developed and the efficacy of this combined therapy in preventing functional deterioration and adverse remodeling post-MI was assessed.

Contributions of Authors

Animal surgeries were performed by Rick Seymour and assisted by me. ECHO-guided myocardial injections were performed by Brian McNeill. Echocardiography and analysis was performed principally by me, though baseline echos were taken by Brian McNeill. I traveled to Soochow University in Suzhou, China to help develop and test the nanoparticles with Drs. Chao Deng and Zhiyuan Zhong, who also kindly provided the nanoparticles polymers. All cell culture was performed by me. Flow cytometry was stained and prepared for by me. The Fisetin release experiments were performed by me. Fisetin measurements using fluorescence spectrophotometry and Dynamic Light Scattering (DLS) measurements were performed by Drs. Manuel Ahumada and Emilio Alarcon. Tissue sectioning was performed by me and Brian McNeill. Tissue staining using Masson-trichrome and immunofluorescence, and analysis was performed by me. Dicarbonyl tissue content assessment using commercially available ELISA was performed by me.

3.3.1 Fisetin Prevents MG-mediated Impairment of Angiogenesis and does not Affect Cell Viability

Fisetin is a dietary flavonoid shown to increase GSH (Khan et al., 2013) and to reduce MG levels through both increased GLO1 activity and direct MG scavenging (Maher et al., 2011). However, Fisetin has also been reported to potentially be anti-angiogenic (Bhat et al., 2012). Therefore, our first goal was to clarify whether Fisetin was anti-angiogenic and/or cytotoxic and at what concentrations. To confirm whether Fisetin was anti-angiogenic we cultured HUVECs in media containing Fisetin at various concentrations (0µM, 10µM, 50µM, 100µM, 500µM) for 48 hours. As shown in Figure 3.14 A, Fisetin at concentrations of less than 50µM did not affect network length in a HUVEC angiogenesis assay. There was a slight drop in total network length at 50µM Fisetin, while 10µM appeared to increase network length, neither of which was statistically significant. However, concentrations of 100µM Fisetin did influence *in vitro* angiogenesis, reducing the total network length significantly, and 500µM completely prevented tubule formation (Fig 3.14 A). Since we confirmed that 10uM Fisetin does not prevent tubule formation *in vitro*, our next approach was to assess the cytotoxicity. HUVECs were cultured in the different Fisetin concentrations for 48 hours, and then cell viability was assessed using flow cytometry and 7AAD staining. As shown in Figure 3.14 B, Fisetin concentrations up to 100µM did not influence cell viability, while 500µM Fisetin reduced HUVEC viability significantly. Together, these results indicate that Fisetin does not impair angiogenesis *in vitro* at concentrations less than 50µM nor cell viability at concentrations less than 100µM. Having determined the concentrations at which

Fisetin would not impair angiogenesis or cell viability, we next sought to confirm whether Fisetin could prevent the negative effects of MG on angiogenesis. We cultured HUVECs in either 1) 0.1% DMSO (Control), 2) 10µM Fisetin, 3) 25µM MG, or 4) 10µM Fisetin + 25µM MG, and then used them in the *in vitro* angiogenesis assay. We found that 25µM MG reduced total network length significantly, but this was rescued by treatment with 10µM Fisetin (Fig 3.14 C). Collectively, our results confirm that concentrations of 10-50µM Fisetin do not affect angiogenesis, are not cytotoxic and can rescue impaired angiogenesis mediated by MG.

3.3.2 Designing a Delivery Platform for *in vivo* Fisetin Injection

After having demonstrated that Fisetin can prevent MG mediated effects on angiogenesis, our next approach was to determine how best to deliver the therapy concomitantly with the biomaterial. Fisetin has very poor solubility in aqueous media; therefore, we tested whether this would be appropriate in a nanomedicine platform. Nanoparticles (NPs) have been shown to improve the solubility, pharmacokinetics and biodistribution of many different drugs (Sun et al., 2016). In collaboration with Drs. Deng and Zhong from Soochow University in Suzhou, China we assessed the feasibility of encapsulating Fisetin in various NP formulations. Two different polymers were assessed including one on a hyaluronic acid (HA) backbone (Sun et al., 2016), and the other on a polyethylene glycol (PEG) backbone (table 1).

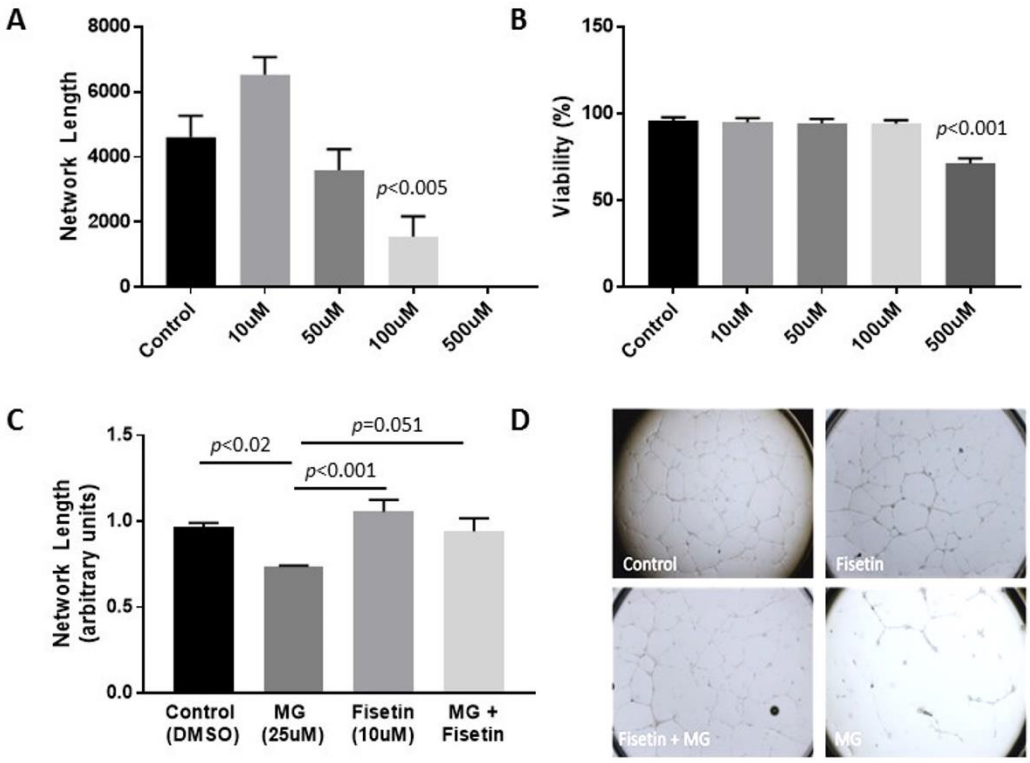

Figure 3.14 Fisetin is not cytotoxic and does not impair angiogenesis *in vitro*. (A) Fisetin dose effect (0µM, 10µM, 50µM, 100µM, 500µM) on total network length in a HUVEC angiogenesis assay, (*n*=6). Fisetin (0µM, 10µM, 50µM, 100µM, 500µM) dose effect on HUVEC viability assessed via flow cytometry and 7AAD staining, (*n*=4). (C) Effect of 10µM fisetin on MG mediated impairment of angiogenesis in HUVEC tube formation assay, (*n=5*). (D) Representative bright field microscopy images of HUVEC angiogenesis assay. Data are presented as mean ± SEM. Analyzed using one way ANOVA with Tukey post-hoc test for multiple comparisons.

Various formulations of the polymers alone in solution or combined with Fisetin were assessed using dynamic light scattering (DLS) to measure the size and polydispersion indices (PDI) of the formulations. As shown in table 1, encapsulating Fisetin within the HA NPs only resulted in a slight increase in the size and PDI of the NPs, whereas the increases in the PEG NPs were greater. Moreover, visual inspection of the solutions revealed that Fisetin was quickly precipitated from solution with the PEG formulation (<12 hours), whereas the Fisetin – HA NPs appeared more stable and maintained Fisetin in solution. Therefore, we decided to pursue the HA NP platform and determine 1) if the NPs could promote solubility of Fisetin within the collagen biomaterial and 2) alter the release kinetics of Fisetin from the biomaterial.

We started by comparing the release behavior of Fisetin HA NPs vs. free Fisetin from the biomaterial. We assessed two different concentrations of Fisetin including a low concentration (40μM) and a high concentration (80μM). We measured Fisetin concentration in solution using fluorescence spectroscopy (365nm excitation: 540nm emission) (Appendix A - Figure A2 A,B)(Guharay et al., 1999).

Table 1. Size and poly-dispersion indices for various nanoparticle formulations with or without Fisetin.

Sample	Size (nm)	PDI
Hyaluronic Acid Nanoparticle (10% DMSO)	61.14	0.149
Hyaluronic Acid Nanoparticle (5% DMSO)	69.56	0.258
5 µL Fisetin (10mg/mL) + 100uL HA polymer (5mg/mL)	81.00	0.202
10 µL Fisetin (10mg/mL) + 100uL HA polymer (5mg/mL)	70.40	0.157
PEG – polyC – 1mg/mL	61.29	0.149
PEG – polyC – 0.5mg/mL	68.61	0.251
PEG – polyC – 1mg/mL + 100ug/mL Fisetin	143.8	0.290
PEG – polyC – 0.5mg/mL + 100ug/mL Fisetin	141.7	0.285

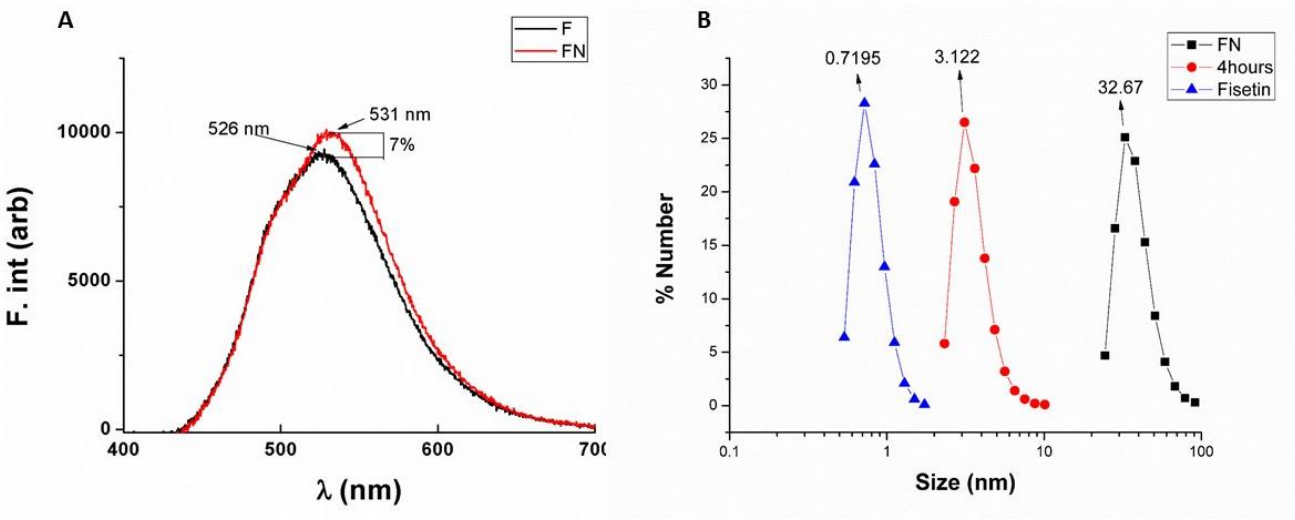

Figure 3.15 Characterizing Fisetin HA NPs. (A) Fluorescence spectra of free Fisetin and Fisetin NPs in solution showing slight shift in emission and fluorescence intensity. (B) Dynamic Light Scattering measurements of free Fisetin (blue, left), release media from 4 hours post-release of Fisetin NP hydrogel (red, center), and freshly prepared Fisetin NPs (right, black).

We found that Fisetin loaded into the HA NP caused a slight shift in fluorescence emission maxima from 526 to 531nm resulting in approximately 7% difference in intensity (Fig 3.15 A). The shift is likely the result of the interaction between the polymer and Fisetin, altering its fluorescent properties, which may minimally affect the measurements of the Fisetin NP release experiments. We also assessed whether we could distinguish between free Fisetin that was released from the biomaterial vs. the release of intact Fisetin HA NPs. We found that the likely scenario is that either the HA NPs stayed within the biomaterial matrix or were degraded, while free Fisetin was released into the release media as shown by the size of particles collected from release media after 4 hours compared against free Fisetin and freshly prepared NPs (Fig 3.15 B).

We next assessed Fisetin release from the biomaterial over time and, as shown in Figure 3.16, we found no difference in the release between free Fisetin vs. Fisetin encapsulated with HA NPs (from within the biomaterial). It appears at both concentrations approximately equal amounts of drug is released from the collagen matrix regardless of whether the biomaterial was made with free Fisetin or Fisetin encapsulated within HA NPs. Given that 1) the HA NPs did not appear to alter the release of Fisetin from the biomaterial; and 2) did not appear to release with the drug from the biomaterial, we abandoned the NP platform and pursued an *in vivo* assessment of the efficacy of free Fisetin release from the biomaterial in a mouse model of MI.

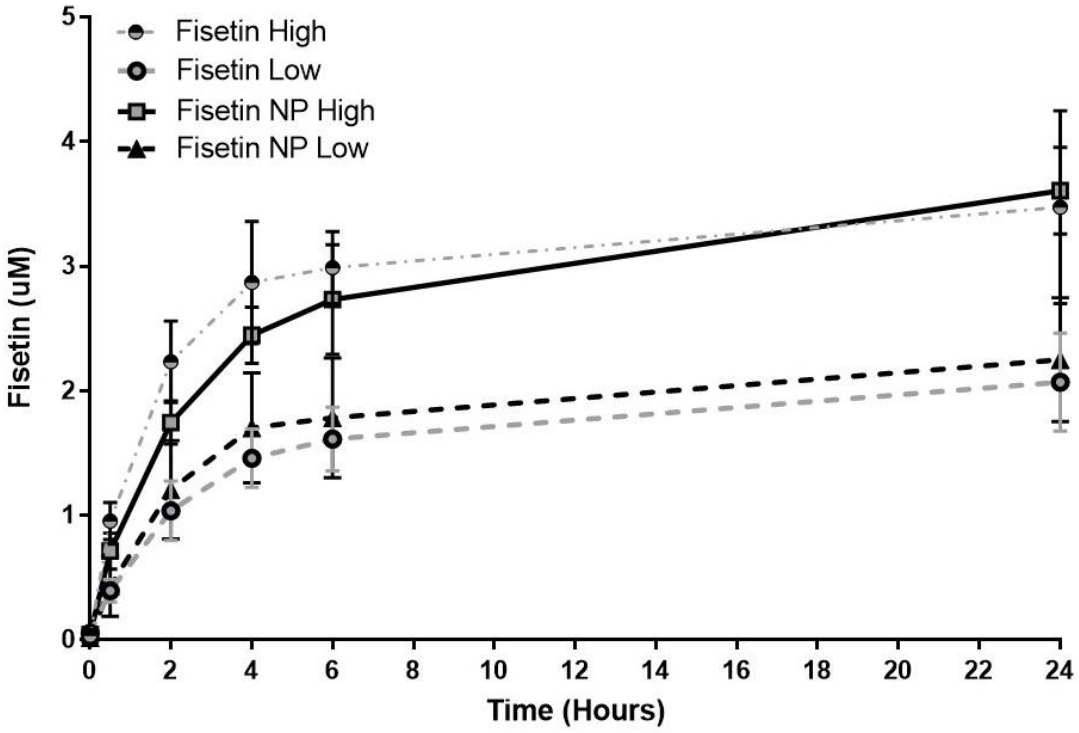

Figure 3.16 Fisetin *in vitro* release from collagen matrix biomaterial. Free fisetin (Fisetin High or Low) or encapsulated in HA NPs (Fisetin NP High or Low) in low (40µM) or high (80µM) concentrations released from collagen matrix biomaterial into release media over 24 hours. Fisetin concentrations were measured using fluorescence spectroscopy (excitation 365nm/emission 540nm) (*n*=3-5). Data are presented as mean ± SEM.

3.3.3 Combined Fisetin - Biomaterial Improves Cardiac Function Post-MI

The biomaterial containing approximately 1.14ug of Fisetin was delivered intramyocardially to infarcted mice at 3 hours post-MI and the animals were followed for 5 weeks post-treatment. The controls for this study were Fisetin (alone, no biomaterial), PBS, and the collagen matrix hydrogel. As shown in Figure 3.17 A, the hydrogel therapy maintained cardiac function while animals treated with PBS saw their cardiac function progressively worsen. Free Fisetin appeared to have no effect on cardiac function, while the Fisetin hydrogel showed a trend in maintained function (p<0.1). The lack of significance found for the Fisetin hydrogel treatment can be due to several reasons (elaborated in discussion section). Notably, we found that mice receiving the Fisetin hydrogel or PBS had a lower baseline (3 hours post-MI / pre-treatment) %LVEF (37.6% and 38.0%, respectively) compared to those receiving the collagen matrix hydrogel (46.6%) (Appendix A - Figure A3). Therefore, we compared the absolute change in %LVEF between baseline and 5 weeks post-treatment in all groups. We found that mice having received the Fisetin hydrogel were the only group to show an improvement in %LVEF over the 5-week period compared to mice receiving only PBS (Fig 3.17 B). To determine if the Fisetin hydrogel influenced remodeling of the myocardium, we also assessed ventricular volumes. Though no differences were observed in end-diastolic volumes at 5 weeks post-MI (Fig 3.17 C) we found a significant reduction in end-systolic volumes in mice having received the Fisetin hydrogel compared to PBS (Fig 3.17 D).

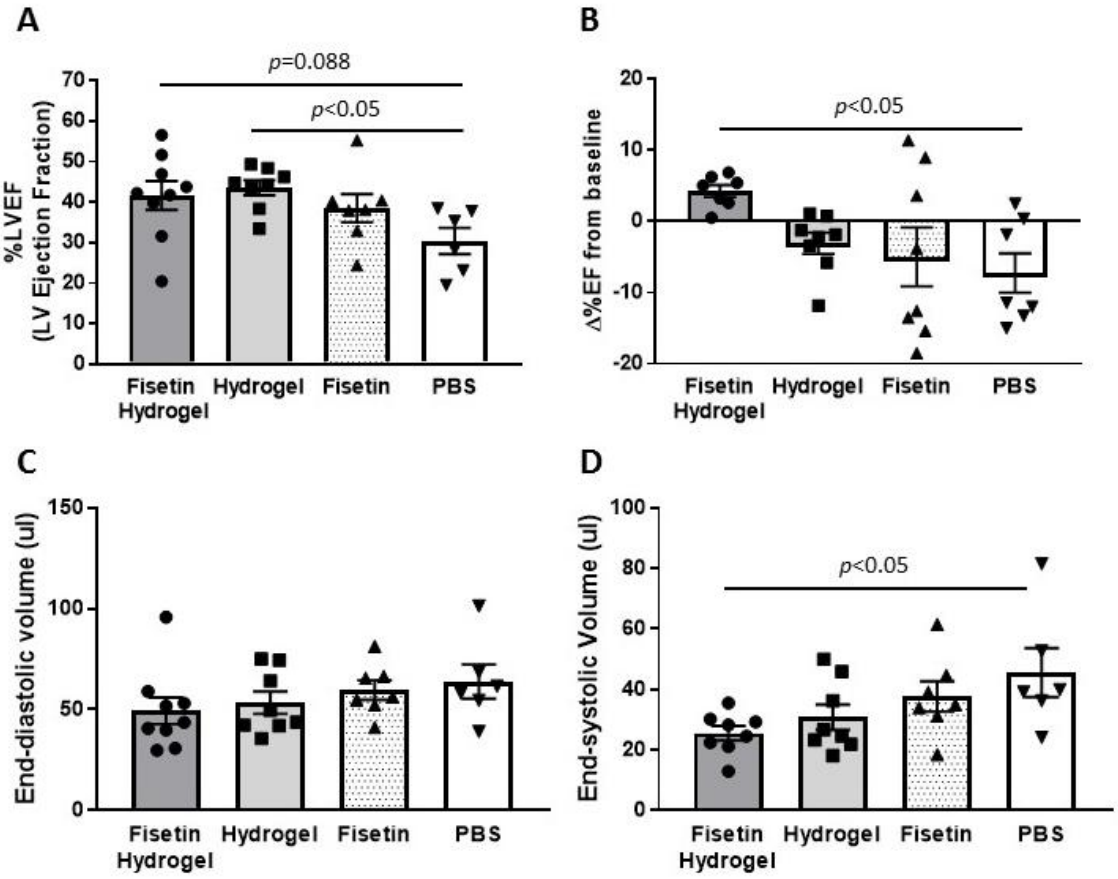

Figure 3.17 Combined Fisetin collagen matrix hydrogel improves cardiac function and ventricular volumes post-MI. (A) Cardiac function, %LVEF, 5 weeks post-treatment in mice treated with the Fisetin hydrogel (*n*=9), collagen matrix hydrogel (*n*=8), free Fisetin (*n*=7) or PBS (*n*=6) at 3 hours post-MI. (B) Difference in cardiac function, %LVEF, from baseline to 5 weeks in mice treated with Fisetin hydrogel, collagen matrix hydrogel, free Fisetin or PBS. (C-D) Ventricular volumes, end-diastolic (C) and end-systolic (D), assessed at 5 weeks post-MI in all treatment groups. Data is presented as a mean ± SEM and analyzed using one way ANOVA with Tukey post-hoc test for multiple comparisons.

3.3.4 Hydrogel Therapies Reduce Final Infarct Sizes Post-MI

We next assessed whether the biomaterial therapies would have an impact on final scar sizes at 5 weeks post-MI. We excluded the Fisetin only therapy from further investigation due to lack of efficacy. We stained frozen tissue section at various levels of the heart using Masson Trichrome and measured infarct sizes using the midline method (Takagawa et al., 2007). As shown in figure 3.18, mice treated with the hydrogel therapy had significantly smaller final infarct sizes compared to animals treated with PBS. Mice treated with the Fisetin hydrogel showed a non-significant decrease in final infarct sizes (p=0.08), though the lack of statistical significance may be due to insufficient sample size.

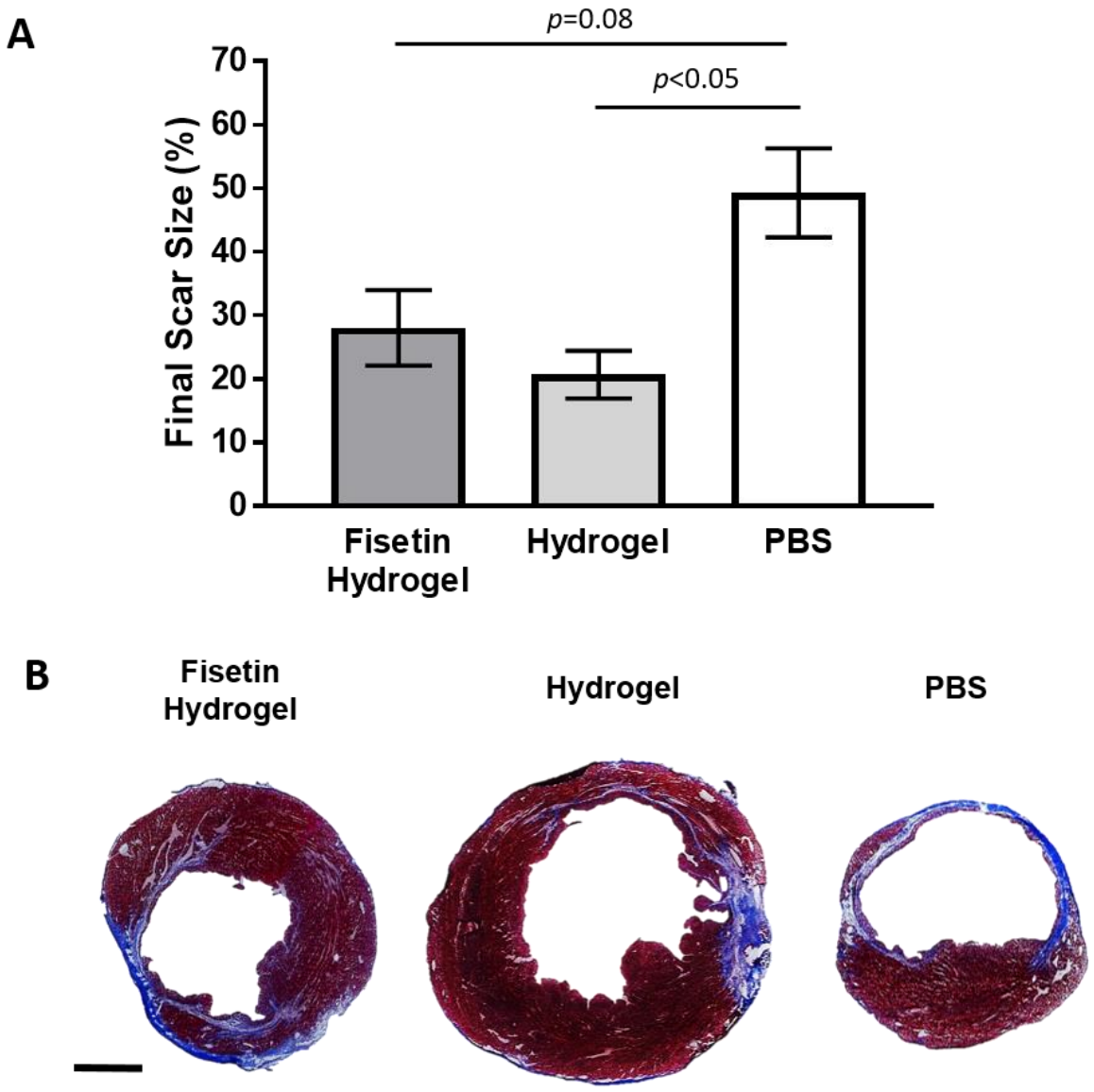

Figure 3.18 Hydrogel therapies reduce final scar sizes at 5 weeks post-treatment. (A) Final scar size assessed using midline method in Masson-Trichrome stained tissue in Fisetin-hydrogel, hydrogel, and PBS treated animals (*n*=3-4). (B) Representative images of Masson-Trichrome stained tissue sections. (scale bar = 1mm). Data is presented as a mean ± SEM and analyzed using one way ANOVA with Tukey post-hoc test for multiple comparisons.

3.3.5 Hydrogel Therapies Improve Vascular Density and Mitigate Chronic Macrophage Recruitment to the Myocardium

In AIM 2 we showed that the hydrogel matrix delivered at 3 hours post-MI improved vascular density and reduced inflammation in the myocardium. Therefore, we endeavored to determine what effect the addition of Fisetin to the biomaterial therapy may have on vascular density and inflammation. Using fresh frozen sectioned tissue, we stained the hearts for CD31+ (endothelial marker) and α-SMA (smooth muscle cell marker) to identify arterioles in the border regions of the infarcts. As shown in Figure 3.19 A, both the hydrogel and the Fisetin hydrogel improved arteriole density in the myocardium at 5 weeks post-treatment compared to PBS treated mice. Both therapies also resulted in the reduction of CD68+ macrophages compared to PBS treated animals (Fig 3.19 B). The hydrogel and Fisetin hydrogel were approximately equivalent in reducing macrophage numbers in the myocardium.

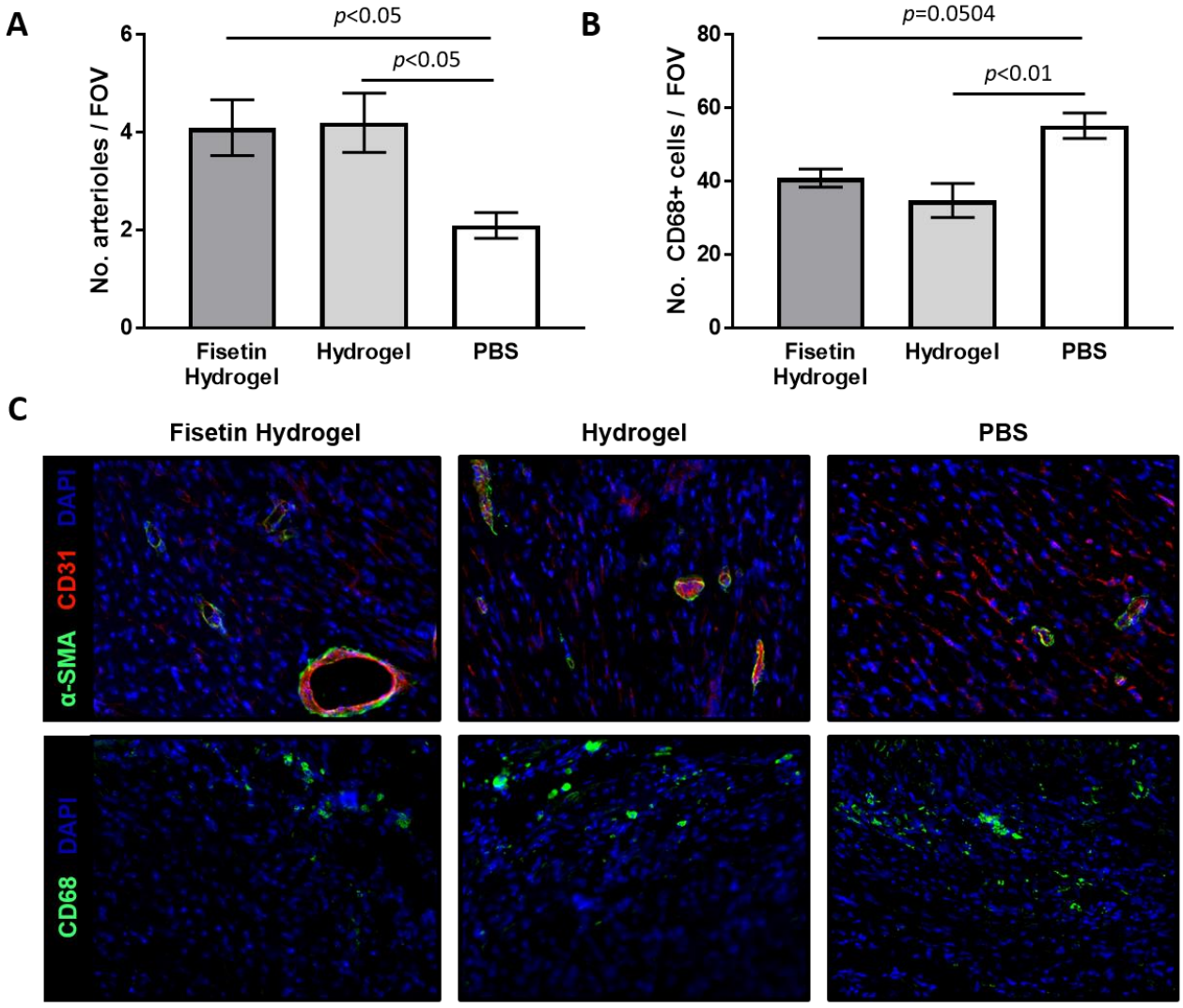

Figure 3.19 Hydrogel therapies improve vascular density and reduce macrophage number at 5 weeks post-treatment. (A) Arteriole density assessed using fluorescence immunohistochemistry with tissue stained for CD31 and α-SMA in Fisetin-hydrogel, hydrogel and PBS treated animals. (*n*=4 per group). (B) Quantification of CD68+ macrophages in Fisetin-hydrogel, hydrogel and PBS treated animals at 5 weeks post-treatment. (*n*=4) (C) Representative images of immunofluorescence stained tissue showing arteriole density (top panels) and macrophages (bottom panels). Data is presented as a mean ± SEM and analyzed using one way ANOVA with Tukey post-hoc test for multiple comparisons.

Chapter 4

Discussion

4.1 Summary

Patients today who suffer from MI are likely to survive the initial insult. However, despite the considerable progress that's been made in the treatment of MI, many patients will progressively decompensate and experience cardiac failure. Up to 30% of patients hospitalized for HF have prior history of MI (Ambrosy et al., 2014). According to a recent study, every 5% increase in infarct size contributed to a 20% increase in the relative hazard for all-cause mortality or hospitalization for HF within 1 year following primary percutaneous coronary intervention (Stone et al., 2016). How the heart remodels in response to the injury determines whether a patient will functionally stabilize or face a clinical syndrome with limited therapeutic tools. Thus, there is a need for new molecular targets and therapies.

Much work has been accomplished that broadens our understanding of the cellular and molecular events that characterize the heart's response to ischemia, yet our knowledge is still incomplete. AIM 1 of this thesis sought to identify a novel mediator of cardiac remodeling. We hypothesized that MG accumulates as a result of cardiac ischemia and that this accumulation is deleterious to the host repair response. As will be discussed, a major contribution of this thesis is the finding that MG participates in the adverse remodeling and functional decompensation that occurs post-MI. Previous studies had alluded to a possible role, though none had causatively shown that MG-derived AGEs accumulate and actively contribute to the worsening of cardiac function and adverse geometric remodeling of the myocardium. We demonstrated this using a

transgenic mouse that over-expresses GLO1 under the control of preproendothelin-1 (PPE-1) (Vulesevic et al., 2014; Vulesevic et al., 2016). Additionally, we highlight several possible means through which MG may be affecting the outcome of remodeling.

AIM 2 of this thesis was to assess the efficacy of a collagen-based hydrogel for the treatment of MI. We had hypothesized that a collagen hydrogel could mediate the host repair response, leading to functional and geometric preservation. It was observed that the hydrogel could interact with the host tissue and positively direct the repair response resulting in the preservation of cardiac function and mitigation of adverse remodeling. Additionally, we showed that delivery timing is a crucial clinical parameter for hydrogel therapies. Indeed, though we characterized an ideal time point for the delivery of our material, our results combined with those from other groups leads us to believe that the optimal time to deliver a biomaterial for therapy will likely be dependent on its specific construction and how it is intended to interact with the host (Kadner et al., 2012; Landa et al., 2008; Yoshizumi et al., 2016). This indicates that delivery timing is an important element to consider for any cardiac therapy going forward.

The final contribution of this thesis was to combine the knowledge gained from AIMs 1 and 2 into developing a hydrogel therapy that could target MG post-MI. We hypothesized that the combination would lead to additive benefits in preservation of function and remodeling over either therapy alone. Indeed, we showed that the flavonoid Fisetin combined with a collagen hydrogel can lead to functional improvements in the MI mouse heart.

Together the work covered in this thesis provides new insights into post-MI remodeling, specifically the identification of a novel mediator MG, and characterizes a biomaterial therapy design to limit adverse remodeling and improve cardiac function, including a strategy to act on this novel mediator.

4.2 The Contribution of MG to Post-MI Cardiac Remodeling

The primary goal of AIM 1 was to determine if MG production post-MI contributes to adverse remodeling and cardiac dysfunction. Our main findings are that: 1) MG-AGEs are produced acutely post-MI and accumulate in the myocardium; 2) over-expressing GLO1 prevents MG production and accumulation post-MI resulting in less cell death, reduced scar size and preserved cardiac function; 3) GLO1 over-expression promotes greater c-kit+ cell recruitment and higher vascular density; and 4) MG-modified collagen impairs the angiogenic properties of human PBMCs. Taken together, this is the first evidence that MI stimulates the acute production of MG-AGEs and causally links their accumulation to on-going cardiac remodeling and dysfunction in non-diabetic post-MI hearts.

4.2.1 Clinical Studies on the Effects of MG and AGEs in CVD

The toxic effects of MG have been researched widely in aging, obesity, chronic renal disease, and most extensively in diabetes (Maessen et al., 2015; Rabbani et al., 2016b). Knowledge of the role that dicarbonyl stress plays in diabetic CVD is expanding,

but comparatively little is known of it in non-diabetic heart disease (Hartog et al., 2007a; Hartog et al., 2007b; Rabbani et al., 2016b; Vulesevic et al., 2016). In one clinical study, Hartog et al. found that the levels of the CML adduct in the plasma of patients with congestive HF was related to the severity and prognosis of the disease. CML levels also predicted patient outcome despite adjustments for age, gender, aetiology and some other known HF predictors (Hartog et al., 2007b). The concept of AGE involvement in HF was born from studies showing that AGE crosslink breakers improved arterial and ventricular function in older rhesus monkeys (Vaitkevicius et al., 2001) and can rescue cardiac dysfunction and AGE accumulation in experimental diabetic rats (Cheng et al., 2005). Hanssen et al. found that both CML and MG-H1 were associated with a rupture prone phenotype of human carotid atherosclerotic plaques (Hanssen et al., 2014). Additionally, they found that CML and MG-H1 expression co-localized with cells staining positive for CD68 (macrophages) and active caspase 3 (apoptotic), suggesting a possible inflammatory axis. CML and MG-H1 adducts also localized to hypoxic regions of the plaque, and when the authors cultured U937 monocytes in hypoxic conditions they found reduced GLO1 activity (Hanssen et al., 2014). Adding TNF-α to the cultured cells further impaired GLO1 activity resulting in increased MG-H1 formation (Hanssen et al., 2014), which helps to explain why MI may be stimulating the production of MG-H1. The effects of TNF-α on GLO1 activity had been reported before (Van Herreweghe et al., 2002). Indeed, some of the strongest evidence to surface recently implicating a role for MG-AGEs in CVD was the finding that *GLO1* was identified as a key driver in a gene network strongly associated with CAD (Makinen et al., 2014).

4.2.2 *In vivo* and *in vitro* Studies of the Effects of MG and AGEs in CVD

Our group recently published a study highlighting the effects of MG-AGE on endothelial cell survival and inflammation in a mouse model of diabetic cardiomyopathy (Vulesevic et al., 2016). In this study, GLO1 over-expression mitigated the loss of endothelial cells and reduced TNF-α production from BMDMs (Vulesevic et al., 2016). The results of Vulesevic et al. are consistent with other studies that demonstrate that MG contributes to diminished neovascularization, endothelial cell death, and impaired remodeling in diabetic animals (Crisostomo et al., 2013; Pedchenko et al., 2005; Talior-Volodarsky et al., 2012; Thangarajah et al., 2009; Van Herreweghe et al., 2002). These studies have demonstrated the impact of MG on diabetes related CVD and some of the hallmark mechanisms; however, such an understanding of MG-AGEs in non-diabetic related CVD is lacking. The central thesis of AIM 1 was that MG-AGEs contributed to impaired MI remodeling and repair in non-diabetic animals. However, given the known susceptibility of diabetics to MG-mediated damage, this may be a mechanism involved in the higher incidence of CVD in diabetes.

No research, to our knowledge, has explicitly investigated MG in a chronic MI model. However, there are some studies that have provided some insights. One study investigated GLO1 over-expression in a renal ischemia-reperfusion injury in rats (Kumagai et al., 2009). The authors reported that I/R impaired the activity of GLO1 and resulted in increased CEL staining assessed by histology (Kumagai et al., 2009). GLO1 over-expression appeared to mitigate I/R induced cell death, the accumulation of CEL

and modestly improved kidney function as shown by reductions in blood urea nitrogen (BUN) levels (Kumagai et al., 2009). The authors reported that impaired GLO1 activity did not correlate with reduced protein or mRNA levels, suggesting secondary means, possibly through inflammatory cytokines such as TNF-α (Van Herreweghe et al., 2002).

A few cardiac I/R studies have been reported. Bucciarelli et al. assessed I/R in WT and RAGE-null mice (Bucciarelli et al., 2006). The authors reported that I/R stimulated the production of MG, and that both exogenously administered soluble RAGE (sRAGE) to rats and RAGE-KO mice completely prevented this increase (Bucciarelli et al., 2006). Moreover, hearts from RAGE-KO mice showed higher left-ventricular diastolic pressure (LVDP) recovery and decreased release of lactate dehydrogenase (LDH) (Bucciarelli et al., 2006). However, the experiments were conducted in a perfused isovolumic isolated heart preparation, complicating the interpretation given that this eliminates the bone-marrow, kidney and neurohormonal axis to the injury. Moreover, the results still did not establish whether it was decreased RAGE signaling or MG production that contributed to the observed benefits. Another study used a surgical model of I/R in RAGE-KO and sRAGE treated mice (Aleshin et al., 2008). Both the RAGE-KO, and sRAGE treated mice were protected from I/R injury and demonstrated similar histological findings to our own, including reduced caspase activation and TUNEL+ cells, reduced infarct sizes, and improved function of the heart (Aleshin et al., 2008). The authors also identified JAK and STAT signal transduction as possible downstream effector pathways. Interestingly, the authors presented results showing that ischemia contributed to the production of MG and reperfusion to the accumulation of AGE epitopes, but these experiments were not

repeated in the sRAGE or RAGE-KO mice. Therefore, the specific role(s) of MG-AGEs in this model remain unknown.

4.2.3 GLO1 Over-expression Improves Cardiac Remodeling and Function Post-MI

Our results present a compelling argument that, though MG-AGE production may initially be a consequence of MI, MG-AGEs are also a contributor to the ensuing cellular changes, LV remodeling and deterioration of cardiac function. We found that MG levels were elevated in mice as soon as 6h post-MI with 52% more MG-H1 production in the myocardium compared to non-MI mice. Moreover, our histological analysis demonstrated that these adducts accumulate in the myocardium up to 4 weeks post-MI. GLO1 over-expression reduced MG-AGE accumulation and conferred cardioprotection. We observed functional benefits as early as 1 week, which persisted to 4 weeks post-MI. This suggests that MG-AGE accumulation was deleterious from the onset of ischemia. Specifically, GLO1 mice had greater LVEF, showed improved chamber dimensions, and had smaller infarct scar size. Though no difference in cardiac output between WT and GLO1 mice was observed at 4 weeks, this effect may be temporary. The maintained cardiac output with the progressive loss of contractility and increased dilatation in the WT cohort may be indicative of early stage HF (Kemp and Conte, 2012). In contrast, the protective effect of GLO1 over-expression may either delay this process or altogether prevent it; however, a comparison of the progression to HF remains to be investigated in future long-term studies with our model. Overall, our results

demonstrate that MI, in the absence of diabetes, stimulates MG and AGE accumulation, which contribute to the negative remodeling and progressive loss of cardiac function.

4.2.4 Mechanisms of MG Action

4.2.4a Cell Death

Identifying a precise mechanism for the action of MG is challenging, as MG is a chemically promiscuous molecule that affects numerous signaling pathways and cell functions (Rabbani et al., 2016b). Furthermore, as mentioned, many of the reported *in vitro* studies have been performed with concentrations of MG that far exceed the levels present in (patho)physiological systems (Rabbani and Thornalley, 2014), possibly confounding the interpretation of the *in vivo* actions of MG. Our GLO1 transgenic mouse model provides the advantage of studying physiologically relevant concentrations of MG and its consequences in the pathology of disease. For example, our lab recently reported that MG contributes to the development of diabetic cardiomyopathy through inflammation and endothelial cell death in a mouse model of type 1 diabetes (Vulesevic et al., 2016). In the literature, MG has been shown to influence cell death and apoptosis, to impair angiogenesis and neovascularization, and to modify and impair ECM signaling (Rabbani and Thornalley, 2012; Rabbani et al., 2016b). Since these are prominent processes in post-MI cardiac remodeling, we investigated them in the present study. Apoptosis during LV remodeling (independent of the immediate post-MI necrotic death) appears to contribute to myocardial ischemia and HF (Kang and Izumo, 2003). In HF,

usually less than 1% of cells are dying at a given time, leading to a progressive loss of cardiomyocytes and deterioration of the heart (Kang and Izumo, 2003). Expression of active caspase-3, one of the final effectors of apoptosis, is increased in HF patient hearts, and its over-expression in an MI mouse model increased scar size and reduced cardiac function (Condorelli et al., 2001). Moreover, MG-AGEs have been shown to induce caspase-3 activation and cardiomyocyte apoptosis via oxidative stress and the MAP-kinase pathway (Li et al., 2007). In our study, GLO1 mice had less active caspase-3+ and TUNEL+ cardiomyocytes at 28d post-MI demonstrating the potential for GLO1 over-expression to confer protection from apoptosis. Caspase 3 activation has been shown to be involved in the hypertrophic response of cardiomyocytes (Putinski et al., 2013), which is why we also stained for TUNEL+ cells. Reduced cell death was also observed in non-cardiomyocyte cells in GLO1 compared to WT mice. Limiting the on-going cell death in the myocardium may partially explain the functional benefits and reduced infarct size in GLO1 mice. Despite the low numbers of cells implicated, it could still be reasoned that even a low amount of persistent, ongoing death is enough to impair remodeling of the myocardium, particularly since myocytes seem to have near negligible turnover (Bergmann et al., 2009). Whether these effects are the result of a direct action of GLO1 or secondary to other mechanisms is unclear. A likely scenario is that multiple GLO1-mediated factors contribute to preserving myocardial viability, including secondary effects of improved post-MI neovascularization.

4.2.4b Contributions of the Bone Marrow

The extent of continued cell death and adverse remodeling post-MI is related, in part, to the loss of myocardial vascularity. A number of studies have highlighted the role that MG plays in impaired angiogenesis in diseases such as diabetes (Rabbani et al., 2016b). Our results suggest that similar MG-mediated anti-angiogenic mechanisms exist in MI. We demonstrated that greater vascular density post-MI could be achieved by limiting the production of MG-AGEs (via GLO1 over-expression). Important to neovascularization of the MI heart is the recruitment of angiogenic BM cells (Fazel et al., 2006). Stimulating greater recruitment of BM cells has been shown to increase capillary density, reduce remodeling and improve function in MI mice (Ohtsuka et al., 2004). Notably, the contribution of mobilized c-kit+ BM cells has been shown to be critical for promoting angiogenesis post-MI (Fazel et al., 2006). In the present study, the recruitment of c-kit+ cells, their adoption of an endothelial phenotype (c-kit+CD31+) and their incorporation into arterioles in the infarcted heart was greater in GLO1 mice compared to WT mice. Although we did not identify the source of these cells, we observed increased mobilization of angiogenic c-kit+VEGFR2+ cells in the peripheral circulation, and there is strong evidence in the literature to suggest that cardioprotective c-kit+ cell populations originate largely from the BM and participate in driving efficient cardiac repair (Fazel et al., 2006). In addition to improved recruitment to the myocardium, it is likely that GLO1 over-expression in the recruited BM cells protects them in the high dicarbonyl stress environment and improves their pro-angiogenic capacity, as our lab has previously demonstrated with these transgenic mice

(Vulesevic et al., 2014; Vulesevic et al., 2016). Nevertheless, our results still cannot exclude a contribution from c-kit+ cardiac cells originating from the myocardium, which have also been shown to possess greater pro-angiogenic function in GLO1 mice (Molgat et al., 2014). To address this limitation, future work could involve the use of a bone marrow transplant model, as we have done previously (Vulesevic et al., 2014). In this experiment, the bone marrow of GLO1 mice would be transplanted into sub-lethally irradiated wild-type littermates, and the bone marrow from wild-type mice could be transplanted into GLO1 mice. Overall, four groups would be assessed: GLO1 mice with GLO1 bone marrow, WT mice with WT bone marrow, GLO1 mice with WT bone marrow, WT mice with GLO1 bone marrow. This experiment would serve to demonstrate the relative contribution, if any, that GLO1 over-expression in the bone marrow has on the total effect of GLO1 over-expression on the preservation of cardiac function and improved post-MI repair response.

4.2.4c Modifications to the ECM

In addition to cellular effects, MG modification of the cardiac ECM may be an important contributor to CVD given that it has a >10-fold longer turn-over than other cardiac proteins (Talior-Volodarsky et al., 2012; Yuen et al., 2010). Collagens and the arginine residues within their integrin recognition domains constitute major targets for MG-mediated glycation (Dobler et al., 2006; Venkatraman et al., 2001; Verzijl et al., 2000), potentially disrupting cell-ECM interactions that are essential for cell phenotype and function (Discher et al., 2009). Notably, collagen glycation has been shown to

negatively affect angiogenesis and vascular repair *in vitro* and *in vivo* and promote pro-fibrogenic myofibroblast differentiation in diabetic cardiomyopathy (Francis-Sedlak et al., 2010; Kuzuya et al., 1998; Talior-Volodarsky et al., 2012), but this has not been established in the context of MI. In our study, there was decreased MG-AGE content in the infarcted tissue of GLO1 mice, and more specifically, a marked reduction in MG-AGE modified collagen surrounding the vasculature, compared to WT mice. This suggests that MG-modification of collagen in the ECM may contribute to defective neovascularization post-MI. Given that the recruitment of PBMCs is important for promoting vascular repair post-MI, we performed *in vitro* experiments to elucidate the effect of MG-modified collagen on the phenotype and function of human PBMCs. MG-modified collagen supported less PBMC adhesion and impaired their ability to promote and participate in angiogenesis. Furthermore, collagen glycation has been shown to induce endothelial cell anoikis (cell death resulting from detachment) (Dobler et al., 2006), and we similarly observed reduced viability of CD133+ progenitors and CD31+ and CD144+ endothelial fractions in apoptosis-inducing conditions for PBMCs cultured on the MG-modified collagen.

It is worth noting that many *in vitro* cell studies employ concentrations of MG of 200uM, 1mM or higher. The best estimates place MG concentrations in the 50 – 150nM in human plasma and 1-4μM in cells, with possibly a 1.5-3 fold increase in pathophysiological states (Rabbani and Thornalley, 2014). Therefore, whether the results of many *in vitro* MG studies are physiologically applicable is difficult to assess. In our study, we employed 1mM MG to experimentally glycate collagen. We feel this is

different from the MG cell studies for several reasons. For one, there appears to be physiological justification. Talior-Volodarsky et al. investigated ECM glycation in a rodent model of diabetic cardiomyopathy (Talior-Volodarsky et al., 2012). In their study, the authors reported that 1mM MG glycation *in vitro* approximated the extent of ECM glycation in their *in vivo* model. One difference is that our animals are not diabetic, and thus it is possible that our *in vitro* studies are slightly over-estimated. Another consideration is that our *in vitro* studies using experimentally glycated collagen asks a separate question from *in vitro* studies using 1mM MG in cell culture. Most, if not all, 1mM MG culture studies are attempting to determine the targets of MG glycation and downstream mediators and impact. However, given the reactivity of MG they may be identifying targets that are not normally modified by MG in nature. Our studies have already assumed collagen as the target; therefore, we are attempting to assess the impact of MG-modified collagen on the behavior of angiogenic PBMCs that subsequently interact with the modified collagen substrate. Using a lower concentration may run the risk of diluting the effects, where the majority of cells would be interacting with native collagen vs. "modified" collagen. Our model ensures cells interact with the modified substrate and, thus provides some insight into what may occur *in situ* when PBMCs arrive to the myocardium and interact with modified ECM.

Taken together, our results suggest that MG-mediated collagen glycation may interfere with cell-ECM interactions and limit the recruitment, viability and function of angiogenic cells leading to reduced vascularization in the MI heart.

4.2.4d Additional Mechanisms of MG

MG has been shown through various studies to be promiscuous and given the numerous intra- and extra-cellular targets for MG glycation, several mechanisms likely contribute to its detrimental effects post-MI. Although we identified ECM glycation as a possible mechanism, the modification of intracellular signaling cannot be excluded (Maessen et al., 2015). One likely signaling pathway negatively affected by MG in the post-MI heart is the hypoxia-inducible factor-1α (HIF-1α) pathway, which is essential in the adaptive responses of cells to hypoxia. MG inhibits HIF-1α activity leading to decreased transcription of its targets genes and reduced angiogenesis (Ceradini et al., 2008). HIF-1α target genes include VEGF, stromal cell-derived factor-1 and erythropoietin, which are cardioprotective against MI (Cochain et al., 2013; Tekin et al., 2010). Thus, GLO1 over-expression may have increased the production of such growth factors by preventing MG interference on HIF-1α activity. Identifying the various MG targets and distinguishing between primary and secondary effects of MG post-MI presents a future research opportunity. Regardless, our study highlights that targeting MG-AGE production post-MI offers cardioprotective benefits.

4.2.5 The PPE-1 *hGLO1* Animal Model to Study Effects of MG on Post-MI Cardiac Remodeling

We studied the influence of MG on post-MI cardiac remodeling using a transgenic mouse model designed to over-express *hGLO1* under the control of PPE-1. GLO1 over-expressing rats have been used to investigate the contribution of MG to

diabetic complications *in vivo* such as diabetic nephropathy (Brouwers et al., 2011). Using this specific transgenic animal model, our lab has shown that GLO1 over-expression in the bone marrow can rescue defective neovascularization caused by streptozotocin (STZ) induced-diabetes in mice (Vulesevic et al., 2014). Our lab has also reported that GLO1 over-expression can rescue cardiac dysfunction in a model of diabetic cardiomyopathy (Vulesevic et al., 2016).

A limitation of our study is that we confirmed elevated GLO1 activity in our mouse model at the whole tissue level in non-infarcted hearts (Vulesevic et al., 2016); however, we have not evaluated GLO1 activity in either infarcted hearts or at the cellular level. The *hGlo1* transgene is under the control of the preproendothelin-1 (PPE-1) promoter, which is highly expressed in the vasculature of the heart (Harats et al., 1995). However, during MI, elevated PPE-1 mRNA expression has been reported in salvaged cardiomyocytes, endothelial cells, vascular smooth muscle cells, and inflammatory cells within the fibrotic tissue (Tonnessen et al., 1998). Also, we have confirmed GLO1 transgene expression in the BM compartment (Vulesevic et al., 2014); therefore, it is likely that GLO1 over-expression is present in most, if not all, cardiac cells in the infarcted hearts of GLO1 mice. The presence of GLO1 expression in the vascular and BM cells likely explains the benefits we found with neovascularization and the recruitment of bone marrow cells. However, whether the rescue of cardiomyocytes and other cardiac cells is a primary effect of the model or secondary to the survival of the vasculature and recruitment of pro-survival bone marrow cells is unknown. Likely, both mechanisms contribute. Future interrogations of the mechanism through which MG

effects in specific cell types contributes to post-MI cardiac remodeling could be conducted. Nevertheless, the model used in the work conducted as a part of this thesis provided compelling evidence of the role that MG plays in post-MI cardiac remodeling.

4.3 Timing underpins the benefits associated with injectable collagen biomaterial therapy for the treatment of myocardial infarction

The principal objectives of AIM 2 were: 1) to assess the efficacy of our collagen matrix biomaterial for the treatment of post-MI adverse cardiac remodeling and 2) determine whether timing of the delivery post-MI played a significant role in the efficacy of the treatment. The results show that the collagen matrix hydrogel mitigates cardiac functional loss, prevents negative cardiac remodeling, reduces final scar size, and positively impacts the host repair response. Additionally, we demonstrated that delivery timing underpins the benefits associated with the hydrogel therapy, showing that delivering the material early, possibly coinciding with the inflammatory phase, produces the most benefits.

4.3.1 Timing the Injection of Hydrogels Post-MI

One of the principal objectives of this AIM was to delineate the ideal time point to deliver our acellular collagen biomaterial post-MI. The ideal time point to deliver hydrogels post-MI is an important clinical parameter owing largely to the dynamic and time dependent evolution of molecular and cellular events that occurs following myocardial tissue ischemia. Interestingly, despite this being an important consideration, the impact of timing on injectable hydrogels for treating MI had been largely overlooked in most study designs (Burdick et al., 2013; Johnson and Christman, 2013; Radhakrishnan et al., 2014). In the literature, most studies evaluating a potential

hydrogel therapy investigate a single time-point ranging from immediately (often immediately following LAD occlusion to 30 minutes post-infarct), 1 week, to 2 months post-MI (Burdick et al., 2013; Johnson and Christman, 2013; Radhakrishnan et al., 2014). Though many therapies delivered immediately post-MI (time = 0 hours) have shown benefits in rodent models, the clinical translation of this time-point is questionable given that it is unlikely any patient would be able to receive the therapy so soon following the onset of ischemia. Indeed, patients presenting with acute coronary symptoms arrive in the clinic in the range of 1.5 to 15.2 hours after the MI event (Goldberg et al., 2000; Khraim and Carey, 2009).

An advantage of 1 or 2 week time-point delivery is that the heart condition is stabilized prior to injection. Materials delivered at such a time may also intervene on the global cardiac remodeling that often occurs following the maturation of the scar. Most time-points in most animal models have demonstrated some degree of efficacy on either cardiac function, LV remodeling or both (Burdick et al., 2013; Johnson and Christman, 2013; Kadner et al., 2012; Landa et al., 2008; Radhakrishnan et al., 2014; Yoshizumi et al., 2016). However, in most rodent models by 1 week post-MI, significant myocardial deterioration and functional decompensation has already occurred, which may limit the potential for the therapy to rescue viable myocardium. Therefore, we chose our early time point to be 3 hours post-MI, which is, arguably, more clinically relevant than immediate delivery of the material. Indeed, it is feasible that a narrow window exists where the most myocardial salvage can occur (Fig 4.1), which may also be

dependent on the specific material being used and the mechanism of its benefits, as discussed further below.

Our results demonstrate that our earliest time-point, 3 hours post-MI, was the most effective. Specifically, when we delivered the material at this time-point the deterioration of cardiac function (%LVEF, SV, CO, and %FS) and remodeling of the myocardium (scar size, ESV, EDV, fibrosis) was mitigated and, in a subset of animals, cardiac function appeared to be stabilized long-term (3 months post-treatment). Later delivery time-points were not as effective at preventing functional decompensation or myocardial remodeling. The 7 day delivery of the material conferred modest benefits to cardiac function and the 14 day therapy did not offer any improvement. Moreover, we witnessed a higher mortality associated with the 14 day delivery. This is likely owing to the fragile nature of the myocardium (i.e. thinner myocardial scar at 14 days) with repeated injections increasing the risk of cardiac rupture significantly. Together, these results indicate that the collagen matrix, when delivered early, can significantly improve myocardial function post-MI.

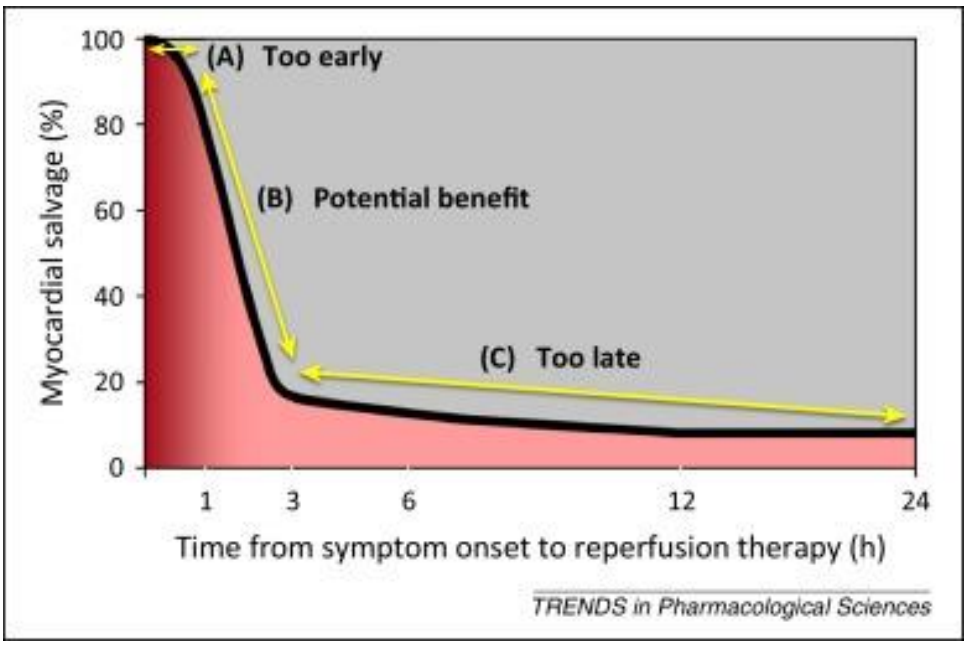

Figure 4.1 Application of potential therapies to reduce myocardial salvage in relation to ischemic time. (A) No benefit: infarct size too small to make a difference. (B) Potential benefit: during the rapid loss of potential myocardial viability. (C) No benefit: too late to make a difference.

From Fordyce CB, Gersh, BJ, Stone, GW, and Granger, CB (2015). Novel therapeutics in myocardial infarction: targeting microvascular dysfunction and reperfusion injury. Trends in Pharmacological Sciences 36, 605-616. Reprinted with permission from Elsevier Ltd.

To our knowledge, only one other study has investigated multiple time-points for a naturally derived material for the treatment of MI. Landa et al. injected alginate based hydrogels into 1 week and 8 week old infarcts in rats and reported more favorable effects on wall thickness and parameters of remodeling for the 1 week treatment group (Landa et al., 2008). Their results appear consistent with our own, that earlier delivery was more effective. However, their study did not include an injection time sooner post-injury. Further comparison between the two studies is complicated by hydrogel design, alginate vs. collagen, and animal model (i.e. rat vs. mouse). To our knowledge no direct comparison between the responses of rats and mice in the experimental MI procedure has been conducted, though qualitatively others have reported differences between the two (Lutgens et al., 1999) and other species specific differences have been reported (Dewald et al., 2004).

In contrast to our results, and those published by Landa et al., others have shown that for synthetic hydrogels, later delivery may be more appropriate. Both Kadner et al. and Yoshizumi et al. have reported that delayed injections for synthetic materials were more beneficial to cardiac function and remodeling (Kadner et al., 2012; Yoshizumi et al., 2016). Kadner et al. assessed two delivery time-points, immediately and 7 days post-MI for a PEG hydrogel and found that immediate delivery of the material did not result in any observable improvements (Kadner et al., 2012). Rats receiving the material at 7 days had higher % fractional shortening (%FS), improved end-systolic diameters (ESD), and increased scar thickness at 4 weeks post-MI compared to saline treated animals (Kadner et al., 2012). How exactly their hydrogel proved

beneficial to myocardial remodeling was left relatively unexplored. The authors did report a greater resistance to degradation of their hydrogel when delivered at 7 days vs. immediately post-MI (Kadner et al., 2012). More recently, Yoshizumi et al. compared the influence of delivery timing using a relatively stiff, biodegradable, synthetic hydrogel (Yoshizumi et al., 2016). In their study, the authors delivered their hydrogel immediately after, 3 days and 2 weeks post-MI in rats. They found that delivering the hydrogel 3 days post-MI had the greatest impact on cardiac function, end-systolic and end-diastolic areas (ESA, ESD), and infarct size, while delivering the material at 2 weeks had a more modest impact and early delivery almost no observable benefits (Yoshizumi et al., 2016).

Several of the aforementioned studies appear to suggest that the length of time that a material persists in the myocardium influences its efficacy; however, the mechanisms behind delivery timing are likely more complex. Materials designed to participate in the host repair process may not be required in the myocardium indefinitely, while those designed to increase wall thickness and decrease stress through Laplace's law (Burchfield et al., 2013) may be required to persist longer. As such, there appears to be a mix of results between when the material is delivered, how long it persists in the myocardium and the overall benefit of the delivery. For example, some materials delivered immediately post-MI have been shown to persist in the myocardium long-term, though having almost no impact on function (Dobner et al., 2009). Similarly, using a synthetic bioinert PEG hydrogel material designed to remain within and passively reinforce the myocardium, Rane et al. demonstrated that this was insufficient to improve or preserve cardiac function (Rane et al., 2011).

Together, it appears that a specific, optimal time to deliver a broad range of hydrogels is impossible to recommend. Proper delivery timing for a material likely depends much on its design and how it is intended to interact with the host and mediate the repair response. In summary, timing the delivery of a hydrogel post-MI is an important clinical parameter that should be considered for any study for hydrogels moving forward.

4.3.2 Mechanisms of Action

4.3.2a Mechanical Reinforcement vs. Bioactivity

As indicated, a number of injectable hydrogels have been shown to improve or preserve cardiac function or mitigate remodeling post-MI (Johnson and Christman, 2013; Radhakrishnan et al., 2014). However, the precise mechanisms that govern their benefits remain poorly understood. Whether the material is synthetic, or naturally derived, or whether the material is soft or stiff, or native or functionalized, likely contributes significantly to the underlying mechanisms. For example, some synthetic, stiff hydrogels may be theoretically able to stabilize the injury by increasing wall thickness and decreasing stress in the infarcted zone, border and remote healthy areas of the myocardium (Burchfield et al., 2013; Wall et al., 2006). It's further possible that the reduction in mechanical load would influence signaling pathways and cell behavior via mechanoreceptors (Discher et al., 2009; Sutton and Sharpe, 2000). Indeed, Yoshizumi et al. found that the benefits associated with their relatively stiff, synthetic

hydrogel delivered at 3 days post-MI, though not specifically investigated, were likely a result of mechanical stabilization of the myocardium (Yoshizumi et al., 2016). It's feasible that if the design principle was to mechanically stabilize the myocardium, then immediate delivery would result in premature degradation, since the early post-MI myocardium is characterized by profound changes to MMP and TIMP regulation (Webb et al., 2006). Although, it appears that was unlikely the sole mechanism at play. Other hydrogels have been shown to preserve wall thickness, but failed to provide functional benefits (Dobner et al., 2009; Ifkovits et al., 2010; Sun and Nunes, 2015), despite being delivered early and found to persist in the myocardium. Therefore, whether altering myocardial stress profiles influences remodeling is debatable. As mentioned earlier, Rane et al. assessed the role that mechanical stabilization plays in preventing adverse remodeling using a bioinert PEG hydrogel delivered at 7 days post-MI (Rane et al., 2011). They showed that despite increased wall thickness resulting from the material injection, animals receiving the hydrogel did not experience benefits in ESV, EDV, or cardiac function (Rane et al., 2011). The authors concluded that passive structural reinforcement was insufficient to prevent post-MI remodeling. In contrast, injection of alginate has shown to produce functional benefits while the material appeared to be completely degraded prior to the onset of the observed benefits (Landa et al., 2008). This suggests, as mentioned previously, that a hydrogel's persistence in the myocardium isn't an absolute requirement to produce benefits with the therapy and that the contribution of mechanical reinforcement in the benefits of hydrogel therapies is not a given.

For softer hydrogels, such as the one investigated in this thesis, imparted bioactivity of the material is what is expected to contribute to the benefits of the therapy (Kuraitis et al., 2012). Indeed, the goal of many hydrogel designs is to interact with various host processes. For example, the hydrogel developed by Kadner et al. was polymerized with an MMP-1 enzymatically degradable peptide sequence (Kadner et al., 2012). Hydrogels designed to specifically interact with the remodeling process seem to produce considerable benefits (Eckhouse et al., 2014; Purcell et al., 2014). Meanwhile, ECM-derived materials similar to our own likely take advantage of native ECM-cell signaling to influence remodeling (Seif-Naraghi et al., 2013). Naturally derived ECM biomaterials (Dai et al., 2005; Seif-Naraghi et al., 2013) or functionalized hydrogels (Eckhouse et al., 2014; Garbern et al., 2011; Lin et al., 2012) may surface as candidate hydrogel choices for therapeutic targeting of post-MI remodeling. Rather than relying on passive reinforcement of the myocardium, these strategies appear to provide natural binding sites and/or promote ECM-cell responses and signaling to modulate the host wound repair cascade (Kuraitis et al., 2012; Rosso et al., 2004). Dr. Christman's group recently published on their myocardial matrix hydrogel, one derived from decellularized porcine ventricular myocardium, and found that their hydrogel interacted with the host repair responses (Wassenaar et al., 2016). They found that the transcriptomes of animals treated with the ECM hydrogel clustered differently than those treated with saline. In their study, matrix-treated animals showed an altered inflammatory response, reduced myocyte apoptosis, enhance neovascularization, lessened fibrosis, altered metabolic enzyme expression and increased progenitor cell recruitment (Wassenaar et

al., 2016). As will be discussed below, these findings are similar to our observations. We expected the hydrogel to offer bioactive benefits and given the importance of cell-ECM interactions, we investigated similar processes in post-MI repair that would be altered by our matrix therapy including inflammation and cell death.

4.3.2b Inflammation and Cell Death

We found that the greatest benefit of our therapy was when it was delivered at 3 hours post-MI, which coincides with the early inflammatory phase of post-infarction repair. Though chronic, unabridged inflammation is a major determinant of adverse cardiac remodeling, interfering with the early inflammatory process has been shown to be detrimental as well. This impairs efferocytosis and delays the removal of other necrotic cell debris and worsens the deterioration of cardiac function. Therefore, we deemed it important to investigate the hydrogels effect on the inflammatory response. We assessed early inflammation at 2 days post-MI from sectioned tissue and did not find the hydrogel to impair the recruitment of the Ly6G+ neutrophil or F4/80+ macrophage populations to the infarct or border zones. This suggested to us that the hydrogel did not exacerbate, nor did it likely impede debris removal from the myocardium. Notably, there was a reduction in CD86+ cells (M1 macrophages) in matrix-treated hearts at 2 days post-MI. Together, these results seem to indicate the suitability of the collagen hydrogel for cardiac therapy, suggesting that it may offer pro-wound healing effects on macrophage function.

We also assessed the hydrogel's influence on persistent inflammation. We observed a reduction in TNF-α levels in matrix treated animals. TNF-α is a pleiotropic cytokine, considered to be one of the master regulators of inflammation (Hedayat et al., 2010). It is not constitutively expressed in the heart, but is released as a stress response to ischemic injury in the myocardium (Hedayat et al., 2010). Some of its dichotomous behaviour may be via its action through the TNF receptors, TNFR1 and TNFR2. TNF-α appears to be cytoprotective at low physiological concentrations through TNFR2, while at high concentrations it appears to be pro-inflammatory and pro-apoptotic through TNFR1 (Hedayat et al., 2010). The reduction in TNF-α expression in the hearts of mice treated with the hydrogel may be contributing to the decreased cell death observed at both the short- (2 days) and long-term (4 weeks) endpoints by activating the cytoprotective pathways. The differences in cytokine secretion between macrophages cultured on TCPS and those on the hydrogel seem to support this hypothesis. BMDMs were cultured on the material to assess its influence on their function, given their important role in the wound repair process. Indeed, macrophages have surfaced as not only important mediators of inflammation, but they have also been shown to be involved in tissue remodeling and regeneration (Santini and Rosenthal, 2012). The importance of macrophages in tissue regeneration is highlighted in papers that have shown that macrophages are required to provide signals for vascularization of the regenerating neonatal mouse heart (Aurora et al., 2014), and are necessary for adult salamander limb regeneration (Godwin et al., 2013). Our hydrogel appears to modify the secretion behavior of macrophages as shown by our *in vitro* studies. Culturing

BMDMs on the material reduced the secretion of pro-inflammatory cytokines (MIP-1α, MIP-1γ and CCL5) and the soluble TNF receptors, TNFR1 and TNFR2. Increased concentrations of the soluble TNF receptors have been associated with cardiac rupture and impaired remodeling (Monden et al., 2007). Matrix culture also resulted in increased levels of anti-inflammatory and pro-angiogenic cytokines (IL-4 and CXCL5), and matrix remodeling cytokine TIMP-2. Over-expressing TIMP-2 has been shown to improve survival and alter myocardial remodeling post-MI in mice (Ramani et al., 2011). Altogether, our *in vitro* and *in vivo* assessment of macrophages appears to suggest a positive pro-wound healing, anti-inflammatory influence of the hydrogel on these cells and, in turn, post-MI repair.

4.3.2c Angiogenesis and Cell-ECM Interactions

We found that hydrogel treatment, when delivered at 3 hours post-MI, resulted in significant increases in FGF-2 expression at 4 weeks post-treatment. FGF-2 has been associated with reduced expansion of the infarct and preserved function post-MI, likely due to its potent angiogenic and anti-apoptotic properties (Virag et al., 2007). This is consistent with our own results of improved neovascularization, reduced cell death and superior function in hydrogel vs. PBS treated animals. Hydrogel therapy promoted a greater density of capillaries and arterioles, and along with the observed increase in the number of proliferating endothelial cells suggests that the treatment is stimulating the formation of new vessels, and not only protecting existing ones from death.

Previous publications from our lab and others seem to suggest that the cell-ECM interaction is the primary mechanism that explains the effects of hydrogel therapy (Ahmadi et al., 2014; Rane et al., 2011). Indeed, modifications to ECM proteins, including collagens, set upon by the initial inflammatory phase post-MI results in ECM changes that may disrupt ECM-cell interactions required for signaling, survival and function (Bayomy et al., 2012; Dobaczewski et al., 2010). It is probable that our ECM-based hydrogel preserves or restores some element of the host cell-ECM signaling prior to the proliferative phase or maturation of the injury, resulting in improved tissue repair and mitigation of adverse remodeling and functional deterioration.

4.3.3 Limitations – Injection Methods, Animal Models, Additional Mechanisms

Our data provides compelling evidence that timing the delivery of a cardiac therapy, namely hydrogels, is an important clinical parameter requiring further study. Moreover, we've provided evidence of the efficacy of our collagen derived hydrogel in preserving function and preventing adverse remodeling when delivered early post-injury. However, there are limitations to this study.

4.3.3a Injection Methods

One limitation to this work is that we employed ECHO-guided intramyocardial injections of the hydrogel. This approach allows direct visualization of the infarct region to better direct hydrogel injections. Although, it is a practical approach for use in rodent

studies it also constitutes a more invasive approach for patients compared to alternatives. Percutaneous transendocardial delivery may prove favorable and less invasive for patients and may be visualized using NOGA mapping. NOGA guided injections have been used in similar studies conducted in pigs (Singelyn et al., 2012) and were found to be safe (Schussler et al., 2010; Seif-Naraghi et al., 2013). NOGA guiding injections may be technically unfeasibly in rodents, though constitutes a viable opportunity moving forward with our material in larger animal models.

4.3.3b Disease Models

Another limitation of the work conducted in this Aim is that we employed a chronic infarction rodent model (Lutgens et al., 1999). The chronic infarction model offers the opportunity of studying ventricular remodeling resulting from ischemic injury of the myocardium and the progression to failure (Lutgens et al., 1999); however, in the clinical scenario patients are often reperfused and receive other supportive therapies. Additionally, though mice are cost-effective method, they cannot completely recapitulate the human disease. Therefore, a next step in the research should involve moving the study into a larger mammal and assessing the effect of applying the material when the heart is also reperfused. Primary percutaneous coronary intervention is the gold-standard treatment and to gain acceptance in the community, novel therapies will invariably need to be tested in this scenario and provide additional benefits (Fordyce et al., 2015). It is unlikely that a new therapy will gain much acceptance if it cannot be shown to provide additional benefits alongside conventional therapies.

4.3.3c Additional Mechanisms

Another limitation of this work was the limited molecular characterization of the effects of hydrogel therapy on the host post-MI repair processes. Though we did characterize some influences on angiogenesis and inflammation, and our results were consistent with other similar hydrogels (Seif-Naraghi et al., 2013; Wassenaar et al., 2016), not all possible effects of the hydrogel were characterized. For example, fibroblast activity and the MMP/TIMP regulation are important determinants of remodeling post-MI (Spinale, 2007), and other hydrogel strategies that have been designed to target these processes have provided positive outcomes on cardiac function (Eckhouse et al., 2014; McGarvey et al., 2014; Purcell et al., 2014). Given that secretion of TIMP2 was elevated *in vitro* in matrix-cultured BMDMs and reduced penetrating fibrosis was observed in hydrogel-treated hearts, it is possible that the hydrogel may have influenced fibroblast activity and the regulation of matrix remodeling MMPs and TIMPs. These, and other possible mechanisms, constitute further avenues of study in future projects. Nevertheless, the results we presented provide strong evidence of the benefits associated with our hydrogel therapy for post-MI remodeling and that this occurs through the regulation of multiple processes.

4.4 A Functionalized Hydrogel for Targeting MG Post-MI

In AIM 3, we provide results from a study investigating the possible combination of a MG scavenger/GLO1 activator (Fisetin) and our collagen hydrogel to treat post-MI cardiac remodeling. We confirmed that Fisetin concentrations of less than 50uM are not cytotoxic and do not impair angiogenesis *in vitro*. Additionally, we showed that the 10uM MG concentration can reverse the anti-angiogenic effects of 25uM MG on HUVECs. When we attempted to encapsulate the drug within a hyaluronic acid nanoparticle platform we did not find it to produce any differences in the release of the drug from the biomaterial *in vitro*, nor did the NPs appear to release with the drug. Therefore, for the *in vivo* studies, we favored a simpler approach of embedding the drug directly within the material for the treatment of mice at 3 hours post-MI. Animals were followed for 5 weeks and we did not observe any difference in cardiac function between the hydrogel only groups and the combined therapy at study endpoint. However, Fisetin-hydrogel treated animals were the only group to show an improvement in function between baseline and the 5 week time-point. Baseline function was measured at 3 hours post-MI just prior to receiving treatment; this is a time at which, in our experience, some cardiac dysfunction is already present (Figure A4, Appendix A). Additionally, both hydrogel and Fisetin hydrogel treated animals had smaller infarcts, reduced inflammation and improved arteriole density compared to PBS treated animals, though we did not observe any differences between the combined therapy or the hydrogel only treated animals. Therefore, further study is warranted into the possible ability of the Fisetin hydrogel to rescue early loss of function post-MI.

4.4.1 Targeting MG, and AGEs – a Role for Fisetin

As had been previously mentioned, Fisetin is a dietary flavonoid that has been shown to be anti-carcinogenic, anti-oxidant, immune-stimulatory and anti-inflammatory (Khan et al., 2013). Consumption of dietary flavonoids have been associated with a reduced risk of death from CAD in elderly men (Hertog et al., 1993). It is found predominantly in fruits and vegetables in concentrations ranging from approximately 2-160ug/g (Arai et al., 2000). Fisetin's antioxidant properties are the result of direct scavenging of free radicals and other mechanisms (Khan et al., 2013; Markovic et al., 2009). Fisetin has been shown to increase GSH levels (Ishige et al., 2001), and to be protective against peroxynitrite (ROS) possibly though increasing GSH biosynthesis and maintaining Nrf2 expression (Burdo et al., 2008). Specifically in endothelial cells, Fisetin has been shown to induce heme-oxygenase-1 expression and activity through Nrf2 (Lee et al., 2011). Combined with the knowledge that Fisetin upregulates GLO1, potentially through Nrf2, activity and scavenges MG (Maher et al., 2011), we deemed Fisetin as an ideal candidate to target MG *in vivo* combined with our hydrogel therapy.

We delivered our combined Fisetin hydrogel to mice at 3 hours post-MI. We chose this time-point for delivery based on the results obtained in AIM 2. Moreover, in AIM 1, we found that MG-AGE accumulation occurs as early as 6 hours post-MI, and others have found increased MG in the myocardium even sooner post-I/R injury (Aleshin et al., 2008; Bucciarelli et al., 2006). Therefore, we deemed the 3-hour time-point to be appropriate since it both maintained clinical relevance and would likely target MG at a

time when it may be most important; i.e. near the onset of its production. We found that the hydrogel alone and the Fisetin hydrogel maintained cardiac function, reduced the final scar size, increased neovascularization and reduced inflammation. The Fisetin alone delivery produced very discrepant results between animals. It is likely that this bolus dose was quickly flushed from the myocardium, lacking the viscosity of the hydrogels, thus impairing its intended efficacy. Since we did not see benefits associated with the Fisetin only study, this group was abandoned from further study. Although daily or every second day dosing of Fisetin either *po* (oral administration) or subcutaneously may be another strategy for Fisetin administration, we pursued an approach involving biomaterial delivery in part because of its ability to locally target the drug to the relevant tissue, thus reducing the possibility of unwanted off-target effects.

Interestingly, at study endpoint the combined Fisetin hydrogel did not appear to produce additional benefits over the hydrogel therapy in terms of absolute end-point %LVEF. However, we did find that the mean baseline %LVEF (pre-injection) of the cohort of animals receiving the Fisetin hydrogel was lower than those receiving the hydrogel therapy (Figure A4, appendix A). This prompted us to investigate how, individually, cardiac function evolved over the 5-week period for mice treated with the various therapies. We noted that animals receiving the Fisetin hydrogel showed an improvement in cardiac function from baseline to 5 weeks. This could be for several reasons, and warrants further investigation. It is possible that the additional benefits of this therapy may only apply to animals with the weakest baseline cardiac function or the Fisetin hydrogel rescues stunned or hibernating myocardium (Braunwald and Kloner,

1982; Camici et al., 2008; Fordyce et al., 2015). Future studies could investigate the various treatment groups using a cut-off baseline %LVEF (<35-40%). This would allow to fully discriminate whether the Fisetin hydrogel, indeed, does allow functional recovery post-MI over the hydrogel only therapy, or whether this was simply an artifact of the low sample size and skewed distribution of baseline %LVEFs among groups. Other work could also investigate the early repair processes (1-2 days post-injection) in the myocardium, as it may be possible that Fisetin hydrogel allows for quicker recovery. Furthermore, the efficacy of the hydrogel in an I/R model of MI could be examined. As mentioned previously, most patients are reperfused post-MI, which also has the consequence of causing significant ROS formation resulting in reperfusion injury (Fordyce et al., 2015; Hori and Nishida, 2009; Yellon and Hausenloy, 2007). MG and ROS appear to stimulate the production of the other, resulting in positive feedback (Brouwers et al., 2011; Cai et al., 2006; Ceradini et al., 2008; Giacco and Brownlee, 2010), and Fisetin appears to be a potent anti-oxidant and MG scavenger (Burdo et al., 2008; Hou et al., 2001; Ishige et al., 2001; Khan et al., 2013; Lee et al., 2011; Maher et al., 2011; Maher et al., 2007). Therefore, it is likely that in an I/R MI model, the benefits of the combined therapy would be more pronounced.

4.4.2 Functionalizing Hydrogel Biomaterials for Post-MI Cardiac Therapy with Nanoparticles

As previously mentioned, hydrogels for the treatment of MI have shown considerable promise in preventing adverse remodeling and functional decompensation. A number of research groups have attempted to further refine their

therapies through different strategies, for example, by incorporating bioactive ligands (Eckhouse et al., 2014; Fujita et al., 2004; Garbern et al., 2011); electrically coupling their material to the heart (Mihic et al., 2015); combining synthetic and natural derived components to alter mechanical and degradation properties (Xu et al., 2015); or altering their mechanical properties over time (Young and Engler, 2011). An advantage of attempting to deliver bioactive molecules is the ability to target specific processes or signaling cascades such as MMP and TIMP imbalances (Eckhouse et al., 2014). However, the activity of many bioactive compounds has been hindered by short half-lives *in vivo* (Sun and Nunes, 2015). As mentioned, our study involved targeting MG-AGE production that we identified in AIM 1 as being causative in the loss of function and impaired reparative processed post-MI. Our candidate compound, Fisetin, has been shown to target MG either directly through scavenging MG (Maher et al., 2011)(Maher et al., 2011)(Lee et al., 2011; Maher et al., 2011), or via anti-oxidant mediated reduction of MG (Khan et al., 2013; Lee et al., 2011; Maher et al., 2011). However, it is worth mentioning that the majority of the study presented in AIM 3 is observation/phenomenon based vs. mechanism based. Though we described positive effects of the novel hydrogel therapy, future work should involve some interrogation of the mechanisms involved in the benefits. This work could include a determination of MG-AGE levels via liquid chromatography with tandem mass spectrometry (LC-MS/MS) similar to the experiments conducted in AIM 1, as well as assaying the expression and activity of GLO1 and Nrf2. Such experiments could begin to identify the source of the additive effects of

the Fisetin and collagen biomaterial and possibly direct future avenues to further refine the therapy.

As mentioned previously, Fisetin exhibits poor water solubility, chemical instability, poor absorption and extensive and rapid metabolism (Shia et al., 2009). Therefore, in an effort to overcome these pharmacokinetic limitations others have attempted to encapsulate the drug using different nanomedicine strategies (Ghosh et al., 2016; Rengarajan and Yaacob, 2016). Indeed, we also attempted to improve the pharmacokinetics of Fisetin delivered from our material using a hyaluronic acid based polymer (Sun et al., 2016). However, we did not find the HA polymer to alter the release of Fisetin from the hydrogel or to release with Fisetin. Therefore, in this first attempt, it was unlikely that HA-encapsulated Fisetin would provide additional benefits, thus we proceeded with a hydrogel recipe that did not include encapsulating Fisetin. Previous studies that have used different nanomedicine strategies to improve the pharmacokinetics of Fisetin were relying on its *po* or subcutaneous delivery. Given that we were delivering the drug with the biomaterial directly to the heart, encapsulating Fisetin may have been unnecessary. Of course, we cannot exclude the possibility that the lack of efficacy we observed may have been due to the aforementioned limitations of the drug. Therefore, future work could involve further refinement of the HA polymer or alternate strategies at improving the solubility and bioavailability of the drug.

4.5 General Summary and Conclusions

It appears that the tremendous progress that has been made in the acute rescue of patients from MI seems to have preceded a growing prevalence of HF worldwide. Though a patient has a better chance than any other time in human history to survive an MI, there is still a significant portion of these patients that experience a global remodeling of their hearts and will require novel therapies given that presently the only curative therapy is heart transplantation.

In this thesis, we sought to better understand the process of cardiac repair and remodeling and to investigate a novel therapy to intervene on the process presumably before it begins. We identified that a small bi-product of glycolysis, MG, with no known physiological function to-date, participates in the damage and adverse remodeling that occurs post-MI. Intervening on MG production post-MI by manipulating its principle detoxifying enzyme, GLO1, produced significant improvements to function and remodeling in mice. Hopefully, the work conducted in this thesis will rationalize the design of drugs that could be provided to target MG-AGE accumulation post-MI, resulting in more advantageous resolution of MI repair processes for patients.

This thesis also assessed the efficacy of a collagen-based hydrogel for the treatment of MI. Prior to our study, very little research had been conducted on how timing the materials' delivery post-MI would influence its efficacy. Our research was one of the first comprehensively conducted studies to show that: 1) timing is an important clinical parameter to consider for the delivery of a material therapy for treating MI; and

2) that our hydrogel therapy may be an excellent candidate to intervene on the post-MI repair mechanisms and prevent further myocardial and functional decompensation. It is our hope that this work motivates more groups to consider timing effects when developing biomaterials for cardiac therapy. Moreover, it is hoped that this expands our knowledge on the mechanisms governing ECM based hydrogels for the treatment of MI.

The final contribution of this thesis was to functionalize our hydrogel to target the glycolytic bi-product MG post-MI. The results suggest the possibility that intervening on MG production with a functionalized biomaterial may confer greater recovery post-MI. Further work on this will clarify the mechanisms of action, but the work provided in this thesis shows promising early results.

In summary, it is hoped that knowledge gained from this work on the processes of post-MI repair and remodeling will ultimately contribute to advances in therapies that will one day lead to the elimination of ischemic heart failure.

Appendices

Appendix A - Supplemental Data

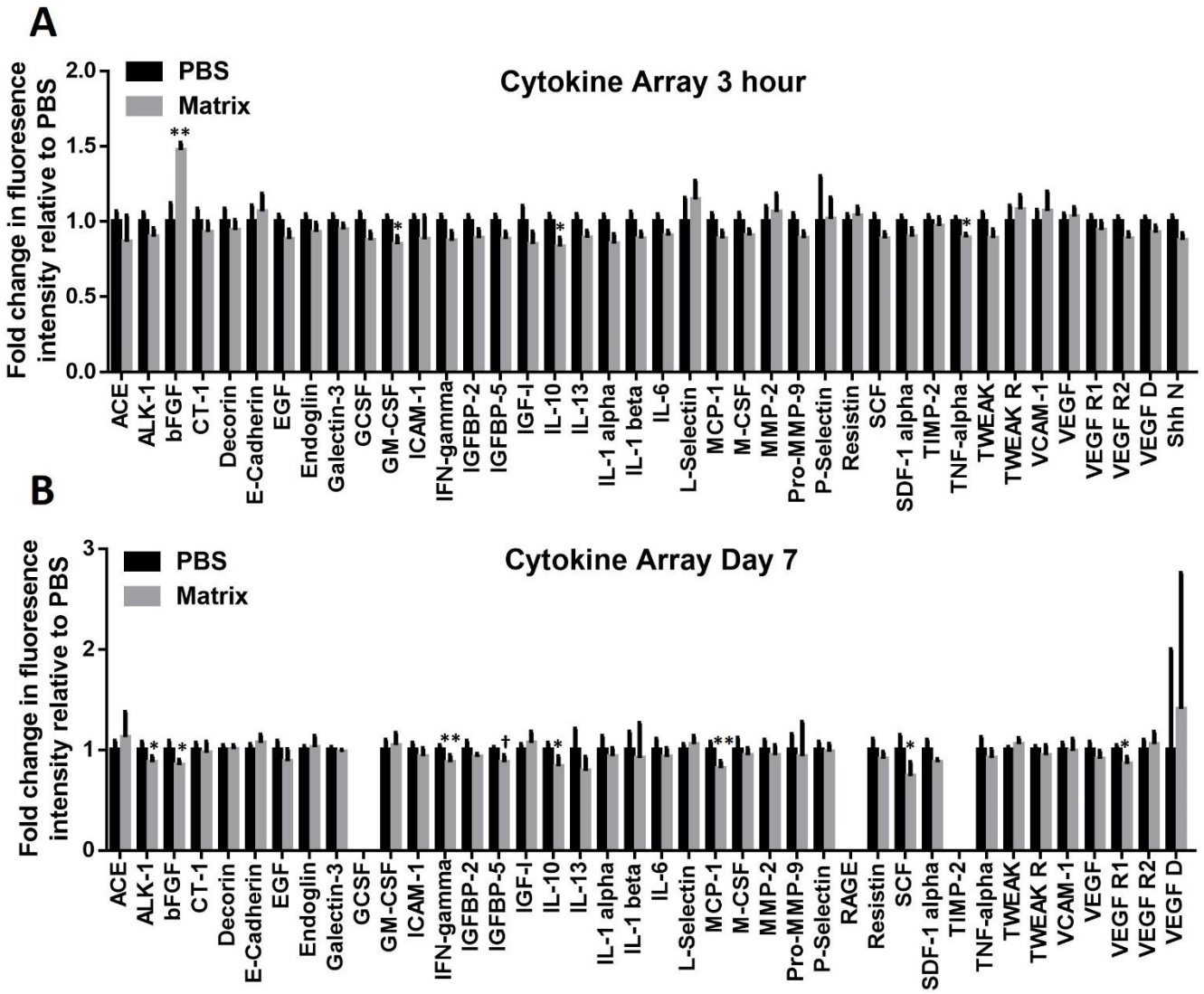

Figure A1 Collagen matrix effects on tissue level cytokine profile. (A & B) Cytokine profile of infarct and peri-infarct tissue harvested at 4 weeks post-treatment in animals treated with collagen matrix or PBS at 3 hours post-MI (A) or 7 days post-MI (B). *p<0.05, **p<0.01, and † p<0.005 vs. PBS; n=5-6.

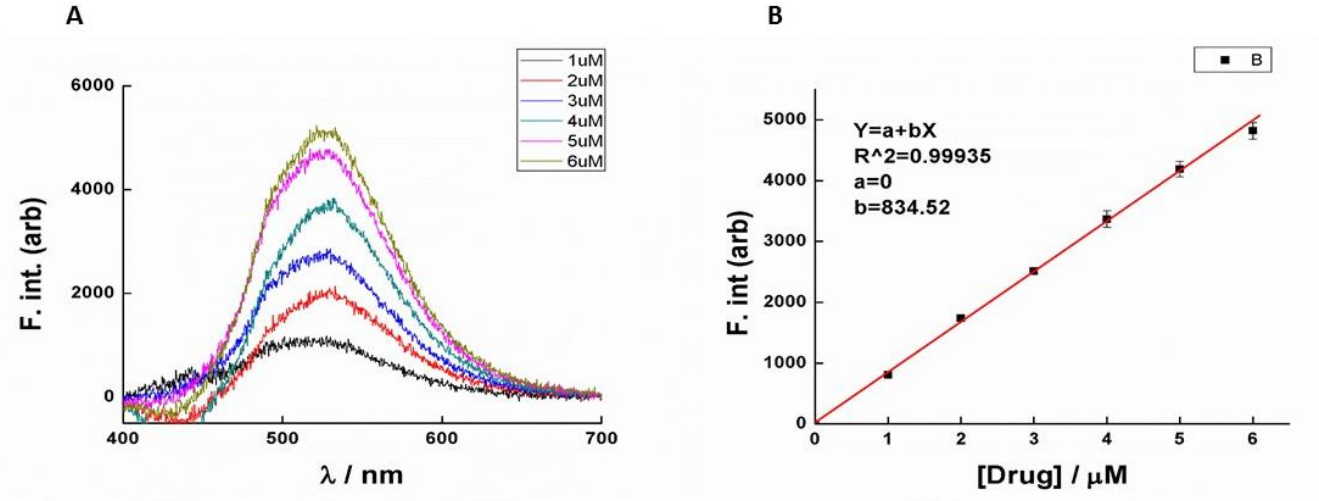

Figure A2 Measuring Fisetin using fluorescence spectroscopy at 365nm excitation and 540nm emission. (A) Representative Fisetin dose response (1-6μM) fluorescence spectra. (B) Representative calibration curve for Fisetin fluorescence spectroscopic measurements.

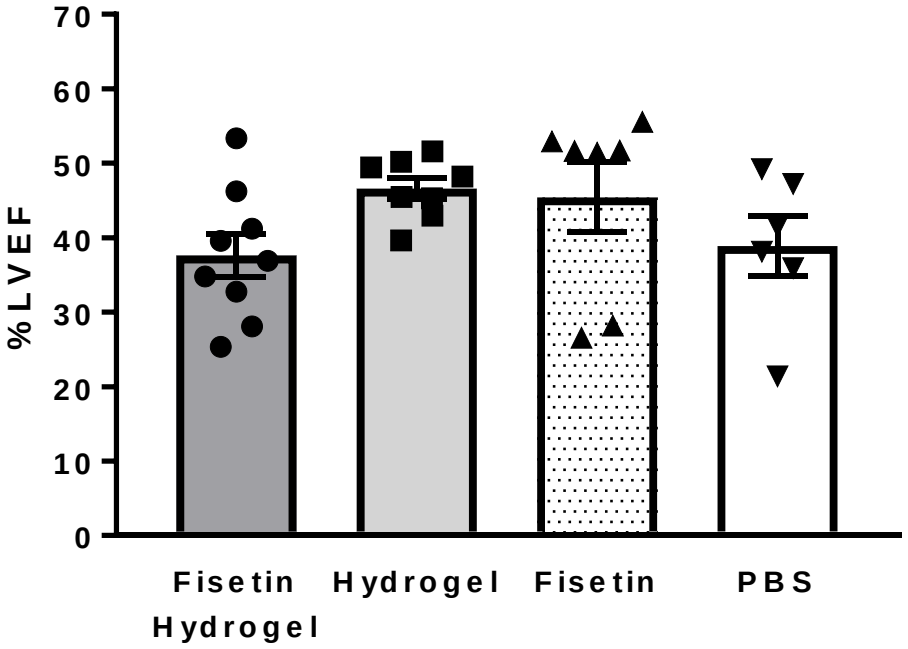

Figure A3. Baseline LVEF (post-MI / pre-injection) of animals treated with fisetin hydrogel, hydrogel, fisetin and PBS 3 hours post-MI.

Appendix B – Permissions and authorizations

Chapter 1, Figure 1.1

Permission for Authors

If you are the author of the article that was published in The New England Journal of Medicine ("NEJM"), please visit the **NEJM Author Center**.

Reuse of Content within a Thesis or Dissertation

Content (full-text or portions thereof) may be used in print and electronic versions of your dissertation or thesis without formal permission from the Massachusetts Medical Society, Publisher of the New England Journal of Medicine.

> **The following credit line must be printed along with the copyrighted material**:
>
> "Reproduced with permission from (scientific reference citation), Copyright Massachusetts Medical Society.

Third-Party Content

Grants of permissions apply only to copyrighted material that the MMS owns, and not to copyrighted text or illustrations for other sources.

Prohibited Uses

The New England Journal of Medicine (and its logo design) are registered trademarks of the Massachusetts Medical Society. We do not grant permission for our logo, cover or brand identity to be used in materials. Permission will not be granted for photographs depicting identifiable individuals.

Chapter 1, Figure 1.2

ELSEVIER LICENSE
TERMS AND CONDITIONS

Jan 05, 2017

This Agreement between Nick Blackburn ("You") and Elsevier ("Elsevier") consists of your license details and the terms and conditions provided by Elsevier and Copyright Clearance Center.

License Number	4022611145754
License date	Jan 05, 2017
Licensed Content Publisher	Elsevier
Licensed Content Publication	Journal of Molecular and Cellular Cardiology
Licensed Content Title	The extracellular matrix as a modulator of the inflammatory and reparative response following myocardial infarction
Licensed Content Author	Marcin Dobaczewski,Carlos Gonzalez-Quesada,Nikolaos G. Frangogiannis
Licensed Content Date	March 2010
Licensed Content Volume Number	48
Licensed Content Issue Number	3
Licensed Content Pages	8
Start Page	504
End Page	511
Type of Use	reuse in a thesis/dissertation
Portion	figures/tables/illustrations
Number of figures/tables/illustrations	1
Format	both print and electronic
Are you the author of this Elsevier article?	No
Will you be translating?	No
Order reference number	
Original figure numbers	Figure 1
Title of your thesis/dissertation	Targeting Novel Mediator of MI, Methylglyoxal, with Biomaterial Therapy
Expected completion date	Jan 2017
Estimated size (number of pages)	200
Elsevier VAT number	GB 494 6272 12
Requestor Location	Nick Blackburn 4 ruskin ottawa, ON K1Y 4W7 Canada Attn: Nick Blackburn
Total	0.00 CAD
Terms and Conditions	

Chapter 1, Figure 1.3

This Agreement between Nick Blackburn ("You") and John Wiley and Sons ("John Wiley and Sons") consists of your license details and the terms and conditions provided by John Wiley and Sons and Copyright Clearance Center.

License Number	4006221508286
License date	Dec 11, 2016
Licensed Content Publisher	John Wiley and Sons
Licensed Content Publication	European Journal of Heart Failure
Licensed Content Title	Advanced glycation end-products (AGEs) and heart failure: Pathophysiology and clinical implications
Licensed Content Author	Jasper W.L. Hartog,Adriaan A. Voors,Stephan J.L. Bakker,Andries J. Smit,Dirk J. Veldhuisen
Licensed Content Date	Dec 1, 2007
Licensed Content Pages	10
Type of use	Dissertation/Thesis
Requestor type	University/Academic
Format	Print and electronic
Portion	Figure/table
Number of figures/tables	1
Original Wiley figure/table number(s)	Figure 3
Will you be translating?	No
Title of your thesis / dissertation	Targeting Novel Mediator of MI, Methylglyoxal, with Biomaterial Therapy
Expected completion date	Jan 2017
Expected size (number of pages)	200
Requestor Location	Nick Blackburn 4 ruskin ottawa, ON K1Y 4W7 Canada Attn: Nick Blackburn
Publisher Tax ID	EU826007151
Billing Type	Invoice
Billing Address	Nick Blackburn 4 ruskin ottawa, ON K1Y 4W7 Canada Attn: Nick Blackburn
Total	0.00 CAD
Terms and Conditions	

Chapter 1, Figure 1.6

THE AMERICAN ASSOCIATION FOR THE ADVANCEMENT OF SCIENCE LICENSE TERMS AND CONDITIONS

Jan 04, 2017

This Agreement between Nick Blackburn ("You") and The American Association for the Advancement of Science ("The American Association for the Advancement of Science") consists of your license details and the terms and conditions provided by The American Association for the Advancement of Science and Copyright Clearance Center.

License Number	4006220530087
License date	Dec 11, 2016
Licensed Content Publisher	The American Association for the Advancement of Science
Licensed Content Publication	Science Translational Medicine
Licensed Content Title	Acellular Biomaterials: An Evolving Alternative to Cell-Based Therapies
Licensed Content Author	Jason A. Burdick,Robert L. Mauck,Joseph H. Gorman,Robert C. Gorman
Licensed Content Date	Mar 13, 2013
Licensed Content Volume Number	5
Licensed Content Issue Number	176
Volume number	5
Issue number	176
Type of Use	Thesis / Dissertation
Requestor type	Scientist/individual at a research institution
Format	Print and electronic
Portion	Figure
Number of figures/tables	2
Order reference number	
Title of your thesis / dissertation	Targeting Novel Mediator of MI, Methylglyoxal, with Biomaterial Therapy
Expected completion date	Jan 2017
Estimated size(pages)	200
Requestor Location	Nick Blackburn 4 ruskin ottawa, ON K1Y 4W7 Canada Attn: Nick Blackburn
Billing Type	Invoice
Billing Address	Nick Blackburn 4 ruskin ottawa, ON K1Y 4W7 Canada Attn: Nick Blackburn
Total	0.00 CAD
Terms and Conditions	

Authorization for Chapter 3 – Figures 3.7 – 3.13, and Figure 3.S1

Chapter 3 provides results from our manuscript published in the journal Biomaterials.

ELSEVIER LICENSE
TERMS AND CONDITIONS

Jan 04, 2017

This Agreement between Nick Blackburn ("You") and Elsevier ("Elsevier") consists of your license details and the terms and conditions provided by Elsevier and Copyright Clearance Center.

License Number	4001420613070
License date	Dec 03, 2016
Licensed Content Publisher	Elsevier
Licensed Content Publication	Biomaterials
Licensed Content Title	Timing underpins the benefits associated with injectable collagen biomaterial therapy for the treatment of myocardial infarction
Licensed Content Author	Nick J.R. Blackburn,Tanja Sofrenovic,Drew Kuraitis,Ali Ahmadi,Brian McNeill,Chao Deng,Katey J. Rayner,Zhiyuan Zhong,Marc Ruel,Erik J. Suuronen
Licensed Content Date	January 2015
Licensed Content Volume Number	39
Licensed Content Issue Number	n/a
Licensed Content Pages	11
Start Page	182
End Page	192
Type of Use	reuse in a thesis/dissertation
Portion	full article
Format	both print and electronic
Are you the author of this Elsevier article?	Yes
Will you be translating?	No
Order reference number	
Title of your thesis/dissertation	Targeting Novel Mediator of MI, Methylglyoxal, with Biomaterial Therapy
Expected completion date	Jan 2017
Estimated size (number of pages)	200
Elsevier VAT number	GB 494 6272 12
Requestor Location	Nick Blackburn 4 ruskin ottawa, ON K1Y 4W7 Canada Attn: Nick Blackburn
Total	0.00 CAD
Terms and Conditions	

Chapter 4, Figure 4.1

ELSEVIER LICENSE
TERMS AND CONDITIONS

Jan 04, 2017

This Agreement between Nick Blackburn ("You") and Elsevier ("Elsevier") consists of your license details and the terms and conditions provided by Elsevier and Copyright Clearance Center.

License Number	4020980716184
License date	Jan 02, 2017
Licensed Content Publisher	Elsevier
Licensed Content Publication	Trends in Pharmacological Sciences
Licensed Content Title	Novel therapeutics in myocardial infarction: targeting microvascular dysfunction and reperfusion injury
Licensed Content Author	Christopher B. Fordyce,Bernard J. Gersh,Gregg W. Stone,Christopher B. Granger
Licensed Content Date	September 2015
Licensed Content Volume Number	36
Licensed Content Issue Number	9
Licensed Content Pages	12
Start Page	605
End Page	616
Type of Use	reuse in a thesis/dissertation
Portion	figures/tables/illustrations
Number of figures/tables/illustrations	1
Format	both print and electronic
Are you the author of this Elsevier article?	No
Will you be translating?	No
Order reference number	
Original figure numbers	Figure 2
Title of your thesis/dissertation	Targeting Novel Mediator of MI, Methylglyoxal, with Biomaterial Therapy
Expected completion date	Jan 2017
Estimated size (number of pages)	200
Elsevier VAT number	GB 494 6272 12
Requestor Location	Nick Blackburn 4 ruskin ottawa, ON K1Y 4W7 Canada Attn: Nick Blackburn
Total	0.00 CAD
Terms and Conditions	

References

Abordo, E.A., Minhas, H.S., and Thornalley, P.J. (1999). Accumulation of alpha-oxoaldehydes during oxidative stress: a role in cytotoxicity. Biochem Pharmacol *58*, 641-648.

Ahmadi, A., McNeill, B., Vulesevic, B., Kordos, M., Mesana, L., Thorn, S., Renaud, J.M., Manthorp, E., Kuraitis, D., Toeg, H.*, et al.* (2014). The role of integrin alpha2 in cell and matrix therapy that improves perfusion, viability and function of infarcted myocardium. Biomaterials *35*, 4749-4758.

Ahmed, N., Argirov, O.K., Minhas, H.S., Cordeiro, C.A., and Thornalley, P.J. (2002). Assay of advanced glycation endproducts (AGEs): surveying AGEs by chromatographic assay with derivatization by 6-aminoquinolyl-N-hydroxysuccinimidyl-carbamate and application to Nepsilon-carboxymethyl-lysine- and Nepsilon-(1-carboxyethyl)lysine-modified albumin. Biochem J *364*, 1-14.

Ahmed, N., Dobler, D., Dean, M., and Thornalley, P.J. (2005). Peptide mapping identifies hotspot site of modification in human serum albumin by methylglyoxal involved in ligand binding and esterase activity. J Biol Chem *280*, 5724-5732.

Aleshin, A., Ananthakrishnan, R., Li, Q., Rosario, R., Lu, Y., Qu, W., Song, F., Bakr, S., Szabolcs, M., D'Agati, V.*, et al.* (2008). RAGE modulates myocardial injury consequent to LAD infarction via impact on JNK and STAT signaling in a murine model. Am J Physiol Heart Circ Physiol *294*, H1823-1832.

Ambrosy, A.P., Fonarow, G.C., Butler, J., Chioncel, O., Greene, S.J., Vaduganathan, M., Nodari, S., Lam, C.S., Sato, N., Shah, A.N.*, et al.* (2014). The global health and economic burden of

hospitalizations for heart failure: lessons learned from hospitalized heart failure registries. J Am Coll Cardiol *63*, 1123-1133.

Amin, P., Singh, M., and Singh, K. (2011). beta-Adrenergic Receptor-Stimulated Cardiac Myocyte Apoptosis: Role of beta1 Integrins. J Signal Transduct *2011*, 179057.

Anker, S.D., Coats, A.J., Cristian, G., Dragomir, D., Pusineri, E., Piredda, M., Bettari, L., Dowling, R., Volterrani, M., Kirwan, B.A*., et al.* (2015). A prospective comparison of alginate-hydrogel with standard medical therapy to determine impact on functional capacity and clinical outcomes in patients with advanced heart failure (AUGMENT-HF trial). Eur Heart J *36*, 2297-2309.

Arai, Y., Watanabe, S., Kimira, M., Shimoi, K., Mochizuki, R., and Kinae, N. (2000). Dietary intakes of flavonols, flavones and isoflavones by Japanese women and the inverse correlation between quercetin intake and plasma LDL cholesterol concentration. J Nutr *130*, 2243-2250.

Artym, V.V., and Matsumoto, K. (2010). Imaging cells in three-dimensional collagen matrix. Curr Protoc Cell Biol *Chapter 10*, Unit 10 18 11-20.

Aurora, A.B., Porrello, E.R., Tan, W., Mahmoud, A.I., Hill, J.A., Bassel-Duby, R., Sadek, H.A., and Olson, E.N. (2014). Macrophages are required for neonatal heart regeneration. J Clin Invest *124*, 1382-1392.

Aversa, C.R., Oparil, S., Caro, J., Li, H., Sun, S.D., Chen, Y.F., Swerdel, M.R., Monticello, T.M., Durham, S.K., Minchenko, A*., et al.* (1997). Hypoxia stimulates human preproendothelin-1 promoter activity in transgenic mice. Am J Physiol *273*, L848-855.

Baldi, A., Abbate, A., Bussani, R., Patti, G., Melfi, R., Angelini, A., Dobrina, A., Rossiello, R., Silvestri, F., Baldi, F*., et al.* (2002). Apoptosis and post-infarction left ventricular remodeling. J Mol Cell Cardiol *34*, 165-174.

Basta, G. (2002). Advanced Glycation End Products Activate Endothelium Through Signal-Transduction Receptor RAGE: A Mechanism for Amplification of Inflammatory Responses. Circulation *105*, 816-822.

Bayomy, A.F., Bauer, M., Qiu, Y., and Liao, R. (2012). Regeneration in heart disease-Is ECM the key? Life Sci *91*, 823-827.

Beisswenger, P.J., Howell, S.K., Russell, G., Miller, M.E., Rich, S.S., and Mauer, M. (2014). Detection of diabetic nephropathy from advanced glycation endproducts (AGEs) differs in plasma and urine, and is dependent on the method of preparation. Amino Acids *46*, 311-319.

Bento, C.F., Fernandes, R., Matafome, P., Sena, C., Seica, R., and Pereira, P. (2010a). Methylglyoxal-induced imbalance in the ratio of vascular endothelial growth factor to angiopoietin 2 secreted by retinal pigment epithelial cells leads to endothelial dysfunction. Exp Physiol *95*, 955-970.

Bento, C.F., Fernandes, R., Ramalho, J., Marques, C., Shang, F., Taylor, A., and Pereira, P. (2010b). The chaperone-dependent ubiquitin ligase CHIP targets HIF-1alpha for degradation in the presence of methylglyoxal. PLoS One *5*, e15062.

Bento, C.F., Marques, F., Fernandes, R., and Pereira, P. (2010c). Methylglyoxal alters the function and stability of critical components of the protein quality control. PLoS One *5*, e13007.

Bergmann, O., Bhardwaj, R.D., Bernard, S., Zdunek, S., Barnabe-Heider, F., Walsh, S., Zupicich, J., Alkass, K., Buchholz, B.A., Druid, H.*, et al.* (2009). Evidence for cardiomyocyte renewal in humans. Science *324*, 98-102.

Bhat, T.A., Nambiar, D., Pal, A., Agarwal, R., and Singh, R.P. (2012). Fisetin inhibits various attributes of angiogenesis in vitro and in vivo--implications for angioprevention. Carcinogenesis *33*, 385-393.

Blackburn, N.J., Sofrenovic, T., Kuraitis, D., Ahmadi, A., McNeill, B., Deng, C., Rayner, K.J., Zhong, Z., Ruel, M., and Suuronen, E.J. (2015). Timing underpins the benefits associated with injectable collagen biomaterial therapy for the treatment of myocardial infarction. Biomaterials *39C*, 182-192.

Blom, N., Sicheritz-Ponten, T., Gupta, R., Gammeltoft, S., and Brunak, S. (2004). Prediction of post-translational glycosylation and phosphorylation of proteins from the amino acid sequence. Proteomics *4*, 1633-1649.

Braunwald, E. (2013). Research advances in heart failure: a compendium. Circ Res *113*, 633-645.

Braunwald, E., and Kloner, R.A. (1982). The stunned myocardium: prolonged, postischemic ventricular dysfunction. Circulation *66*, 1146-1149.

Brouwers, O., Niessen, P.M., Ferreira, I., Miyata, T., Scheffer, P.G., Teerlink, T., Schrauwen, P., Brownlee, M., Stehouwer, C.D., and Schalkwijk, C.G. (2011). Overexpression of glyoxalase-I reduces hyperglycemia-induced levels of advanced glycation end products and oxidative stress in diabetic rats. J Biol Chem *286*, 1374-1380.

Bucciarelli, L.G., Kaneko, M., Ananthakrishnan, R., Harja, E., Lee, L.K., Hwang, Y.C., Lerner, S., Bakr, S., Li, Q., Lu, Y.*, et al.* (2006). Receptor for advanced-glycation end products: key modulator of myocardial ischemic injury. Circulation *113*, 1226-1234.

Burchfield, J.S., Xie, M., and Hill, J.A. (2013). Pathological ventricular remodeling: mechanisms: part 1 of 2. Circulation *128*, 388-400.

Burdick, J.A., Mauck, R.L., Gorman, J.H., 3rd, and Gorman, R.C. (2013). Acellular biomaterials: an evolving alternative to cell-based therapies. Sci Transl Med *5*, 176ps174.

Burdo, J., Schubert, D., and Maher, P. (2008). Glutathione production is regulated via distinct pathways in stressed and non-stressed cortical neurons. Brain Res *1189*, 12-22.

Cai, W., He, J.C., Zhu, L., Lu, C., and Vlassara, H. (2006). Advanced glycation end product (AGE) receptor 1 suppresses cell oxidant stress and activation signaling via EGF receptor. Proc Natl Acad Sci U S A *103*, 13801-13806.

Cai, W., Ramdas, M., Zhu, L., Chen, X., Striker, G.E., and Vlassara, H. (2012). Oral advanced glycation endproducts (AGEs) promote insulin resistance and diabetes by depleting the antioxidant defenses AGE receptor-1 and sirtuin 1. Proc Natl Acad Sci U S A *109*, 15888-15893.

Camici, P.G., Prasad, S.K., and Rimoldi, O.E. (2008). Stunning, hibernation, and assessment of myocardial viability. Circulation *117*, 103-114.

Cecchini, M.G., Felix, R., Fleisch, H., and Cooper, P.H. (1987). Effect of bisphosphonates on proliferation and viability of mouse bone marrow-derived macrophages. J Bone Miner Res *2*, 135-142.

Ceradini, D.J., Yao, D., Grogan, R.H., Callaghan, M.J., Edelstein, D., Brownlee, M., and Gurtner, G.C. (2008). Decreasing intracellular superoxide corrects defective ischemia-induced new vessel formation in diabetic mice. J Biol Chem *283*, 10930-10938.

Chan, W.H., and Wu, H.J. (2008). Methylglyoxal and high glucose co-treatment induces apoptosis or necrosis in human umbilical vein endothelial cells. J Cell Biochem *103*, 1144-1157.

Cheng, G., Wang, L.L., Qu, W.S., Long, L., Cui, H., Liu, H.Y., Cao, Y.L., and Li, S. (2005). C16, a novel advanced glycation endproduct breaker, restores cardiovascular dysfunction in experimental diabetic rats. Acta Pharmacol Sin *26*, 1460-1466.

Cochain, C., Channon, K.M., and Silvestre, J.S. (2013). Angiogenesis in the infarcted myocardium. Antioxid Redox Signal *18*, 1100-1113.

Condorelli, G., Roncarati, R., Ross, J., Jr., Pisani, A., Stassi, G., Todaro, M., Trocha, S., Drusco, A., Gu, Y., Russo, M.A.*, et al.* (2001). Heart-targeted overexpression of caspase3 in mice increases infarct size and depresses cardiac function. Proc Natl Acad Sci U S A *98*, 9977-9982.

Crisostomo, J., Matafome, P., Santos-Silva, D., Rodrigues, L., Sena, C.M., Pereira, P., and Seica, R. (2013). Methylglyoxal chronic administration promotes diabetes-like cardiac ischaemia disease in Wistar normal rats. Nutr Metab Cardiovasc Dis *23*, 1223-1230.

Dai, W., Wold, L.E., Dow, J.S., and Kloner, R.A. (2005). Thickening of the infarcted wall by collagen injection improves left ventricular function in rats: a novel approach to preserve cardiac function after myocardial infarction. J Am Coll Cardiol *46*, 714-719.

Dewald, O., Ren, G., Duerr, G.D., Zoerlein, M., Klemm, C., Gersch, C., Tincey, S., Michael, L.H., Entman, M.L., and Frangogiannis, N.G. (2004). Of mice and dogs: species-specific differences in the inflammatory response following myocardial infarction. Am J Pathol *164*, 665-677.

Discher, D.E., Mooney, D.J., and Zandstra, P.W. (2009). Growth factors, matrices, and forces combine and control stem cells. Science *324*, 1673-1677.

Dobaczewski, M., Gonzalez-Quesada, C., and Frangogiannis, N.G. (2010). The extracellular matrix as a modulator of the inflammatory and reparative response following myocardial infarction. J Mol Cell Cardiol *48*, 504-511.

Dobler, D., Ahmed, N., Song, L., Eboigbodin, K.E., and Thornalley, P.J. (2006). Increased dicarbonyl metabolism in endothelial cells in hyperglycemia induces anoikis and impairs angiogenesis by RGD and GFOGER motif modification. Diabetes *55*, 1961-1969.

Dobner, S., Bezuidenhout, D., Govender, P., Zilla, P., and Davies, N. (2009). A synthetic non-degradable polyethylene glycol hydrogel retards adverse post-infarct left ventricular remodeling. J Card Fail *15*, 629-636.

Eckhouse, S.R., Purcell, B.P., McGarvey, J.R., Lobb, D., Logdon, C.B., Doviak, H., O'Neill, J.W., Shuman, J.A., Novack, C.P., Zellars, K.N.*, et al.* (2014). Local hydrogel release of recombinant TIMP-3 attenuates adverse left ventricular remodeling after experimental myocardial infarction. Sci Transl Med *6*, 223ra221.

Eltzschig, H.K., and Carmeliet, P. (2011). Hypoxia and inflammation. N Engl J Med *364*, 656-665.

Eyman, D., Damodarasamy, M., Plymate, S.R., and Reed, M.J. (2009). CCL5 secreted by senescent aged fibroblasts induces proliferation of prostate epithelial cells and expression of genes that modulate angiogenesis. J Cell Physiol *220*, 376-381.

Fadini, G.P., Losordo, D., and Dimmeler, S. (2012). Critical reevaluation of endothelial progenitor cell phenotypes for therapeutic and diagnostic use. Circ Res *110*, 624-637.

Fazel, S., Cimini, M., Chen, L., Li, S., Angoulvant, D., Fedak, P., Verma, S., Weisel, R.D., Keating, A., and Li, R.K. (2006). Cardioprotective c-kit+ cells are from the bone marrow and regulate the myocardial balance of angiogenic cytokines. J Clin Invest *116*, 1865-1877.

Fedak, P.W., Verma, S., Weisel, R.D., Skrtic, M., and Li, R.K. (2005). Cardiac remodeling and failure: from molecules to man (Part III). Cardiovasc Pathol *14*, 109-119.

Fesus, L., Muszbek, L., and Laki, K. (1981). The effect of methylglyoxal on actin. Biochem Biophys Res Commun *99*, 617-622.

Fomovsky, G.M., Thomopoulos, S., and Holmes, J.W. (2010). Contribution of extracellular matrix to the mechanical properties of the heart. J Mol Cell Cardiol *48*, 490-496.

Fordyce, C.B., Gersh, B.J., Stone, G.W., and Granger, C.B. (2015). Novel therapeutics in myocardial infarction: targeting microvascular dysfunction and reperfusion injury. Trends Pharmacol Sci *36*, 605-616.

Fraccarollo, D., Galuppo, P., and Bauersachs, J. (2012). Novel therapeutic approaches to post-infarction remodelling. Cardiovasc Res *94*, 293-303.

Francis-Sedlak, M.E., Moya, M.L., Huang, J.J., Lucas, S.A., Chandrasekharan, N., Larson, J.C., Cheng, M.H., and Brey, E.M. (2010). Collagen glycation alters neovascularization in vitro and in vivo. Microvasc Res *80*, 3-9.

Frangogiannis, N.G. (2012). Regulation of the inflammatory response in cardiac repair. Circ Res *110*, 159-173.

Frey, N., Linke, A., Suselbeck, T., Muller-Ehmsen, J., Vermeersch, P., Schoors, D., Rosenberg, M., Bea, F., Tuvia, S., and Leor, J. (2014). Intracoronary delivery of injectable bioabsorbable scaffold (IK-5001) to treat left ventricular remodeling after ST-elevation myocardial infarction: a first-in-man study. Circ Cardiovasc Interv *7*, 806-812.

Fujita, M., Ishihara, M., Simizu, M., Obara, K., Ishizuka, T., Saito, Y., Yura, H., Morimoto, Y., Takase, B., Matsui, T.*, et al.* (2004). Vascularization in vivo caused by the controlled release of fibroblast growth factor-2 from an injectable chitosan/non-anticoagulant heparin hydrogel. Biomaterials *25*, 699-706.

Gallet, X., Charloteaux, B., Thomas, A., and Brasseur, R. (2000). A fast method to predict protein interaction sites from sequences. J Mol Biol *302*, 917-926.

Garbern, J.C., Minami, E., Stayton, P.S., and Murry, C.E. (2011). Delivery of basic fibroblast growth factor with a pH-responsive, injectable hydrogel to improve angiogenesis in infarcted myocardium. Biomaterials *32*, 2407-2416.

Geoffrion, M., Du, X., Irshad, Z., Vanderhyden, B.C., Courville, K., Sui, G., D'Agati, V.D., Ott-Braschi, S., Rabbani, N., Thornalley, P.J.*, et al.* (2014). Differential effects of glyoxalase 1

overexpression on diabetic atherosclerosis and renal dysfunction in streptozotocin-treated, apolipoprotein E-deficient mice. Physiol Rep *2*.

Ghosh, P., Singha Roy, A., Chaudhury, S., Jana, S.K., Chaudhury, K., and Dasgupta, S. (2016). Preparation of albumin based nanoparticles for delivery of fisetin and evaluation of its cytotoxic activity. Int J Biol Macromol *86*, 408-417.

Giacco, F., and Brownlee, M. (2010). Oxidative stress and diabetic complications. Circ Res *107*, 1058-1070.

Godwin, J.W., Pinto, A.R., and Rosenthal, N.A. (2013). Macrophages are required for adult salamander limb regeneration. Proc Natl Acad Sci U S A *110*, 9415-9420.

Goh, S.Y., and Cooper, M.E. (2008). Clinical review: The role of advanced glycation end products in progression and complications of diabetes. J Clin Endocrinol Metab *93*, 1143-1152.

Goldberg, R.J., Yarzebski, J., Lessard, D., and Gore, J.M. (2000). Decade-long trends and factors associated with time to hospital presentation in patients with acute myocardial infarction: the Worcester Heart Attack study. Arch Intern Med *160*, 3217-3223.

Goldin, A., Beckman, J.A., Schmidt, A.M., and Creager, M.A. (2006). Advanced glycation end products: sparking the development of diabetic vascular injury. Circulation *114*, 597-605.

Guharay, J., Moses Dennison, S., and Sengupta, P.K. (1999). Influence of differencet environments on the excited-state proton transfer and dual fluorescence of fisetin. Spectrochimica Acta Part A *55*, 1091-1099.

Haberstroh, U., Pocock, J., Gomez-Guerrero, C., Helmchen, U., Hamann, A., Gutierrez-Ramos, J.C., Stahl, R.A., and Thaiss, F. (2002). Expression of the chemokines MCP-1/CCL2 and

RANTES/CCL5 is differentially regulated by infiltrating inflammatory cells. Kidney Int *62*, 1264-1276.

Hanssen, N.M., Wouters, K., Huijberts, M.S., Gijbels, M.J., Sluimer, J.C., Scheijen, J.L., Heeneman, S., Biessen, E.A., Daemen, M.J., Brownlee, M.*, et al.* (2014). Higher levels of advanced glycation endproducts in human carotid atherosclerotic plaques are associated with a rupture-prone phenotype. Eur Heart J *35*, 1137-1146.

Harats, D., Kurihara, H., Belloni, P., Oakley, H., Ziober, A., Ackley, D., Cain, G., Kurihara, Y., Lawn, R., and Sigal, E. (1995). Targeting gene expression to the vascular wall in transgenic mice using the murine preproendothelin-1 promoter. J Clin Invest *95*, 1335-1344.

Hartog, J.W., Smit, A.J., van Son, W.J., Navis, G., Gans, R.O., Wolffenbuttel, B.H., and de Jong, P.E. (2004). Advanced glycation end products in kidney transplant patients: a putative role in the development of chronic renal transplant dysfunction. Am J Kidney Dis *43*, 966-975.

Hartog, J.W., Voors, A.A., Bakker, S.J., Smit, A.J., and van Veldhuisen, D.J. (2007a). Advanced glycation end-products (AGEs) and heart failure: pathophysiology and clinical implications. Eur J Heart Fail *9*, 1146-1155.

Hartog, J.W., Voors, A.A., Schalkwijk, C.G., Scheijen, J., Smilde, T.D., Damman, K., Bakker, S.J., Smit, A.J., and van Veldhuisen, D.J. (2007b). Clinical and prognostic value of advanced glycation end-products in chronic heart failure. Eur Heart J *28*, 2879-2885.

Hedayat, M., Mahmoudi, M.J., Rose, N.R., and Rezaei, N. (2010). Proinflammatory cytokines in heart failure: double-edged swords. Heart Fail Rev *15*, 543-562.

Heino, J. (2000). The collagen receptor integrins have distinct ligand recognition and signaling functions. Matrix Biol *19*, 319-323.

Hertog, M.G., Feskens, E.J., Hollman, P.C., Katan, M.B., and Kromhout, D. (1993). Dietary antioxidant flavonoids and risk of coronary heart disease: the Zutphen Elderly Study. Lancet *342*, 1007-1011.

Heusch, G., and Rassaf, T. (2016). Time to Give Up on Cardioprotection? A Critical Appraisal of Clinical Studies on Ischemic Pre-, Post-, and Remote Conditioning. Circ Res *119*, 676-695.

Hofmann, U., and Frantz, S. (2013). How can we cure a heart "in flame"? A translational view on inflammation in heart failure. Basic Res Cardiol *108*, 356.

Hori, M., and Nishida, K. (2009). Oxidative stress and left ventricular remodelling after myocardial infarction. Cardiovasc Res *81*, 457-464.

Hou, D.X., Fukuda, M., Johnson, J.A., Miyamori, K., Ushikai, M., and Fujii, M. (2001). Fisetin induces transcription of NADPH:quinone oxidoreductase gene through an antioxidant responsive element-involved activation. Int J Oncol *18*, 1175-1179.

Huyer, L.D., Montgomery, M., Zhao, Y., Xiao, Y., Conant, G., Korolj, A., and Radisic, M. (2015). Biomaterial based cardiac tissue engineering and its applications. Biomed Mater *10*, 034004.

Ifkovits, J.L., Tous, E., Minakawa, M., Morita, M., Robb, J.D., Koomalsingh, K.J., Gorman, J.H., 3rd, Gorman, R.C., and Burdick, J.A. (2010). Injectable hydrogel properties influence infarct expansion and extent of postinfarction left ventricular remodeling in an ovine model. Proc Natl Acad Sci U S A *107*, 11507-11512.

Ishige, K., Schubert, D., and Sagara, Y. (2001). Flavonoids protect neuronal cells from oxidative stress by three distinct mechanisms. Free Radic Biol Med *30*, 433-446.

Jahan, H., and Choudhary, M.I. (2015). Glycation, carbonyl stress and AGEs inhibitors: a patent review. Expert Opin Ther Pat *25*, 1267-1284.

Jessup, M., and Brozena, S. (2003). Heart failure. N Engl J Med *348*, 2007-2018.

Johnson, T.D., and Christman, K.L. (2013). Injectable hydrogel therapies and their delivery strategies for treating myocardial infarction. Expert Opin Drug Deliv *10*, 59-72.

Kadner, K., Dobner, S., Franz, T., Bezuidenhout, D., Sirry, M.S., Zilla, P., and Davies, N.H. (2012). The beneficial effects of deferred delivery on the efficiency of hydrogel therapy post myocardial infarction. Biomaterials *33*, 2060-2066.

Kang, P.M., and Izumo, S. (2003). Apoptosis in heart: basic mechanisms and implications in cardiovascular diseases. Trends in Molecular Medicine *9*, 177-182.

Kemp, C.D., and Conte, J.V. (2012). The pathophysiology of heart failure. Cardiovasc Pathol *21*, 365-371.

Khan, N., Syed, D.N., Ahmad, N., and Mukhtar, H. (2013). Fisetin: a dietary antioxidant for health promotion. Antioxid Redox Signal *19*, 151-162.

Khraim, F.M., and Carey, M.G. (2009). Predictors of pre-hospital delay among patients with acute myocardial infarction. Patient Educ Couns *75*, 155-161.

Kilhovd, B.K., Juutilainen, A., Lehto, S., Ronnemaa, T., Torjesen, P.A., Hanssen, K.F., and Laakso, M. (2009). Increased serum levels of methylglyoxal-derived hydroimidazolone-AGE are

associated with increased cardiovascular disease mortality in nondiabetic women. Atherosclerosis *205*, 590-594.

Koenig, R.J., Peterson, C.M., Jones, R.L., Saudek, C., Lehrman, M., and Cerami, A. (1976). Correlation of glucose regulation and hemoglobin AIc in diabetes mellitus. N Engl J Med *295*, 417-420.

Kraaijeveld, A.O., de Jager, S.C., de Jager, W.J., Prakken, B.J., McColl, S.R., Haspels, I., Putter, H., van Berkel, T.J., Nagelkerken, L., Jukema, J.W.*, et al.* (2007). CC chemokine ligand-5 (CCL5/RANTES) and CC chemokine ligand-18 (CCL18/PARC) are specific markers of refractory unstable angina pectoris and are transiently raised during severe ischemic symptoms. Circulation *116*, 1931-1941.

Kumagai, T., Nangaku, M., Kojima, I., Nagai, R., Ingelfinger, J.R., Miyata, T., Fujita, T., and Inagi, R. (2009). Glyoxalase I overexpression ameliorates renal ischemia-reperfusion injury in rats. Am J Physiol Renal Physiol *296*, F912-921.

Kuraitis, D., Berardinelli, M.G., Suuronen, E.J., and Musaro, A. (2013). A necrotic stimulus is required to maximize matrix-mediated myogenesis in mice. Dis Model Mech *6*, 793-801.

Kuraitis, D., Giordano, C., Ruel, M., Musaro, A., and Suuronen, E.J. (2012). Exploiting extracellular matrix-stem cell interactions: a review of natural materials for therapeutic muscle regeneration. Biomaterials *33*, 428-443.

Kuraitis, D., Hou, C., Zhang, Y., Vulesevic, B., Sofrenovic, T., McKee, D., Sharif, Z., Ruel, M., and Suuronen, E.J. (2011). Ex vivo generation of a highly potent population of circulating angiogenic cells using a collagen matrix. J Mol Cell Cardiol *51*, 187-197.

Kurrelmeyer, K.M., Michael, L.H., Baumgarten, G., Taffet, G.E., Peschon, J.J., Sivasubramanian, N., Entman, M.L., and Mann, D.L. (2000). Endogenous tumor necrosis factor protects the adult cardiac myocyte against ischemic-induced apoptosis in a murine model of acute myocardial infarction. Proc Natl Acad Sci U S A *97*, 5456-5461.

Kuzuya, M., Satake, S., Ai, S., Asai, T., Kanda, S., Ramos, M.A., Miura, H., Ueda, M., and Iguchi, A. (1998). Inhibition of angiogenesis on glycated collagen lattices. Diabetologia *41*, 491-499.

Landa, N., Miller, L., Feinberg, M.S., Holbova, R., Shachar, M., Freeman, I., Cohen, S., and Leor, J. (2008). Effect of injectable alginate implant on cardiac remodeling and function after recent and old infarcts in rat. Circulation *117*, 1388-1396.

Lee, S.E., Jeong, S.I., Yang, H., Park, C.S., Jin, Y.H., and Park, Y.S. (2011). Fisetin induces Nrf2-mediated HO-1 expression through PKC-delta and p38 in human umbilical vein endothelial cells. J Cell Biochem *112*, 2352-2360.

Li, A.H., Liu, P.P., Villarreal, F.J., and Garcia, R.A. (2014). Dynamic changes in myocardial matrix and relevance to disease: translational perspectives. Circ Res *114*, 916-927.

Li, S.Y., Sigmon, V.K., Babcock, S.A., and Ren, J. (2007). Advanced glycation endproduct induces ROS accumulation, apoptosis, MAP kinase activation and nuclear O-GlcNAcylation in human cardiac myocytes. Life Sci *80*, 1051-1056.

Lin, Y.D., Luo, C.Y., Hu, Y.N., Yeh, M.L., Hsueh, Y.C., Chang, M.Y., Tsai, D.C., Wang, J.N., Tang, M.J., Wei, E.I.*, et al.* (2012). Instructive nanofiber scaffolds with VEGF create a microenvironment for arteriogenesis and cardiac repair. Sci Transl Med *4*, 146ra109.

Lister, Z., Rayner, K.J., and Suuronen, E.J. (2016). How Biomaterials Can Influence Various Cell Types in the Repair and Regeneration of the Heart after Myocardial Infarction. Front Bioeng Biotechnol *4*, 62.

Lo, T.W., Westwood, M.E., McLellan, A.C., Selwood, T., and Thornalley, P.J. (1994). Binding and modification of proteins by methylglyoxal under physiological conditions. A kinetic and mechanistic study with N alpha-acetylarginine, N alpha-acetylcysteine, and N alpha-acetyllysine, and bovine serum albumin. J Biol Chem *269*, 32299-32305.

Lutgens, E., Daemen, M.J., de Muinck, E.D., Debets, J., Leenders, P., and Smits, J.F. (1999). Chronic myocardial infarction in the mouse: cardiac structural and functional changes. Cardiovasc Res *41*, 586-593.

Ma, H., Li, S.Y., Xu, P., Babcock, S.A., Dolence, E.K., Brownlee, M., Li, J., and Ren, J. (2009). Advanced glycation endproduct (AGE) accumulation and AGE receptor (RAGE) up-regulation contribute to the onset of diabetic cardiomyopathy. J Cell Mol Med *13*, 1751-1764.

Maekawa, N., Wada, H., Kanda, T., Niwa, T., Yamada, Y., Saito, K., Fujiwara, H., Sekikawa, K., and Seishima, M. (2002). Improved myocardial ischemia/reperfusion injury in mice lacking tumor necrosis factor-alpha. J Am Coll Cardiol *39*, 1229-1235.

Maessen, D.E., Stehouwer, C.D., and Schalkwijk, C.G. (2015). The role of methylglyoxal and the glyoxalase system in diabetes and other age-related diseases. Clin Sci (Lond) *128*, 839-861.

Maher, P., Dargusch, R., Ehren, J.L., Okada, S., Sharma, K., and Schubert, D. (2011). Fisetin lowers methylglyoxal dependent protein glycation and limits the complications of diabetes. PLoS One *6*, e21226.

Maher, P., Salgado, K.F., Zivin, J.A., and Lapchak, P.A. (2007). A novel approach to screening for new neuroprotective compounds for the treatment of stroke. Brain Res *1173*, 117-125.

Makinen, V.P., Civelek, M., Meng, Q., Zhang, B., Zhu, J., Levian, C., Huan, T., Segre, A.V., Ghosh, S., Vivar, J.*, et al.* (2014). Integrative genomics reveals novel molecular pathways and gene networks for coronary artery disease. PLoS Genet *10*, e1004502.

Mann, D.L., Lee, R.J., Coats, A.J., Neagoe, G., Dragomir, D., Pusineri, E., Piredda, M., Bettari, L., Kirwan, B.A., Dowling, R.*, et al.* (2016). One-year follow-up results from AUGMENT-HF: a multicentre randomized controlled clinical trial of the efficacy of left ventricular augmentation with Algisyl in the treatment of heart failure. Eur J Heart Fail *18*, 314-325.

Markovic, Z.S., Mentus, S.V., and Dimitric Markovic, J.M. (2009). Electrochemical and density functional theory study on the reactivity of fisetin and its radicals: implications on in vitro antioxidant activity. J Phys Chem A *113*, 14170-14179.

McGarvey, J.R., Pettaway, S., Shuman, J.A., Novack, C.P., Zellars, K.N., Freels, P.D., Echols, R.L., Jr., Burdick, J.A., Gorman, J.H., 3rd, Gorman, R.C.*, et al.* (2014). Targeted injection of a biocomposite material alters macrophage and fibroblast phenotype and function following myocardial infarction: relation to left ventricular remodeling. J Pharmacol Exp Ther *350*, 701-709.

Mihic, A., Cui, Z., Wu, J., Vlacic, G., Miyagi, Y., Li, S.H., Lu, S., Sung, H.W., Weisel, R.D., and Li, R.K. (2015). A Conductive Polymer Hydrogel Supports Cell Electrical Signaling and Improves Cardiac Function After Implantation into Myocardial Infarct. Circulation *132*, 772-784.

Molgat, A.S., Tilokee, E.L., Rafatian, G., Vulesevic, B., Ruel, M., Milne, R., Suuronen, E.J., and Davis, D.R. (2014). Hyperglycemia inhibits cardiac stem cell-mediated cardiac repair and angiogenic capacity. Circulation *130*, S70-76.

Monden, Y., Kubota, T., Tsutsumi, T., Inoue, T., Kawano, S., Kawamura, N., Ide, T., Egashira, K., Tsutsui, H., and Sunagawa, K. (2007). Soluble TNF receptors prevent apoptosis in infiltrating cells and promote ventricular rupture and remodeling after myocardial infarction. Cardiovasc Res *73*, 794-805.

Monnier, V.M., Mustata, G.T., Biemel, K.L., Reihl, O., Lederer, M.O., Zhenyu, D., and Sell, D.R. (2005). Cross-linking of the extracellular matrix by the maillard reaction in aging and diabetes: an update on "a puzzle nearing resolution". Ann N Y Acad Sci *1043*, 533-544.

Morcos, M., Du, X., Pfisterer, F., Hutter, H., Sayed, A.A., Thornalley, P., Ahmed, N., Baynes, J., Thorpe, S., Kukudov, G.*, et al.* (2008). Glyoxalase-1 prevents mitochondrial protein modification and enhances lifespan in Caenorhabditis elegans. Aging Cell *7*, 260-269.

Mozaffarian, D., Benjamin, E.J., Go, A.S., Arnett, D.K., Blaha, M.J., Cushman, M., Das, S.R., de Ferranti, S., Despres, J.P., Fullerton, H.J.*, et al.* (2016). Heart Disease and Stroke Statistics-2016 Update: A Report From the American Heart Association. Circulation *133*, e38-360.

Mulder, D.J., van Haelst, P.L., Graaff, R., Gans, R.O., Zijlstra, F., and Smit, A.J. (2009). Skin autofluorescence is elevated in acute myocardial infarction and is associated with the one-year incidence of major adverse cardiac events. Neth Heart J *17*, 162-168.

Murata-Kamiya, N., Kaji, H., and Kasai, H. (1999). Deficient nucleotide excision repair increases base-pair substitutions but decreases TGGC frameshifts induced by methylglyoxal in Escherichia coli. Mutat Res *442*, 19-28.

Murata-Kamiya, N., and Kamiya, H. (2001). Methylglyoxal, an endogenous aldehyde, crosslinks DNA polymerase and the substrate DNA. Nucleic Acids Res *29*, 3433-3438.

Nabel, E.G., and Braunwald, E. (2012). A tale of coronary artery disease and myocardial infarction. N Engl J Med *366*, 54-63.

Nam, D.H., Han, J.H., Lee, T.J., Shishido, T., Lim, J.H., Kim, G.Y., and Woo, C.H. (2015). CHOP deficiency prevents methylglyoxal-induced myocyte apoptosis and cardiac dysfunction. J Mol Cell Cardiol *85*, 168-177.

Neubauer, S. (2007). The failing heart--an engine out of fuel. N Engl J Med *356*, 1140-1151.

Ohtsuka, M., Takano, H., Zou, Y., Toko, H., Akazawa, H., Qin, Y., Suzuki, M., Hasegawa, H., Nakaya, H., and Komuro, I. (2004). Cytokine therapy prevents left ventricular remodeling and dysfunction after myocardial infarction through neovascularization. FASEB J *18*, 851-853.

Pedchenko, V.K., Chetyrkin, S.V., Chuang, P., Ham, A.J., Saleem, M.A., Mathieson, P.W., Hudson, B.G., and Voziyan, P.A. (2005). Mechanism of perturbation of integrin-mediated cell-matrix interactions by reactive carbonyl compounds and its implication for pathogenesis of diabetic nephropathy. Diabetes *54*, 2952-2960.

Phillips, S.A., and Thornalley, P.J. (1993). The formation of methylglyoxal from triose phosphates. Investigation using a specific assay for methylglyoxal. Eur J Biochem *212*, 101-105.

Prabhu, S.D., and Frangogiannis, N.G. (2016). The Biological Basis for Cardiac Repair After Myocardial Infarction: From Inflammation to Fibrosis. Circ Res *119*, 91-112.

Purcell, B.P., Lobb, D., Charati, M.B., Dorsey, S.M., Wade, R.J., Zellars, K.N., Doviak, H., Pettaway, S., Logdon, C.B., Shuman, J.A*., et al.* (2014). Injectable and bioresponsive hydrogels for on-demand matrix metalloproteinase inhibition. Nat Mater *13*, 653-661.

Putinski, C., Abdul-Ghani, M., Stiles, R., Brunette, S., Dick, S.A., Fernando, P., and Megeney, L.A. (2013). Intrinsic-mediated caspase activation is essential for cardiomyocyte hypertrophy. Proc Natl Acad Sci U S A *110*, E4079-4087.

Queisser, M.A., Yao, D., Geisler, S., Hammes, H.P., Lochnit, G., Schleicher, E.D., Brownlee, M., and Preissner, K.T. (2010). Hyperglycemia impairs proteasome function by methylglyoxal. Diabetes *59*, 670-678.

Rabbani, N., and Thornalley, P.J. (2012). Methylglyoxal, glyoxalase 1 and the dicarbonyl proteome. Amino Acids *42*, 1133-1142.

Rabbani, N., and Thornalley, P.J. (2014). Measurement of methylglyoxal by stable isotopic dilution analysis LC-MS/MS with corroborative prediction in physiological samples. Nat Protoc *9*, 1969-1979.

Rabbani, N., Xue, M., and Thornalley, P.J. (2014). Activity, regulation, copy number and function in the glyoxalase system. Biochem Soc Trans *42*, 419-424.

Rabbani, N., Xue, M., and Thornalley, P.J. (2016a). Dicarbonyls and glyoxalase in disease mechanisms and clinical therapeutics. Glycoconj J *33*, 513-525.

Rabbani, N., Xue, M., and Thornalley, P.J. (2016b). Methylglyoxal-induced dicarbonyl stress in aging and disease: first steps towards glyoxalase 1-based treatments. Clin Sci (Lond) *130*, 1677-1696.

Radhakrishnan, J., Krishnan, U.M., and Sethuraman, S. (2014). Hydrogel based injectable scaffolds for cardiac tissue regeneration. Biotechnol Adv *32*, 449-461.

Ramani, R., Nilles, K., Gibson, G., Burkhead, B., Mathier, M., McNamara, D., and McTiernan, C.F. (2011). Tissue inhibitor of metalloproteinase-2 gene delivery ameliorates postinfarction cardiac remodeling. Clin Transl Sci *4*, 24-31.

Ramasamy, R., Yan, S.F., and Schmidt, A.M. (2006). Methylglyoxal comes of AGE. Cell *124*, 258-260.

Ramasamy, R., Yan, S.F., and Schmidt, A.M. (2008). Stopping the primal RAGE reaction in myocardial infarction: capturing adaptive responses to heal the heart? Circulation *117*, 3165-3167.

Ramasamy, R., Yan, S.F., and Schmidt, A.M. (2009). RAGE: therapeutic target and biomarker of the inflammatory response--the evidence mounts. J Leukoc Biol *86*, 505-512.

Ramasamy, R., Yan, S.F., and Schmidt, A.M. (2012). Advanced glycation endproducts: from precursors to RAGE: round and round we go. Amino Acids *42*, 1151-1161.

Ramos, C.D., Canetti, C., Souto, J.T., Silva, J.S., Hogaboam, C.M., Ferreira, S.H., and Cunha, F.Q. (2005). MIP-1alpha[CCL3] acting on the CCR1 receptor mediates neutrophil migration in immune inflammation via sequential release of TNF-alpha and LTB4. J Leukoc Biol *78*, 167-177.

Rane, A.A., and Christman, K.L. (2011). Biomaterials for the treatment of myocardial infarction: a 5-year update. J Am Coll Cardiol *58*, 2615-2629.

Rane, A.A., Chuang, J.S., Shah, A., Hu, D.P., Dalton, N.D., Gu, Y., Peterson, K.L., Omens, J.H., and Christman, K.L. (2011). Increased infarct wall thickness by a bio-inert material is insufficient to prevent negative left ventricular remodeling after myocardial infarction. PLoS One *6*, e21571.

Rengarajan, T., and Yaacob, N.S. (2016). The flavonoid fisetin as an anticancer agent targeting the growth signaling pathways. Eur J Pharmacol *789*, 8-16.

Rosso, F., Giordano, A., Barbarisi, M., and Barbarisi, A. (2004). From cell-ECM interactions to tissue engineering. J Cell Physiol *199*, 174-180.

Ruvinov, E., and Cohen, S. (2016). Alginate biomaterial for the treatment of myocardial infarction: Progress, translational strategies, and clinical outlook: From ocean algae to patient bedside. Adv Drug Deliv Rev *96*, 54-76.

Santini, M.P., and Rosenthal, N. (2012). Myocardial regenerative properties of macrophage populations and stem cells. J Cardiovasc Transl Res *5*, 700-712.

Schlotterer, A., Kukudov, G., Bozorgmehr, F., Hutter, H., Du, X., Oikonomou, D., Ibrahim, Y., Pfisterer, F., Rabbani, N., Thornalley, P.*, et al.* (2009). C. elegans as model for the study of high glucose- mediated life span reduction. Diabetes *58*, 2450-2456.

Schultz, G.S., and Wysocki, A. (2009). Interactions between extracellular matrix and growth factors in wound healing. Wound Repair Regen *17*, 153-162.

Schussler, O., Chachques, J.C., Mesana, T.G., Suuronen, E.J., Lecarpentier, Y., and Ruel, M. (2010). 3-dimensional structures to enhance cell therapy and engineer contractile tissue. Asian Cardiovasc Thorac Ann *18*, 188-198.

Schwanhausser, B., Busse, D., Li, N., Dittmar, G., Schuchhardt, J., Wolf, J., Chen, W., and Selbach, M. (2011). Global quantification of mammalian gene expression control. Nature *473*, 337-342.

Seif-Naraghi, S.B., Singelyn, J.M., Salvatore, M.A., Osborn, K.G., Wang, J.J., Sampat, U., Kwan, O.L., Strachan, G.M., Wong, J., Schup-Magoffin, P.J.*, et al.* (2013). Safety and efficacy of an injectable extracellular matrix hydrogel for treating myocardial infarction. Sci Transl Med *5*, 173ra125.

Sena, C.M., Matafome, P., Crisostomo, J., Rodrigues, L., Fernandes, R., Pereira, P., and Seica, R.M. (2012). Methylglyoxal promotes oxidative stress and endothelial dysfunction. Pharmacol Res *65*, 497-506.

Shah, A.M., and Mann, D.L. (2011). In search of new therapeutic targets and strategies for heart failure: recent advances in basic science. The Lancet *378*, 704-712.

Shah, V.K., and Shalia, K.K. (2011). Stem Cell Therapy in Acute Myocardial Infarction: A Pot of Gold or Pandora's Box. Stem Cells Int *2011*, 536758.

Shamsi, F.A., Partal, A., Sady, C., Glomb, M.A., and Nagaraj, R.H. (1998). Immunological evidence for methylglyoxal-derived modifications in vivo. Determination of antigenic epitopes. J Biol Chem *273*, 6928-6936.

Shang, L., Ananthakrishnan, R., Li, Q., Quadri, N., Abdillahi, M., Zhu, Z., Qu, W., Rosario, R., Toure, F., Yan, S.F.*, et al.* (2010). RAGE modulates hypoxia/reoxygenation injury in adult murine cardiomyocytes via JNK and GSK-3beta signaling pathways. PLoS One *5*, e10092.

Shia, C.S., Tsai, S.Y., Kuo, S.C., Hou, Y.C., and Chao, P.D. (2009). Metabolism and pharmacokinetics of 3,3',4',7-tetrahydroxyflavone (fisetin), 5-hydroxyflavone, and 7-hydroxyflavone and antihemolysis effects of fisetin and its serum metabolites. J Agric Food Chem *57*, 83-89.

Singelyn, J.M., Sundaramurthy, P., Johnson, T.D., Schup-Magoffin, P.J., Hu, D.P., Faulk, D.M., Wang, J., Mayle, K.M., Bartels, K., Salvatore, M.*, et al.* (2012). Catheter-deliverable hydrogel derived from decellularized ventricular extracellular matrix increases endogenous cardiomyocytes and preserves cardiac function post-myocardial infarction. J Am Coll Cardiol *59*, 751-763.

Sousa Silva, M., Gomes, R.A., Ferreira, A.E., Ponces Freire, A., and Cordeiro, C. (2013). The glyoxalase pathway: the first hundred years... and beyond. Biochem J *453*, 1-15.

Spinale, F.G. (2007). Myocardial matrix remodeling and the matrix metalloproteinases: influence on cardiac form and function. Physiol Rev *87*, 1285-1342.

Stone, G.W., Selker, H.P., Thiele, H., Patel, M.R., Udelson, J.E., Ohman, E.M., Maehara, A., Eitel, I., Granger, C.B., Jenkins, P.L.*, et al.* (2016). Relationship Between Infarct Size and Outcomes Following Primary PCI: Patient-Level Analysis From 10 Randomized Trials. J Am Coll Cardiol *67*, 1674-1683.

Sun, B., Deng, C., Meng, F., Zhang, J., and Zhong, Z. (2016). Robust, active tumor-targeting and fast bioresponsive anticancer nanotherapeutics based on natural endogenous materials. Acta Biomater *45*, 223-233.

Sun, X., and Nunes, S.S. (2015). Overview of hydrogel-based strategies for application in cardiac tissue regeneration. Biomed Mater *10*, 034005.

Sutton, M.G., and Sharpe, N. (2000). Left ventricular remodeling after myocardial infarction: pathophysiology and therapy. Circulation *101*, 2981-2988.

Takagawa, J., Zhang, Y., Wong, M.L., Sievers, R.E., Kapasi, N.K., Wang, Y., Yeghiazarians, Y., Lee, R.J., Grossman, W., and Springer, M.L. (2007). Myocardial infarct size measurement in the mouse chronic infarction model: comparison of area- and length-based approaches. J Appl Physiol (1985) *102*, 2104-2111.

Talior-Volodarsky, I., Connelly, K.A., Arora, P.D., Gullberg, D., and McCulloch, C.A. (2012). alpha11 integrin stimulates myofibroblast differentiation in diabetic cardiomyopathy. Cardiovasc Res *96*, 265-275.

Tanaka, N., Yonekura, H., Yamagishi, S., Fujimori, H., Yamamoto, Y., and Yamamoto, H. (2000). The receptor for advanced glycation end products is induced by the glycation products themselves and tumor necrosis factor-alpha through nuclear factor-kappa B, and by 17beta-estradiol through Sp-1 in human vascular endothelial cells. J Biol Chem *275*, 25781-25790.

Tatone, C., Heizenrieder, T., Di Emidio, G., Treffon, P., Amicarelli, F., Seidel, T., and Eichenlaub-Ritter, U. (2011). Evidence that carbonyl stress by methylglyoxal exposure induces DNA damage

and spindle aberrations, affects mitochondrial integrity in mammalian oocytes and contributes to oocyte ageing. Hum Reprod *26*, 1843-1859.

Tekin, D., Dursun, A.D., and Xi, L. (2010). Hypoxia inducible factor 1 (HIF-1) and cardioprotection. Acta Pharmacol Sin *31*, 1085-1094.

Thangarajah, H., Yao, D., Chang, E.I., Shi, Y., Jazayeri, L., Vial, I.N., Galiano, R.D., Du, X.L., Grogan, R., Galvez, M.G.*, et al.* (2009). The molecular basis for impaired hypoxia-induced VEGF expression in diabetic tissues. Proc Natl Acad Sci U S A *106*, 13505-13510.

Thornalley, P.J. (2003a). The enzymatic defence against glycation in health, disease and therapeutics: a symposium to examine the concept. Biochem Soc Trans *31*, 1341-1342.

Thornalley, P.J. (2003b). Glyoxalase I--structure, function and a critical role in the enzymatic defence against glycation. Biochem Soc Trans *31*, 1343-1348.

Thornalley, P.J., Waris, S., Fleming, T., Santarius, T., Larkin, S.J., Winklhofer-Roob, B.M., Stratton, M.R., and Rabbani, N. (2010). Imidazopurinones are markers of physiological genomic damage linked to DNA instability and glyoxalase 1-associated tumour multidrug resistance. Nucleic Acids Res *38*, 5432-5442.

Thygesen, K., Alpert, J.S., Jaffe, A.S., Simoons, M.L., Chaitman, B.R., White, H.D., and Task Force for the Universal Definition of Myocardial, I. (2012). Third universal definition of myocardial infarction. Nat Rev Cardiol *9*, 620-633.

Tonnessen, T., Lunde, P.K., Giaid, A., Sejersted, O.M., and Christensen, G. (1998). Pulmonary and cardiac expression of preproendothelin-1 mRNA are increased in heart failure after myocardial

infarction in rats. Localization of preproendothelin-1 mRNA and endothelin peptide. Cardiovasc Res *39*, 633-643.

Tous, E., Purcell, B., Ifkovits, J.L., and Burdick, J.A. (2011). Injectable acellular hydrogels for cardiac repair. J Cardiovasc Transl Res *4*, 528-542.

Tsoporis, J.N., Izhar, S., Leong-Poi, H., Desjardins, J.F., Huttunen, H.J., and Parker, T.G. (2010). S100B interaction with the receptor for advanced glycation end products (RAGE): a novel receptor-mediated mechanism for myocyte apoptosis postinfarction. Circ Res *106*, 93-101.

Vaitkevicius, P.V., Lane, M., Spurgeon, H., Ingram, D.K., Roth, G.S., Egan, J.J., Vasan, S., Wagle, D.R., Ulrich, P., Brines, M.*, et al.* (2001). A cross-link breaker has sustained effects on arterial and ventricular properties in older rhesus monkeys. Proc Natl Acad Sci U S A *98*, 1171-1175.

van Berlo, J.H., and Molkentin, J.D. (2014). An emerging consensus on cardiac regeneration. Nat Med *20*, 1386-1393.

Van Dyken, S.J., and Locksley, R.M. (2013). Interleukin-4- and interleukin-13-mediated alternatively activated macrophages: roles in homeostasis and disease. Annu Rev Immunol *31*, 317-343.

van Empel, V.P., Bertrand, A.T., Hofstra, L., Crijns, H.J., Doevendans, P.A., and De Windt, L.J. (2005). Myocyte apoptosis in heart failure. Cardiovasc Res *67*, 21-29.

Van Herreweghe, F., Mao, J., Chaplen, F.W., Grooten, J., Gevaert, K., Vandekerckhove, J., and Vancompernolle, K. (2002). Tumor necrosis factor-induced modulation of glyoxalase I activities through phosphorylation by PKA results in cell death and is accompanied by the formation of a specific methylglyoxal-derived AGE. Proc Natl Acad Sci U S A *99*, 949-954.

Venkatraman, J., Aggarwal, K., and Balaram, P. (2001). Helical peptide models for protein glycation: proximity effects in catalysis of the Amadori rearrangement. Chem Biol *8*, 611-625.

Verzijl, N., DeGroot, J., Thorpe, S.R., Bank, R.A., Shaw, J.N., Lyons, T.J., Bijlsma, J.W., Lafeber, F.P., Baynes, J.W., and TeKoppele, J.M. (2000). Effect of collagen turnover on the accumulation of advanced glycation end products. J Biol Chem *275*, 39027-39031.

Virag, J.A., Rolle, M.L., Reece, J., Hardouin, S., Feigl, E.O., and Murry, C.E. (2007). Fibroblast growth factor-2 regulates myocardial infarct repair: effects on cell proliferation, scar contraction, and ventricular function. Am J Pathol *171*, 1431-1440.

Vulesevic, B., McNeill, B., Geoffrion, M., Kuraitis, D., McBane, J.E., Lochhead, M., Vanderhyden, B.C., Korbutt, G.S., Milne, R.W., and Suuronen, E.J. (2014). Glyoxalase-1 overexpression in bone marrow cells reverses defective neovascularization in STZ-induced diabetic mice. Cardiovasc Res *101*, 306-316.

Vulesevic, B., McNeill, B., Giacco, F., Maeda, K., Blackburn, N.J., Brownlee, M., Milne, R.W., and Suuronen, E.J. (2016). Methylglyoxal-Induced Endothelial Cell Loss and Inflammation Contribute to the Development of Diabetic Cardiomyopathy. Diabetes *65*, 1699-1713.

Wall, S.T., Walker, J.C., Healy, K.E., Ratcliffe, M.B., and Guccione, J.M. (2006). Theoretical impact of the injection of material into the myocardium: a finite element model simulation. Circulation *114*, 2627-2635.

Wang, T., Kartika, R., and Spiegel, D.A. (2012). Exploring post-translational arginine modification using chemically synthesized methylglyoxal hydroimidazolones. J Am Chem Soc *134*, 8958-8967.

Wang, X.L., Lau, W.B., Yuan, Y.X., Wang, Y.J., Yi, W., Christopher, T.A., Lopez, B.L., Liu, H.R., and Ma, X.L. (2010). Methylglyoxal increases cardiomyocyte ischemia-reperfusion injury via glycative inhibition of thioredoxin activity. Am J Physiol Endocrinol Metab *299*, E207-214.

Ward, M.S., Fortheringham, A.K., Cooper, M.E., and Forbes, J.M. (2013). Targeting advanced glycation endproducts and mitochondrial dysfunction in cardiovascular disease. Curr Opin Pharmacol *13*, 654-661.

Wassenaar, J.W., Gaetani, R., Garcia, J.J., Braden, R.L., Luo, C.G., Huang, D., DeMaria, A.N., Omens, J.H., and Christman, K.L. (2016). Evidence for Mechanisms Underlying the Functional Benefits of a Myocardial Matrix Hydrogel for Post-MI Treatment. J Am Coll Cardiol *67*, 1074-1086.

Watt, F.M., and Huck, W.T. (2013). Role of the extracellular matrix in regulating stem cell fate. Nat Rev Mol Cell Biol *14*, 467-473.

Webb, C.S., Bonnema, D.D., Ahmed, S.H., Leonardi, A.H., McClure, C.D., Clark, L.L., Stroud, R.E., Corn, W.C., Finklea, L., Zile, M.R.*, et al.* (2006). Specific temporal profile of matrix metalloproteinase release occurs in patients after myocardial infarction: relation to left ventricular remodeling. Circulation *114*, 1020-1027.

Wencker, D., Chandra, M., Nguyen, K., Miao, W., Garantziotis, S., Factor, S.M., Shirani, J., Armstrong, R.C., and Kitsis, R.N. (2003). A mechanistic role for cardiac myocyte apoptosis in heart failure. Journal of Clinical Investigation *111*, 1497-1504.

Xu, G., Wang, X., Deng, C., Teng, X., Suuronen, E.J., Shen, Z., and Zhong, Z. (2015). Injectable biodegradable hybrid hydrogels based on thiolated collagen and oligo(acryloyl carbonate)-

poly(ethylene glycol)-oligo(acryloyl carbonate) copolymer for functional cardiac regeneration. Acta Biomater *15*, 55-64.

Xue, J., Ray, R., Singer, D., Bohme, D., Burz, D.S., Rai, V., Hoffmann, R., and Shekhtman, A. (2014). The receptor for advanced glycation end products (RAGE) specifically recognizes methylglyoxal-derived AGEs. Biochemistry *53*, 3327-3335.

Xue, M., Rabbani, N., Momiji, H., Imbasi, P., Anwar, M.M., Kitteringham, N., Park, B.K., Souma, T., Moriguchi, T., Yamamoto, M.*, et al.* (2012). Transcriptional control of glyoxalase 1 by Nrf2 provides a stress-responsive defence against dicarbonyl glycation. Biochem J *443*, 213-222.

Yan, X., Anzai, A., Katsumata, Y., Matsuhashi, T., Ito, K., Endo, J., Yamamoto, T., Takeshima, A., Shinmura, K., Shen, W.*, et al.* (2013). Temporal dynamics of cardiac immune cell accumulation following acute myocardial infarction. J Mol Cell Cardiol *62*, 24-35.

Yao, D., Taguchi, T., Matsumura, T., Pestell, R., Edelstein, D., Giardino, I., Suske, G., Rabbani, N., Thornalley, P.J., Sarthy, V.P.*, et al.* (2007). High glucose increases angiopoietin-2 transcription in microvascular endothelial cells through methylglyoxal modification of mSin3A. J Biol Chem *282*, 31038-31045.

Yellon, D.M., and Hausenloy, D.J. (2007). Myocardial reperfusion injury. N Engl J Med *357*, 1121-1135.

Yokoyama, T., Nakano, M., Bednarczyk, J.L., McIntyre, B.W., Entman, M., and Mann, D.L. (1997). Tumor necrosis factor-alpha provokes a hypertrophic growth response in adult cardiac myocytes. Circulation *95*, 1247-1252.

Yoshizumi, T., Zhu, Y., Jiang, H., D'Amore, A., Sakaguchi, H., Tchao, J., Tobita, K., and Wagner, W.R. (2016). Timing effect of intramyocardial hydrogel injection for positively impacting left ventricular remodeling after myocardial infarction. Biomaterials *83*, 182-193.

Young, J.L., and Engler, A.J. (2011). Hydrogels with time-dependent material properties enhance cardiomyocyte differentiation in vitro. Biomaterials *32*, 1002-1009.

Yuen, A., Laschinger, C., Talior, I., Lee, W., Chan, M., Birek, J., Young, E.W., Sivagurunathan, K., Won, E., Simmons, C.A*., et al.* (2010). Methylglyoxal-modified collagen promotes myofibroblast differentiation. Matrix Biol *29*, 537-548.